ALGACEUTICAL: WHEN MICROALGAE APPLICATION MEETS INNOVATION

Enrica Giustino

Dottorato in Biotecnologie – XXXVII ciclo

Università di Napoli Federico II

Dottorato in Biotecnologie – XXXVII ciclo

Università di Napoli "Federico II"

ALGACEUTICAL: WHEN MICROALGAE APPLICATION MEETS INNOVATION

Enrica Giustino

Dottoranda:	Enrica Giustino
Relatore:	Prof. Daria Maria Monti
Coordinatore:	Prof. Marco Moracci
Settore Scientifico Disciplinare:	05/BIOS-07

Long live all the mountains we moved

INDEX

Le microalghe sono un gruppo eterogeneo di microorganismi unicellulari ubiquitari, comunemente presenti negli ambienti acquatici. I loro processi fotosintetici non solo favoriscono la produzione di ossigeno, ma contribuiscono anche alla fissazione della CO_2, producendo glucosio e ossigeno, rappresentando quindi una risorsa fondamentale per la mitigazione dei cambiamenti climatici. La loro capacità di prosperare in una vasta gamma di ecosistemi è principalmente dovuta alla loro estrema adattabilità ambientale, che le rende capaci di sopravvivere in condizioni estreme, come in fonti termali, bacini ad alta salinità, in presenza di metalli pesanti o contaminanti del suolo. Per tali caratteristiche, le microalghe sono spesso paragonate alle piante superiori, con le quali condividono i principali meccanismi di fotosintesi e la produzione di metaboliti necessari per la crescita. Tuttavia, le microalghe offrono anche vantaggi in termini di produzione di molecole rispetto alle piante superiori. A differenza di quest'ultime, le microalghe crescono più rapidamente e non dipendono dai cicli stagionali, rendendole ideali per coltivazioni perenni. Inoltre, le microalghe non richiedono terreni agricoli né acqua dolce, permettendo di coltivarle in ambienti alternativi, senza competere con altre colture agricole, il che consente di implementarne la produzione su larga scala. Grazie alle loro caratteristiche, le microalghe rappresentano una risorsa straordinaria in grado di accumulare una vasta gamma di composti bioattivi ad alto valore aggiunto, tra cui proteine, lipidi, zuccheri e altre molecole di interesse per vari settori, come quello cosmetico, nutraceutico, alimentare e farmaceutico. Inoltre, le microalghe sono in grado di cambiare il loro metabolismo senza ricorrere all’ingegneria genetica, ma solo variando le condizioni di crescita. In tal modo, è possibile aumentare la produzione di lipidi o zuccheri, da utilizzare come fonti sostenibili per la produzione di biocarburanti di terza generazione.

Nonostante il loro grande potenziale, l'uso delle microalghe rimane ancora limitato a causa degli elevati costi di produzione, raccolta, estrazione e conversione, che rendono l'intero processo non economicamente sostenibile. Per incentivare lo sviluppo dell'industria delle microalghe, è cruciale implementare una piattaforma integrata che consenta la produzione di diversi prodotti attraverso un processo in cascata. La creazione di sistemi di bioraffineria efficienti e l'adozione di strategie di coltivazione mirate potrebbero contribuire significativamente alla riduzione dei costi totali di produzione.

La ricerca, tuttavia, non può limitarsi a ottimizzare i processi, utilizzando tecniche innovative o sostituendo i solventi chimici con

alternative più sicure per l'uomo e per l'ambiente. È necessario, parallelamente, un costante controllo della qualità dei prodotti estratti, al fine di garantirne una corretta attività biologica, per poterle introdurre nel mercato. Inoltre, è fondamentale valutare attentamente la fetta di mercato di interesse, per assicurarsi che i prodotti possano realmente generare profitti.

Come già accennato, le microalghe possiedono un enorme potenziale dal punto di vista produttivo, venendo spesso identificate come vere e proprie biofabbriche da cui è possibile estrarre una vasta gamma di prodotti. Tali prodotti, dalle più diverse attività biologiche, condividono spesso una marcata attività antiossidante, che è di grande interesse industriale, in particolare nei settori della cosmetica e della nutraceutica. L'esposizione ai raggi UV, lo stile di vita alimentare e sociale, l'inquinamento e la salubrità dei prodotti alimentari sono solo alcuni dei numerosi fattori a cui gli esseri umani sono esposti e che provocano una risposta fisiologica chiamata stress ossidativo. Biologicamente, lo stress ossidativo è definito come lo squilibrio tra la produzione di specie reattive dell'ossigeno (ROS) e la loro detossificazione. Sebbene i ROS siano essenziali per il mantenimento di normali funzioni biologiche cellulari, la loro produzione eccessiva può provocare danni significativi, come la modifica delle macromolecole biologiche (DNA, RNA, proteine e lipidi), con conseguenze cellulari potenzialmente gravi. Questo può tradursi in stati infiammatori, nell'invecchiamento cutaneo, nella deregolazione del differenziamento cellulare e nell'accumulo eccessivo di lipidi nel tessuto adiposo e nel fegato, fenomeni che possono predisporre allo sviluppo di patologie gravi come insulino-resistenza, obesità e steatosi epatica. Di conseguenza, la riduzione dello stress ossidativo rappresenta un obiettivo strategico per migliorare o trattare tali condizioni.

In questo contesto, le microalghe emergono come candidate ideali, poiché producono molecole antiossidanti naturali, la cui estrazione e caratterizzazione può essere ottimizzata per soddisfare i criteri necessari per applicazioni industriali. Il presente progetto di dottorato ha avuto come obiettivo l'impiego di molecole antiossidanti isolate dalle microalghe in ambito cosmeceutico e nutraceutico, con un focus particolare sulla loro capacità di interferire con il metabolismo lipidico. Sono stati utilizzati due modelli sperimentali: le cellule pre-adipocitiche murine 3T3-L1 e le cellule epatiche murine AML12. Le microalghe selezionate sono state: (i) la microalga rossa mesofila marina *Porphyridium cruentum*; (ii) la microalga rossa termo-acidofila *Galdieria phlegrea*; e (iii) la microalga verde *Pseudococcomyxa simplex*. La

selezione di microalghe appartenenti a phyla differenti ha permesso di caratterizzare diverse classi di molecole per natura e composizione, consentendo di ottimizzare il processo di estrazione in cascata per ciascun ceppo. Per *P. cruentum* e *G. phlegrea*, il sistema di bioraffineria e la valutazione chimico-fisica e biologica delle molecole estratte erano già state sviluppate in precedenza. Il processo di estrazione è stato invece completamente ottimizzato per *P. simplex*, una specie poco conosciuta in letteratura, se non per la sua classificazione tassonomica. Sono stati testati vari composti, come la ficoeritrina e gli esopolisaccaridi solfati da *P. cruentum*, e i carotenoidi estratti dalla biomassa di *P. simplex* e dalla biomassa residua di *G. phlegrea*.

Globalmente, tutte le molecole analizzate hanno mostrato buona biocompatibilità e sono state in grado di migliorare positivamente almeno una delle condizioni testate, ad eccezione dei carotenoidi estratti dalla biomassa fresca di *Galdieria phlegrea*, i quali potrebbero aver subito un'influenza negativa da parte di contaminanti non rimossi durante la prima fase di estrazione, riducendo così la qualità dell'estratto. Al contrario, l'estratto ottenuto dalla biomassa residua ha rivelato eccellenti proprietà nel modulare gli enzimi coinvolti nell'iper-pigmentazione della pelle, oltre a inibire il differenziamento dei pre-adipociti, agendo sugli enzimi che regolano l'accumulo intracellulare di lipidi, fin dalle prime fasi della trascrizione. Inoltre, l'estratto, applicato sugli adipociti maturi, ha mostrato risultati promettenti nella modulazione positiva della lipolisi e della lipogenesi.

Gli esopolisaccaridi e la ficoeritrina estratti da *P. cruentum* si sono rivelati attivi in entrambi i modelli cellulari, mostrando la capacità di inibire il differenziamento dei pre-adipociti, incrementando la sintesi di enzimi lipolitici negli adipociti maturi e riducendo l’espressione degli enzimi coinvolti nella sintesi dei trigliceridi, con un’efficacia che variava tra le due molecole.

Per quanto riguarda i carotenoidi ed i lipidi estratti in cascata dalla biomassa di *P. simplex*, la composizione dei carotenoidi ha rivelato una predominanza di due carotenoidi ad alto valore commerciale, la luteina e la neoxantina. La caratterizzazione dell'estratto ha evidenziato una notevole attività antiossidante, soprattutto nell'inibire la produzione di specie reattive dell'ossigeno (ROS) intracellulari, a seguito dell'induzione dello stress ossidativo, e nell'attivazione del *pathway* di Nrf2, una proteina chiave coinvolta nella risposta cellulare allo stress. Questa elevata attività benefica è stata ulteriormente confermata dall’abilità dell'estratto, testato alla sua concentrazione antiossidante,

nell'inibire gli enzimi legati all'invecchiamento cutaneo e al differenziamento cellulare.

Partendo dai risultati promettenti ottenuti, un aspetto cruciale della ricerca ha riguardato l'ottimizzazione del processo di raccolta, utilizzando la flocculazione come metodo alternativo alla tradizionale centrifugazione. Questo approccio ha migliorato ulteriormente l'efficienza del processo, permettendo di bypassare la fase di essiccazione della biomassa prima dell'estrazione, con il vantaggio di ridurre sia i tempi di trasformazione che i costi energetici. Poiché l'obiettivo finale è ottimizzare il processo senza compromettere la qualità della biomassa e dei prodotti ottenuti, è stata condotta un'analisi dell'attività antiossidante dei carotenoidi estratti dalla biomassa flocculata. Sebbene la flocculazione abbia mostrato risultati promettenti, si è osservato che tre dei quattro estratti analizzati hanno mostrato una riduzione dell'attività antiossidante dopo la flocculazione. Questo risultato sottolinea la necessità di adattare il processo in funzione delle caratteristiche specifiche del microrganismo utilizzato, e non il contrario.

In conclusione, il presente progetto di dottorato ha messo in evidenza il grande potenziale delle microalghe come fonte innovativa di molecole antiossidanti, attive in diversi meccanismi cellulari legati al miglioramento dello stress ossidativo, come l'invecchiamento cellulare e le problematiche connesse al metabolismo lipidico. Le microalghe si configurano così come strumenti sia preventivi, grazie alla loro elevata capacità di inibire l'accumulo di lipidi nel tessuto adiposo, sia terapeutici, con applicazioni in ambito cosmeceutico e nutraceutico, suggerendo potenziali applicazioni reali per i composti analizzati. Inoltre, la ricerca ha evidenziato l'importanza dell'uso della bioraffineria, non solo come mezzo per ridurre i costi del processo, ma anche per ottenere molecole con attività biologiche migliorate, come nel caso di *Galdieria phlegrea*.

L'approccio integrato della bioraffineria, insieme all'ottimizzazione dei processi di raccolta ed estrazione, offrono soluzioni concrete per ridurre i costi di produzione e migliorare la sostenibilità dell'intero processo. Tuttavia, sebbene i risultati siano estremamente incoraggianti, il passaggio dalla ricerca di laboratorio alla produzione su scala industriale richiede ulteriori sforzi, non solo in termini di innovazione tecnologica, ma anche nell’affrontare le sfide normative e commerciali legate all'uso delle microalghe. Infatti, le realtà industriali che si basano esclusivamente sull'uso delle microalghe sono ancora

piuttosto limitate, sebbene grandi aziende cosmetiche stiano immettendo sul mercato prodotti a base di microalghe, come creme solari e idratanti. Solo con l'integrazione di queste soluzioni si può sperare di concretizzare pienamente il potenziale delle microalghe, creando un futuro sostenibile che unisca innovazione scientifica e applicazioni industriali efficaci, contribuendo significativamente alla salute umana e alla mitigazione dei cambiamenti climatici.

* Gli studi condotti sull'effetto delle molecole antiossidanti sul metabolismo lipidico nei due sistemi cellulari sono stati condotti durante il periodo di studio e ricerca all'estero presso l'Università Dei Paesi Baschi presso il laboratorio di nutrizione ed obesità coordinato dalla prof. Maria Puy Portillo.

Microalgae are unicellular photosynthetic microorganisms that inhabit a wide range of environments and play a significant role in global oxygen production. Their remarkable adaptability to extreme external conditions makes them perfect candidates for sustainable biomass production in regions unsuitable for conventional agriculture. Microalgae can produce a wide variety of bioactive molecules (i.e., phycobiliproteins, carotenoids, lipids, polysaccharides), many endowed with antioxidant properties. In recent years, the potential of microalgae has been increasingly recognized for various industrial applications, including nutraceuticals, cosmeceuticals, biofuels, and pharmaceuticals. In particular, research on the antioxidant potential of microalgae-derived compounds is gaining traction, as oxidative stress is now well recognized for its role in the alteration of cellular differentiation as well as in the modification of different metabolic pathways, like the lipidic ones, which can lead to the onset of a plethora of associated pathologies. The general aim of the present thesis was to evaluate the potential of antioxidant molecules derived from microalgae in different applications, such as the cosmeceuticals and nutraceuticals fields. Investigation was done with a specific emphasis on the impact of different antioxidant molecules on cellular differentiation in murine pre-adipocytes and on lipid metabolism in mature adipocytes and hepatocytes. Three microalgal strains were used: *Porphyridium cruentum*, a red marine mesophile microalga, *Galdieria phlegrea*, a red thermo-acidophilic microalga, and *Pseudococcomyxa simplex*, a green freshwater microalga. The first two strains were already the subject of a tailored biorefinery approach, which allowed obtaining different classes of bioactive molecules, characterized at chemico-physical and antioxidant level. In this study, sulfated exopolysaccharides and phycoerythrin from *P. cruentum*, and carotenoids from *G. phlegrea* residual biomass (i.e., after protein extraction) were used. Results showed that sulfated exopolysaccharides, phycoerythrin and carotenoids were all biocompatible and able to inhibit pre-adipocyte differentiation, but with a different extent. Interestingly, carotenoids from the residual biomass of *G. phlegrea* showed a regulation of lipid metabolism on mature adipocytes, whereas sulfated exopolysaccharides positively inhibited lipid build-up in the hepatic cells. For *P. simplex*, the study started with the design of a novel biorefinery, which enabled the extraction of carotenoids and lipids and the evaluation of the antiadipogenic activity of the extracted carotenoids. Finally, flocculation was explored as an alternative harvesting method, and its efficacy was evaluated through the biological characterization of the extracted molecules after flocculation.

CHAPTER 01

INTRODUCTION

1.1 *Microalgae and their biotechnological interest*

The term *microalgae* refers to a group of unicellular, eukaryotic, photosynthetic microorganisms, typically found in aquatic environments. Recent taxonomic classification has separated microalgae from cyanobacteria, known as blue-green algae, which are prokaryotic unicellular photosynthetic microorganisms. However, despite this distinction, the term *microalgae* is still frequently used to encompass both groups, as both they share similar ecological roles as primary producers in aquatic ecosystems. They utilize light and inorganic carbon for growing, producing approximately half of the atmospheric oxygen[1]. Microalgae are adaptable to a wide range of habitats, including hot springs, extremely saline waters, wastewaters, fresh and marine environments. Thanks to their high adaptability, they can be grown in areas unsuitable for traditional agriculture and do not require fertile soil[2]. Microalgae grow at a higher rate, achieving greater biomass productivity *per* area, compared to terrestrial crops[3] and, due to their lower fiber content, microalgae biomass can be almost completely utilized to extract proteins, lipids, and easily accessible carbohydrates (such as starch)[4]. For these reasons, microalgae can be used in several industrial products, such as aquatic or animal feed, nutraceuticals, biofertilizer and cosmetics[5,6]. Moreover, microalgae are emerging as potential feedstock in different industrial sectors, as food commodities, biofuels, bio-based chemicals, bioplastics, nutraceuticals, and cosmetics[7]. Nevertheless, their scalability, cost-effectiveness and efficient downstream processing remain issues to be addressed, outlining the urgency of optimizing microalgal exploitation in order to establish an algae-based industry[8].

Indeed, despite microalgae can be easily grown and their metabolism may be affected by changing external parameters (no genetic manipulation is needed), research and technological advancements are currently being pursued, focusing on enhancing the cultivation process, lowering freshwater requirements for cultivation, as well as reducing harvesting and transformation costs[9].

Besides the implementation of single steps in microalgae exploitation, the possibility of employing microalgae on large-scale relies on the application of the biorefinery concept[10–14]. Indeed, the obtainment of different class of molecules with high market value in a cascade approach can lower the whole costs, thus economically driving the entire process[9].

1.2 *Microalgae strain selection*

The implementation and efficacy of a biorefinery process based on microalgae starts from an appropriate strain selection. It has been estimated that about 200,000-800,000 species in many different genera exist, but only about 50,000 species have been described so far[2], with only 10 genera used at industrial scale[15]. Among all families, the most interesting are represented by Rhodophyta (red algae), Chlorophyta (green algae) and from Cyanobacteria (blue-green algae), thanks to the vast array of produced molecules[15,16].

1.2.1 Rhodophyta

Rhodophyta, also known as red algae, are eukaryotic unicellular microorganisms, normally spherical shaped with an average size of about 5 μm[15]. Generally speaking, all microalgae belonging to the red division are characterized by: (i) the presence of the phycobilisome, a photosynthetic accessory set of pigments; (ii) chloroplasts containing non-linked thylakoids; (iii) floridoside cytosolic granules used as energy storage; (iv) cell-wall composed of a microfibrillar layer of cellulose or xylan and amorphous polysaccharidic mucilages; and (v) the absence of flagella[17]. Thanks to their high tolerance towards environmental stressors, red microalgae are considered good candidates for large-scale production of biomass and bioactive molecules. Among the different genera, the best known and most simple ones are represented by *Porphyridium*, *Rhodella* and *Rhodosorus* strains.

1.2.1.1 *Porphyridium cruentum*

Porphyridium cruentum (**Figure 1**) is a spherical unicellular microalga, belonging to the class of *Porphyridiophyaceae,* often found in aggregates of cells because of the presence of a water-soluble polysaccharide layer that protects cells from osmotic stress, thus acting as cell wall[18–20]. During cell growth, the layer is gradually dissolved and sugars, namely exopolysaccharides (EPs), are released in the medium. In particular, *P. cruentum* excretes a large amount of sulfated EPs (s-EPSs) with a molecular weight range from 2 to 7 × 10^6 Da, composed of numerous monosaccharides, with xylose, glucose, and galactose the most abundant ones[12,21]. Beside s-EPSs, *P. cruentum* is well known for its ability to synthetize phycoerythrin on high extent, making this

microalga a potential source of interesting biotechnological compounds with high commercial value.

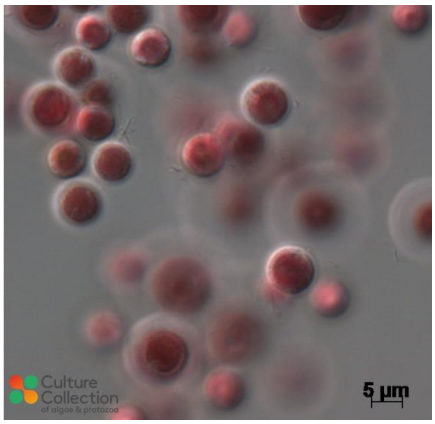

Figure 1. Microscopic image of *Porphyridium cruentum* *(https://www.ccap.ac.uk/catalogue/strain-1380-1a?mfp=61-archived%5BAvailable%5D&search=porphyridium%20cruentum).*

1.2.1.2 *Galdieria phlegrea*

Galdieria phlegrea (**Figure 2**) is a thermo-acidophilic, unicellular, red microalga belonging to the order of Cyanidiales. It is a freshwater microalga characterized by a spherical shape, a thick wall, one chloroplast, 1-3 mitochondria and a vacuole[22–24]. It is able to live at low pH environments, at high temperature, and has peculiar mechanisms for metal tolerance, allowing cells to bloom in ecosystems considered hostile for other microorganisms[25]. The peculiar *G. phlegrea* growth condition represents a further value, as the use of a medium with a low pH and the high temperature used could significantly reduce contaminations, making this microalga suitable for an up-scale in non-controlled systems. Moreover, when grown in autotrophy, it accumulates carotenoids (i.e., β-carotene, astaxanthin, zeaxanthin) and phycocyanin, as well as polyunsaturated fatty acids (PUFAs). Altogether, the production of different classes of bioactive molecules, linked to its unique growth conditions, makes *G. phlegrea* a perfect candidate for biotechnological applications.

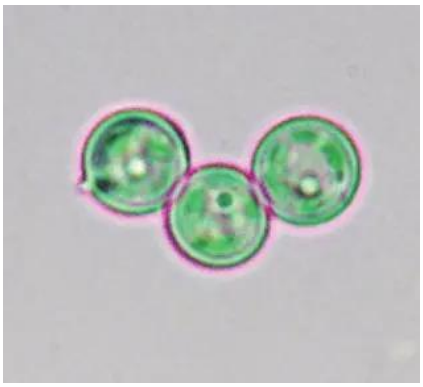

Figure 2. Microscopic image of *Galdieria phlegrea.* *https://www.microbiologiaitalia.it/alghe/galdieria-phlegrea/*

1.2.2 Chlorophyta

The division of Chlorophyta, or green algae, represents the most abundant one of microalgae. Among microalgae, the green ones are the most similar to terrestrial plants; they synthesize chlorophyll *a* and *b*, α- and β- carotene and xanthophylls, generally lutein, violaxanthin, and neoxantin[26,27]. They are surrounded by a typical cell wall, made of cellulose and pectin, which help in starch storage. Many Chlorophyta have attracted attention not only as a source of molecules used in the production of biofuels, but also for their ability to accumulate high-value biological products (e.g., α-tocopherol, carotenoids and PUFAs)[28].

1.2.2.1 *Pseudococcomyxa simplex*

Pseudococcomyxa simplex (**Figure 3**) is a green, freshwater, acid-tolerant microalga belonging to the family of Chlorellaceae. It is characterized by an ellipsoidal shape, occasionally slightly curved, of about 2-7 μm in width and 4-12 μm in length and found either as single cell or in small colonies[29]. This family is known for the ability to store lipids, which could represent the source for biofuel production, even if no evidence is reported in the use of *P. simplex* as feedstock. Moreover, the possibility of growing *P. simplex* at low pH values makes it an interesting candidate for biotechnological applications.

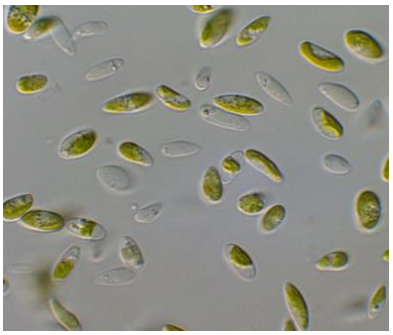

Figure 3. Microscopic image of *Pseudococcomyxa simplex.* *https://www.ccap.ac.uk/catalogue/strain-812-2b*

1.2.3 Cyanobacteria

Cyanobacteria, also known as cyanophytes or blue-green algae due to their pigment content, are prokaryotic organisms that share several characteristics with eukaryotic algal cells, such as size and the ability to perform photosynthesis under both aerobic and anaerobic conditions[30,31]. These traits, along with their significant phenotypic polymorphism, have historically complicated their classification, especially when based solely on morphological characteristics. Molecular studies and comprehensive morphological-functional analyses have clarified their distinction from eukaryotic microalgae in terms of cytology, physiology, and biochemistry. Unlike eukaryotic microalgae, cyanobacteria lack chloroplasts and instead possess thylakoids containing pigments such as chlorophyll *a*, phycocyanin, phycoerythrin, carotenoids, and xanthophylls[32].

1.2.3.1 *Synechococcus bigranulatus*

Synechococcus bigranulatus (**Figure 4**) is a unicellular prokaryotic microalga belonging to the order of Synechococcale[33]. It is found in aquatic environments, including lakes, rivers, and oceans and is characterized by a remarkable ability to rapidly grow at high temperatures (up to 70 °C) and alkaline pH (pH 11)[34]. Its biomass is rich in proteins, carbohydrates, lipids and micronutrients, including vitamins, carotenoids and chlorophylls, with concentrations varying according to growth conditions[35]. These characteristics make *S. bigranulatus* of great interest for biotechnological applications.

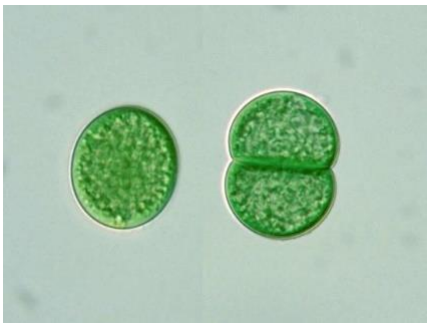

Figure 3. Microscopic image of *Synechococcus bigranulatus.* ttp://protist.i.hosei.ac.jp/pdb/images/Prokaryotes/Chroococcaceae/Synechococcus/sp_02b.html.

1.3 *Bioactive molecules from microalgae*

Due to their diverse nature and adaptability to external conditions, microalgae can produce a vast array of molecules, including polyunsaturated fatty acids (PUFAs), pigments (such as chlorophylls, carotenoids, and phycobiliproteins), carbohydrates and proteins. Many of them possess biological activities, including antioxidant, anticancer, antibacterial, antiviral, and antifungal activity[36]. Additionally, microalgae extracts can be employed in the formulation of anti-aging, emollient, protective, regenerating, and antioxidant skin care products[37], which have the potential to enhance skin structure, morphology, and appearance. Moreover, pigments produced by microalgae have been demonstrated to possess photoprotective, antiadipogenic activity, anti-inflammatory and anti-allergenic properties[38]. Thus, microalgae are considered promising microorganisms that can play a key role in bio-based economy, since they may serve as a continuous and reliable source of safe natural products of industrial interest. In particular, microalgae-derived compounds can be employed in the cosmetic and cosmeceutical fields in a variety of functions, as primary active ingredient or as stabilizer, dye, or thickening agent[39].

1.3.1 Phycobiliproteins

Phycobiliproteins (PBPs) are a family of water-soluble proteins, components of the photosynthetic light-harvesting antenna complex of Cyanobacteria, Rhodophyta, Cryptophytes, and Glaucophytes[40,41] (**Figure 4**). Phycobiliproteins are highly-fluorescent, with bright colors

and are assembled into an organized cellular structure, the phycobilisome (PBS), which is attached in regular arrays to the external surface of the thylakoid membranes. PBS acts as the major light-harvesting system in cyanobacteria and red algae as it is responsible for providing light energy to both PSII and PSI reaction centers[42]. The phycobilisome consists of an allophycocyanin (AP) core, which acts as the bridge between phycobilisomes and the photosynthetic lamella[43], surrounded by phycocyanin (PC), and phycoerythrin (PE) on the periphery, both usually present but in different ratios. PC and PE increase photosynthetic efficiency by collecting light energy at a wavelength at which chlorophyll poorly absorbs[44]. Due to their properties, phycobiliproteins have different biotechnological applications[45,46]. They are widely used in the cosmetics and food industry as dyes (e.g., lipsticks, eyeliners, eye shadows, ice cream, candies), especially because of the potential toxicity of synthetic dyes[47]. Moreover, due to their peculiar fluorescence, if conjugated with molecules that possess a biological specificity (such as biotin or immunoglobulins), phycobiliproteins can be used for immunological analyses[48]. In addition, phycobiliproteins can act as antioxidants: PE reduces ROS levels; PC and APC can either behave in the same way as PE or as preventive antioxidant agents, chelating the metal ions responsible for the production of ROS[49].

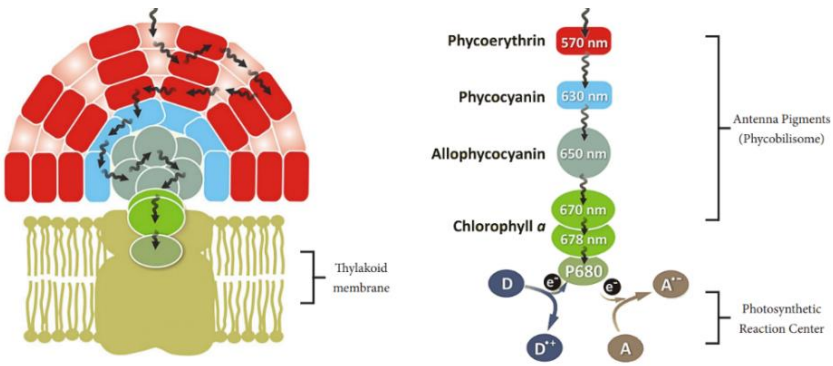

Figure 4. Schematic representation of the phycobilisome. The light-harvesting antenna complex is made of an APC core (dark green circles) closely surrounded by several rods made up of PC (blue rectangles) and PE (red rectangles) with outward orientation. The energy is absorbed by the rods and efficiently transferred to the chlorophyll for the photosynthetic reactions[1].

[1] Aryee, Alberta NA, et al. *Recovery and utilization of seaweed pigments in food processing.* Current Opinion in Food Science, **2018**, 19:113-119. https://doi.org/10.1016/j.cofs.2018.03.013.

1.3.1.1 Phycoerythrin

Like all phycobiliproteins, PE is composed of a protein covalently linked to an organic chromophore, the phycobilin. In the PE family, the most known phycobilins are phycoerythrobilin and sometimes phycourobilin[50]. PE is composed of (αβ) monomers, assembled into disk-shaped trimer $(\alpha\beta)_3$ or hexamer $[(\alpha\beta)_3]_2$. These typical complexes also contain a third type of subunit, the γ chain, which contributes as a linker and has light-harvesting functions, as it contains different chromophores from α and β chains[51] (**Figure 5**). Based on their absorption, excitation, and fluorescence emission spectra, as well as on the nature of the organic chromophore, phycoerythrins can be divided into five main groups forming the most spectroscopically variable class of phycobiliproteins[52]. Industrial demand for natural products led to an increased interest for PE, used as molecular marker, but also in the cosmetics and food industry as dye. However, PE's ability to act as anti-inflammatory molecule and as a preventive antioxidant agent, depicts it as a perfect candidate for therapeutic applications in oxidative stress-related diseases[53]. Unfortunately, to date, only few microalgal strains belonging to the *Porphyridiophyaceae* class are known to synthesize PE at high levels[54].

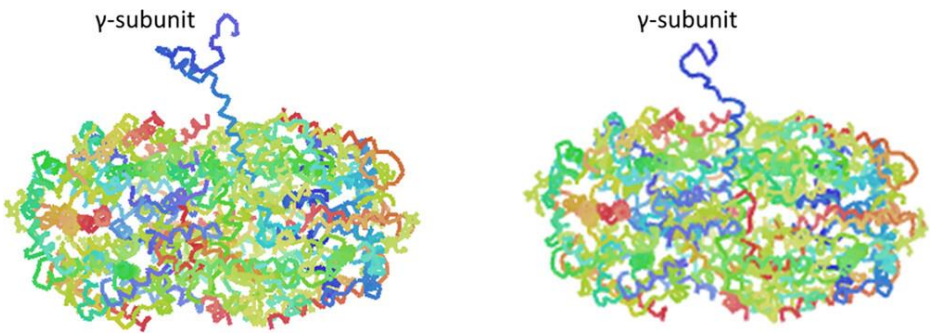

Figure 5. Heptameric $(\alpha\beta)_3\gamma$ structures observed in the phycobilisome from *P. cruentum*[2].

[2] Liberti, D., et al. *Inside out Porphyridium cruentum: Beyond the conventional biorefinery concept.* ACS Sustainable Chemistry & Engineering, **2022**, 11.1: 381-389. https://doi.org/10.1021/acssuschemeng.2c05869

1.3.2 Carotenoids

Carotenoids are considered the most widely distributed lipid-soluble accessory pigments in nature, synthetized by photosynthetic organisms (**Figure 6**)[55]. They can be divided into xanthophylls and carotenes, are responsible for light harvesting, and represent up to 14% of dry algal biomass[56]. During the last years, carotenoids have received increasing attention because of their potent antioxidant activity, which, combined to their natural brilliant color, allow to use them in different industrial fields (e.g. cosmeceutics)[57]. Furthermore, many carotenoids possess anti-inflammatory activity, as well as photoprotective or anti-obesity properties[58–60]. Noteworthy, the carotenoid market, in particular the one concerning astaxanthin, β-carotene, zeaxanthin, lutein, and fucoxanthin, is expected to reach 221.38 billion USD by 2030 with a Compound Annual Growth Rate (CAGR) of 4.79% (https://straitsresearch.com/report/facial-skincare-products-market)[61]. Recently, it has been found that β-carotene, β-cryptoxanthin, lutein, zeaxanthin, and astaxanthin can stimulate hyaluronic acid synthesis, a glycosaminoglycan involved in skin hydration, improving skin health and preventing skin-aging and wrinkles insurgence[16]. It has been reported that topical or oral administration of astaxanthin can suppress skin hyper-pigmentation and improve the condition of all skin layers[62]. Furthermore, some carotenoids are able to prevent fat accumulation[63].

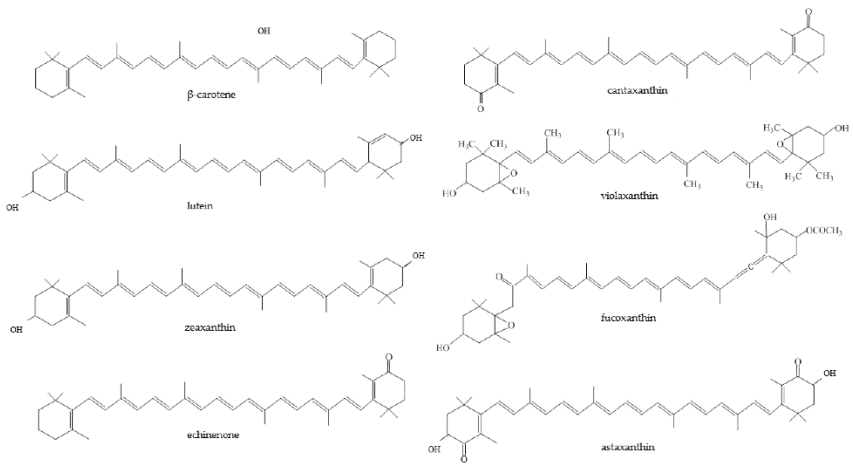

Figure 6. Molecular structure of major microalgal carotenoids.

1.3.3 Exopolysaccharides

Microalgae are also an excellent source of polysaccharides (PSs), which can represent up to 50% of total dry biomass, used as energy storage and/or structural cell-wall elements[39]. A peculiar class of PSs is represented by the so-called exopolysaccharides (EPSs), found in some microalgae cell wall. EPSs are unbound to the cell wall and released in the culture medium during algal growth[64]. They are primarily constituted of linear sulfated galactan polymers; however, their composition is species-specific and can range from a single sugar class to a heterogeneous mixture[65]. EPSs are endowed with different peculiar properties that, although their mechanisms remain unclear, have been attributed to structural characteristics, i.e., sulfate content or sulfation pattern[66].

Indeed, the sulfated EPSs class (s-EPSs) are well-known for their antioxidant, antiviral, and anti-inflammatory activity[67]. The main mechanism by which s-EPSs exert their primary antioxidant action is by scavenging free radicals or by inhibiting their appearance[68]. Thanks to their high bioactivity, s-EPSs may be used for cosmetic or skin-care products, such as anti-aging and wrinkle-removing compounds. As some s-EPSs have film-forming properties, these can be useful in reducing skin water evaporation, allowing a moisturizing effect[69]. S-ESPs can also find applications as emulsifying and gelling compounds, stabilizers, and thickening agents[70].

1.4 *Oxidative stress*

Oxidative stress is defined as the alteration of the balance between the production and detoxification of reactive oxygen species (ROS). While ROS are essentials for cellular function, their deregulation can give rise to adverse effects, resulting in cellular damage and metabolic alterations[71]. When the intracellular ROS level decreases, cell growth is inhibited, and apoptosis may finally occur. On the other hand, high ROS levels can damage cellular macromolecules with dramatic results. In particular, lipid peroxidation starts from the attack of an oxygen radical on a fatty acid's side chain, subtracting a hydrogen atom from a methylene carbon, followed by the rearrangement of the carbon-centered lipid radical. The high reactivity of the resulting peroxyl radical could represent the starting point of a lipid peroxidation chain reaction. Additionally, lipid peroxides can be generated through the attack on PUFAs or their side chains by singlet oxygen. Proteins, instead, can be

affected by (i) oxidation of specific amino acids, (ii) free radical-mediated peptides cleavage, and (iii) proteins cross-linking due to the reaction with lipid peroxidation products. In the case of sugars, ROS production could directly result in glycoxidative damage. Finally, ROS could affect nucleic acid structure inducing base deletions, modifications, frame shift, single or double strand breaks but also in cross-linking with proteins and chromosomal re-arrangements[72–74] (**Figure 7**). Consequently, damages induced by oxidative stress will affect the regulation of intracellular signal transduction. There is substantial evidence that oxidative stress plays a pivotal role in the pathogenesis of lifestyle-related diseases, e.g., obesity, atherosclerosis, hypertension, and diabetes mellitus[75–77].

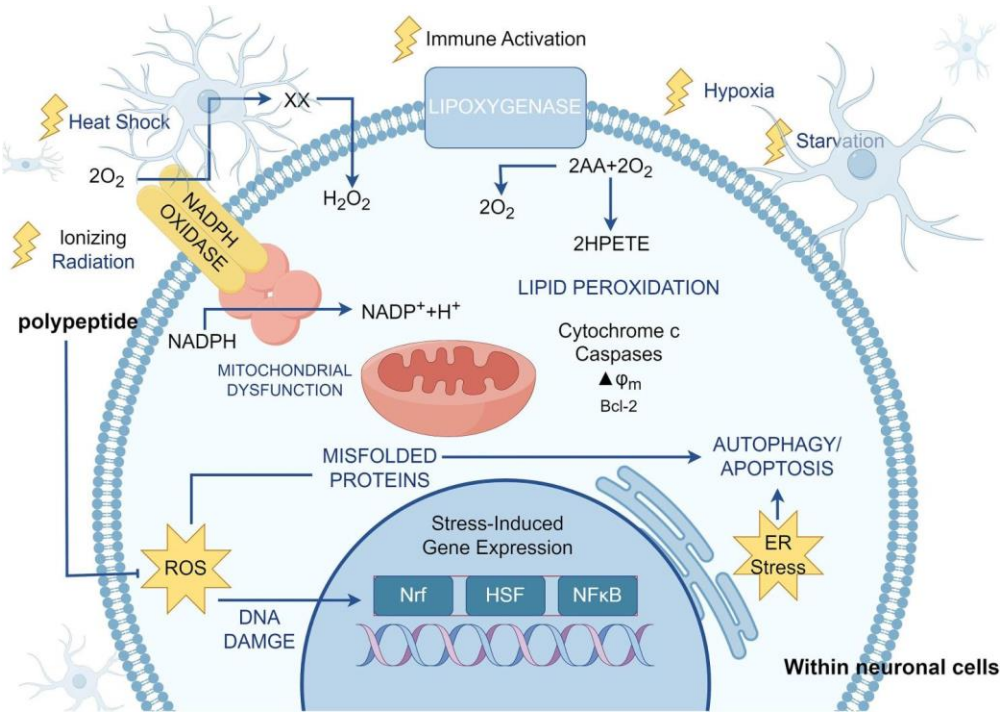

Figure 7. Schematic representation of the effects of ROS on eukaryotic cells[3].

[3] Ding, Xuying, et al., *Research progress on the protection and mechanism of active peptides in Alzheimer's disease and Parkinson's disease*. Neuropeptides, **2024**, 102457. https://doi.org/10.1016/j.npep.2024.102457

1.4.1 Oxidative stress and lipid metabolism

In adult mammals lipids as triglycerides are regulated in, at least, two distinct adipose lineages: (i) unilocular white adipocytes, used as energy storage through triglyceride synthesis, and (ii) multilocular brown adipocytes, mainly devoted to β-oxidation for thermogenesis, thanks to the high number of mitochondria and subsequent over expression of the uncoupling protein 1 (UCP1). However, adipose tissue is considered a heterogenic tissue made also of pre-adipocytes, mature adipocytes, mesenchymal stem cells, macrophages, and endothelial cells in different proportions[78]. Given its complexity, the regulation of lipid metabolism and the onset of related pathological conditions in adipose tissue, as well as in the liver, are finely controlled by an intersection of pathways that share a common feature: the alteration of the cellular redox state[79].

Indeed, the increase in intracellular ROS levels induces the activation of the pro-inflammatory cascade, inducing the synthesis and secretion of the nuclear factor kappaB (NF-kB), which in turn promotes the production of pro-inflammatory cytokines, such as interleukin 1 β (IL-1β) and tumor-necrosis factor α (TNF-α). The latter influences apoptosis of adipose tissues, increases lipogenesis, insulin signaling and enhance ROS synthesis[73,80]. On the other hand, ROS significantly affects long-chain fatty acid β-oxidation pathway in mitochondria by downregulating the key genes involved in the Acil-CoA translocation in the mitochondria (i.e., CPT1α and PPARα)[81]. In particular, the catabolism process starts from the translocation of the acyl-CoAs groups to the mitochondrial matrix *via* carnitine acyltransferase (CPT1α)[81]. Downregulation of CPT1α synthesis stops the β-oxidation inducing lipid storage both in adipose tissue and liver. However, while the oxidation of fatty acids efficiently increases cell energy levels, it also promotes the increase of ROS[82] (**Figure 8**).

Oxidative stress enhances preadipocyte proliferation, adipocyte differentiation and growth[83] leading to adipocyte hypertrophy (i.e., adipocyte increased size) or hyperplasia (i.e., adipocyte increased number), significantly affecting adipose tissue health and structure[84,85]. ROS mainly exert their proliferative activity through the upregulation of genes involved in differentiation processes, such as those of the superfamilies of PPARs (Peroxisome Proliferator-Activated Receptors) and c/EBPs (CCAAT/Enhancer-Binding Proteins)[86].

Consequently, cytokines and adipokines secreted by the enlarged adipose induce insulin resistance, reduce lipolysis and thus directly induce the translocation of fatty acids to the liver. These

changes may represent the starting point for hepatic inflammatory states (also known as hepatic steatosis or nonalcoholic fatty liver disease (NAFLD)) that, in the worst-case scenario, can lead to the development of cirrhosis and hepatocellular carcinoma[74,87].

Overall, the important role that oxidative stress plays in the regulation of lipid metabolism and the occurrence of associated pathological conditions suggest that reducing oxidative stress could be the key strategy in mitigating lipid metabolism related disorders.

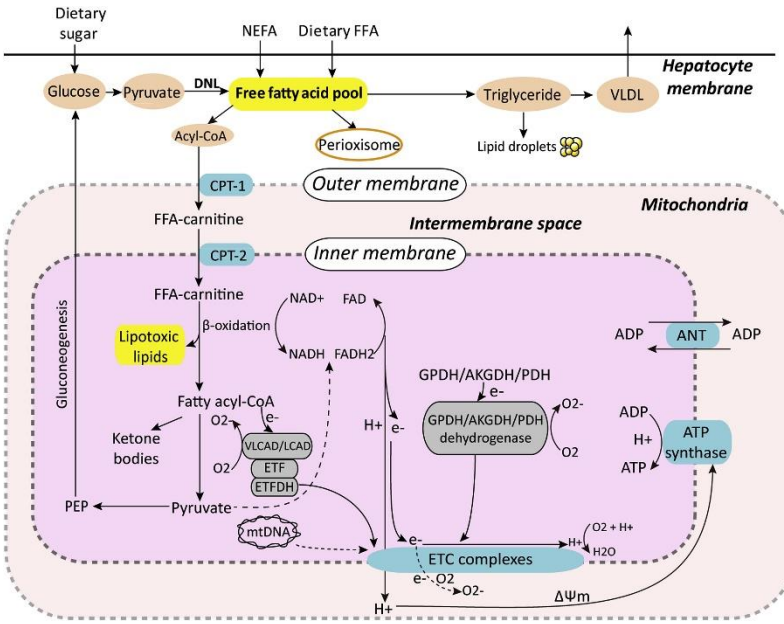

Figure 8. Schematic representation of oxidative stress effect on cellular homeostasis and lipid metabolism alteration[4].

1.5 *Antioxidants*

To overcome alterations in oxidative stress, cells have developed sophisticated mechanisms of intervention and protection based on antioxidants. The term "antioxidant" is defined as any substance that can interact with oxidants, regulating the biological redox-dependent pathways and/or oxidative damage[88]. According to their origin, antioxidants can be classified as either endogenous or exogenous, with the latter encompassing antioxidants obtained from the diet (e.g.,

[4] Chen, Ze, et al. *Role of oxidative stress in the pathogenesis of nonalcoholic fatty liver disease.* Free Radical Biology and Medicine 152, **2020,** 116-141. https://doi.org/10.1016/j.freeradbiomed.2020.02.025.

ascorbic acid, tocopherols, carotenoids, phenolic acids)[89,90] or synthetic ones (e.g., coenzyme Q analogues, GSH precursors [91], nitrones/nitroxides), used as supplements[92]. Synthetic antioxidants have become a popular choice for consumers in past decades, largely due to their low costs and ease of retrieval, frequently employed as alternatives to natural antioxidants thanks to their higher stability[93]. Despite that, synthetic antioxidants' negative effect on human health have been largely discussed[93]. As a result, there is growing interest in natural antioxidant molecules, especially those obtained from plants [47,94–97]. In this scenario, the therapeutic potential of antioxidants derived from microalgae offers promising ways of intervention[98,99].

1.6 *Aim of the thesis*

The aim of the present PhD thesis was the use of antioxidant molecules, isolated from microalgae, for cosmeceutical/nutraceutical applications. In particular, the ability of selected molecules to interfere with lipid metabolism was assessed. Two experimental systems were considered: the murine pre-adipocytes 3T3-L1 cells and the murine hepatic AML12 cells. The selected microalgae were: (i) the red marine mesophile microalga *Porphyridium cruentum*; (ii) the red thermo-acidophilic microalga *Galdieria phlegrea* and (iii) the green microalga *Pseudococcomyxa simplex.* The cascade extractions and the biochemical characterization of the extracted molecules were designed only in the case of *P. simplex*, whereas *P. cruentum* and *G. phlegrea* biorefinery approach were previously reported[11,12].

More in detail, the research activities were:

1. Evaluation of the antiadipogenic activity of Phycoerythrin and sulfated exopolysaccharides from *Porphyridium cruentum*.
Taking advantage of the already established antioxidant and anti-inflammatory activities of PE and s-EPSs[100], their possible anti-adipogenic activity was studied. In particular, the analyses were done to study any inhibitory activity on pre-adipocyte (3T3-L1) maturation, as well as to study a possible lipid metabolism alteration in mature adipocytes and hepatocytes (AML12) (**Chapter 2**).

2. Evaluation of anti-adipogenic activity of Carotenoids extracted from *Galdieria phlegrea*.
Ethanolic carotenoids extracts were obtained from the residual biomass and from the fresh biomass, in order to compare them as anti-adipogenic molecules. In particular, pre-adipocyte maturation was studied in the presence of carotenoids and their biological activity was measured also on mature adipocytes; finally, their anti-aging activity was tested *in vitro* (**Chapter 3**).

3. Set-up of a biorefinery using *Pseudococcomyxa simplex* biomass and biochemical characterization of the extracted molecules.
Carotenoids and lipids were isolated from the biomass of *P. simplex* in a cascade approach. The extracted molecules were chemically characterized. The obtained carotenoids were tested *in vitro* for their anti-aging properties. Then, the biocompatibility and the antioxidant

activity were done on a cell-based model (**Chapter 4**). Finally, carotenoids anti-adipogenic activity was analyzed on a well-known cell-based model (**Chapter 5**).

4. Preliminary optimization of downstream process.

To lower the costs related to microalgae cultivation, an alternative to centrifugation was proposed. In particular, different flocculating agents and experimental parameters were tested. Flocculation effects were tested also from a biological point of view, i.e., on extraction quality and yield. Thus, carotenoids were extracted from the flocculated biomass and compared to the ones obtained from the centrifuged wet biomass. To check the quality of the extracts, their antioxidant activity was evaluated *in vitro* (**Chapter 6**).

1.7 *References*

1. Benemann, J. R. Hydrogen production by microalgae. *J. Appl. Phycol.* **12**, 291–300 (2000).
2. Novoveská, L. *et al.* Overview and Challenges of Large-Scale Cultivation of Photosynthetic Microalgae and Cyanobacteria. *Mar. Drugs* **21**, 1–23 (2023).
3. Jacob-Lopes, *et al. Pigments from Microalgae Handbook*. *Pigments from Microalgae Handbook* (2020).
4. Maghzian, A., *et al.* How to effectively produce value-added products from microalgae? *Renew. Energy* **204**, 262–276 (2023).
5. Devi, A. *et al.* Microalgae: A green eco-friendly agents for bioremediation of tannery wastewater with simultaneous production of value-added products. *Chemosphere* **336**, 139192 (2023).
6. Nagappan, S. *et al.* Potential of microalgae as a sustainable feed ingredient for aquaculture. *J. Biotechnol.* **341**, 1–20 (2021).
7. You, N. *et al.* Review and Opinions on the Research, Development and Application of Microalgae Culture Technologies for Resource Recovery from Wastewater. *Water* vol. 15 (2023).
8. Ummalyma, S. B. *et al.* Sustainable microalgal biomass production in food industry wastewater for low-cost biorefinery products: a review. *Phytochem. Rev.* **22**, 969–991 (2023).
9. Uma, V. S. *et al.* Valorisation of algal biomass to value-added metabolites: emerging trends and opportunities. *Phytochem. Rev.* **22**, 1015–1040 (2023).
10. Imbimbo, P. *et al.* Unveiling the potential of *Pseudococcomyxa simplex*: a stepwise extraction for cosmetic applications. *Appl. Microbiol. Biotechnol.* (2024).
11. Imbimbo, P. *et al.* Green Compressed Fluid Technologies To Extract Antioxidants and Lipids from *Galdieria phlegrea* in a Biorefinery Approach. *ACS Sustain. Chem. Eng.* **8**, 2939–2947 (2020).
12. Liberti, D. *et al.* Inside out *Porphyridium cruentum*: Beyond the Conventional Biorefinery Concept. *ACS Sustain. Chem. Eng.* (2022).
13. Di Caprio, F., *et al.* Microalgae Biorefinery: Optimization of Starch Recovery for Bioplastic Production. *ACS Sustain. Chem. Eng.* **11**, 16509–16520 (2023).
14. Singh, A. K. *et al.* Microalgal biorefinery as a sustainable and cost-effective platform for co-production of high-value-added products/metabolites: An insight into emerging trends, challenges, and opportunities. *Biocatal. Agric. Biotechnol.* **58**, 103192 (2024).
15. Bayu, A., *et al.* Biological and technical aspects on valorization of red microalgae genera *Porphyridium*. *Biomass Convers. Biorefinery* **13**, 12395–12411 (2023).
16. Razzak, S. A. Comprehensive overview of microalgae-derived carotenoids and their applications in diverse industries. *Algal Res.* **78**, 103422 (2024).
17. Arad, S. *et al.* Natural pigments from red microalgae for use in foods and cosmetics. *Trends in Food Science and Technology* vol. 3 92–97 (1992).
18. Risjani, Y., *et al.* Exopolysaccharide from *Porphyridium cruentum* (*purpureum*) is Not Toxic and Stimulates Immune Response against Vibriosis: The Assessment Using Zebrafish and White Shrimp Litopenaeus vannamei. *Marine Drugs* vol. 19 (2021).
19. Sánchez-Saavedra, M. del P. *et al.* Effects of nitrogen source and irradiance on *Porphyridium cruentum*. *J. Appl. Phycol.* **30**, 783–792 (2018).

20. Pekárková, B., *et al.* Cell morphology and growth characteristics of *Porphyridium aerugineum* (Rhodophyta). *Plant Syst. Evol.* **164**, 263–272 (1989).
21. Gloaguen, V. *et al.* The extracellular polysaccharide of *Porphyridium sp*.: An NMR study of lithium-resistant oligosaccharidic fragments. *Carbohydr. Res.* **339**, 97–103 (2004).
22. Albertano, P., *et al.* The taxonomic position of *Cyanidium*, *Cyanidioschyzon* and *Galdieria*: an update. *Hydrobiologia* **433**, 137–143 (2000).
23. Carfagna, S. *et al.* Dietary supplementation with the microalga *Galdieria sulphuraria* (rhodophyta) reduces prolonged exercise-induced oxidative stress in rat tissues. *Oxid. Med. Cell. Longev.* **2015**, (2015).
24. Ciniglia, C., *et al.* Hidden biodiversity of the extremophilic Cyanidiales red algae. *Mol. Ecol.* **13**, 1827–1838 (2004).
25. Carfagna, S. *et al.* Different characteristics of C-phycocyanin (C-PC) in two strains of the extremophilic *Galdieria phlegrea*. *Algal Res.* **31**, 406–412 (2018).
26. Round, F. E. The taxonomy of the chlorophyta. II. *Br. Phycol. J.* **6**, 235–264 (1971).
27. Yusuff, A. S. Extraction, optimization, and characterization of oil from green microalgae Chlorophyta species. *Energy Sources, Part A Recover. Util. Environ. Eff.* **45**, 7473–7484 (2019).
28. Maltsev, Y. I., *et al.* Analysis of a New Strain of *Pseudomuriella engadinensis* (Sphaeropleales, Chlorophyta) for Possible Use in Biotechnology. *Russ. J. Plant Physiol.* **66**, 609–617 (2019).
29. Broady, P. A. The morphology, distribution and ecology of *Pseudococcomyxa simplex* (Mainx) Fott (Chlorophyta, Chlorellaceae), a widespread terrestrial Antarctic alga. *Polar Biol.* **7**, 25–30 (1987).
30. Whitton, B. A. & Potts, M. Introduction to the Cyanobacteria BT - Ecology of Cyanobacteria II: Their Diversity in Space and Time. in (ed. Whitton, B. A.) 1–13 (Springer Netherlands, Dordrecht, 2012).
31. Allaguvatova, R. Z., *et al.* Study of Biodiversity of Algae and Cyanobacteria of Mutnovsky and Gorely Volcanoes Soils (Kamchatka Peninsula) Using a Polyphasic Approach. (2022).
32. Castenholz, R. W. General Characteristics of the Cyanobacteria. in *Bergey's Manual of Systematics of Archaea and Bacteria* 1–23 (2015).
33. Komárek, J., *et al.* Phylogeny and taxonomy of synechococcus–like cyanobacteria. *Fottea* **20**, 171–191 (2020).
34. Hindák, F., *et al.* Growth characteristics of selected thermophilic strains of cyanobacteria using crossed gradients of temperature and light. **68**, 830–837 (2013).
35. D'Elia, L. *et al.* Switchable Solvent Selective Extraction of Hydrophobic Antioxidants from Synechococcus bigranulatus. *ACS Sustain. Chem. Eng.* **9**, 13798–13806 (2021).
36. Martins, R., *et al.* Food Wastes and Microalgae as Sources of Bioactive Compounds and Pigments in a Modern Biorefinery: A Review. *Antioxidants* vol. 12 328 (2023).
37. Narayanan, M. Promising biorefinery products from marine macro and microalgal biomass: A review. *Renew. Sustain. Energy Rev.* **190**, 114081 (2024).
38. Anusree, M. K. *et al.* Marine microalgae: an emerging source of pharmaceuticals and bioactive compounds. *New Horizons Nat. Compd. Res.* 251–265 (2023).

39. Levasseur, W., *et al.* A review of high value-added molecules production by microalgae in light of the classification. *Biotechnol. Adv.* **41**, 107545 (2020).
40. Kiki, M. J. Biopigments of Microbial Origin and Their Application in the Cosmetic Industry. *Cosmetics* vol. 10 (2023).
41. Barreto, J. V, *et al.* Microbial Pigments: Major Groups and Industrial Applications. *Microorganisms* vol. 11 (2023).
42. Adir, N., *et al.* The amazing phycobilisome. *Biochim. Biophys. Acta - Bioenerg.* **1861**, 148047 (2020).
43. Li, X., *et al.* The Unique Light-Harvesting System of the Algal Phycobilisome: Structure, Assembly Components, and Functions. *International Journal of Molecular Sciences* vol. 24 (2023).
44. Dagnino-Leone, J. *et al.* Phycobiliproteins: Structural aspects, functional characteristics, and biotechnological perspectives. *Comput. Struct. Biotechnol. J.* **20**, 1506–1527 (2022).
45. Ashaolu, T. J. The powerful phycobiliproteins-phycocyanin and phycoerythrin: Pleiotropic applications and biofunctional uses. *Algal Res.* **82**, 103636 (2024).
46. Ji, L. *et al.* Phycobiliproteins from algae: Current updates in sustainable production and applications in food and health. *Food Res. Int.* **167**, 112737 (2023).
47. Nieto, G. *et al.* Applications of Plant Bioactive Compounds as Replacers of Synthetic Additives in the Food Industry. *Foods* vol. 13 (2024).
48. Chini Zittelli, G., *et al.* Valuable pigments from microalgae: phycobiliproteins, primary carotenoids, and fucoxanthin. *Photochem. Photobiol. Sci.* **22**, 1733–1789 (2023).
49. Imchen, T. *et al.* Marine algae colorants: Antioxidant, anti-diabetic properties and applications in food industry. *Algal Res.* **69**, 102898 (2023).
50. Glazer, A. N., *et al.* Phycoerythrins as chemotaxonomic markers in red algae: A survey. *Biochem. Syst. Ecol.* **10**, 203–215 (1982).
51. Ma, J. *et al.* Structural basis of energy transfer in *Porphyridium purpureum* phycobilisome. *Nature* **579**, 146–151 (2020).
52. Stebegg, R., *et al.* Heterotrophy among Cyanobacteria. *ACS Omega* **8**, 33098–33114 (2023).
53. Coulombier, N., *et al.* Antioxidant Compounds from Microalgae: A Review. *Marine Drugs* vol. 19 (2021).
54. George, R. *et al.* Phycoerythrin as a potential natural colourant: A mini review. *Int. J. Food Sci. Technol.* **58**, 513–519 (2023).
55. Generalić Mekinić, I., *et al.* Algal Carotenoids: Chemistry, Sources, and Application. *Foods* vol. 12 (2023).
56. Cervantes-Paz, B., *et al.* Absorption of Carotenoids and Mechanisms Involved in Their Health-Related Properties in Carotenoids in Nature: Biosynthesis, Regulation, and Function. *Carotenoids in nature: biosynthesis, regulation, and function* vol. 79 (2016).
57. Gong, M. *et al.* Carotenoids from microalgae: A review of recent developments. *Biotechnology Advances* vol. 34 1396–1412 (2016).
58. Hwang, S. H., *et al.* Chemical Transformation of Astaxanthin from *Haematococcus pluvialis* Improves Its Antioxidative and Anti-inflammatory Activities. *ACS Omega* **5**, 19120–19130 (2020).
59. Choudhary, B., *et al.* Edible Seaweeds: A Potential Novel Source of Bioactive Metabolites and Nutraceuticals With Human Health Benefits. *Front. Mar. Sci.* **8**, (2021).
60. Ojulari, O. V, *et al.* Therapeutic Effect of Seaweed Derived Xanthophyl

Carotenoid on Obesity Management; Overview of the Last Decade. *International Journal of Molecular Sciences* vol. 21 (2020).
61. Sathasivam, R. *et al.* A review of the biological activities of microalgal carotenoids and their potential use in healthcare and cosmetic industries. *Marine Drugs* vol. 16 (2018).
62. Di Salvo, E. *et al.* Natural Pigments Production and Their Application in Food, Health and Other Industries. *Nutrients* **15**, (2023).
63. Kim, H. J. *et al.* Anti-obesity activity of anthocyanin and carotenoid extracts from color-fleshed sweet potatoes. *J. Food Biochem.* **44**, (2020).
64. Toucheteau, C. *et al.* Role of some structural features in EPS from microalgae stimulating collagen production by human dermal fibroblasts. *Bioengineered* **14**, 2254027 (2023).
65. Li, Y. *et al.* Production, isolation and bioactive estimation of extracellular polysaccharides of green microalga *Neochloris oleoabundans*. *Algal Res.* **48**, 101883 (2020).
66. He, P., *et al.* Structure and bioactivity of a polysaccharide containing uronic acid from *Polyporus umbellatus sclerotia*. *Carbohydr. Polym.* **152**, 222–230 (2016).
67. De Jesus Raposo, M. F., *et al.* Bioactivity and applications of sulphated polysaccharides from marine microalgae. *Marine Drugs* vol. 11 233–252 (2013).
68. Fan, J., *et al.* Potential therapeutic target for polysaccharide inhibition of colon cancer progression. *Front. Med.* **10**, (2024).
69. Zhuang, D. *et al.* Application progress of bioactive compounds in microalgae on pharmaceutical and cosmetics. *Chemosphere* **291**, 132932 (2022).
70. Bernal, P. *et al.* Promising biotechnological applications of antibiofilm exopolysaccharides. *Microb. Biotechnol.* **5**, 670–673 (2012).
71. Klran, T. R., *et al.* Oxidative stress and antioxidants in health and disease. *J. Lab. Med.* **47**, 1–11 (2023).
72. Birben, E., *et al.* Oxidative Stress and Antioxidant Defense Mechanism in. *WAO J.* **22**, 9–19 (2012).
73. Čolak, E. *et al.* The role of oxidative stress in the development of obesity and obesity-related metabolic disorders. *J. Med. Biochem.* **40**, 1–9 (2021).
74. Clemente-Suárez, V. J., *et al.* Global Impacts of Western Diet and Its Effects on Metabolism and Health: A Narrative Review. *Nutrients* vol. 15 (2023).
75. Reddy, V. P. Oxidative Stress in Health and Disease. *Biomedicines* vol. 11 (2023).
76. Jomova, K. *et al.* Reactive oxygen species, toxicity, oxidative stress, and antioxidants: chronic diseases and aging. *Arch. Toxicol.* **97**, 2499–2574 (2023).
77. Hu, B. *et al.* Antioxidant Hydrogels: Antioxidant Mechanisms, Design Strategies, and Applications in the Treatment of Oxidative Stress-Related Diseases. *Adv. Healthc. Mater.* **13**, 2303817 (2024).
78. Corvera, S. Cellular Heterogeneity in Adipose Tissues. *Annu. Rev. Physiol.* **83**, 257–278 (2021).
79. Masenga, S. K., *et al.* Mechanisms of Oxidative Stress in Metabolic Syndrome. *International Journal of Molecular Sciences* vol. 24 (2023).
80. Allen, R. G. & Tresini, M. Oxidative stress and gene regulation. *Free Radic. Biol. Med.* **28**, 463–499 (2000).
81. Lee, J., *et al.* Adipose fatty acid oxidation is required for thermogenesis and potentiates oxidative stress-induced inflammation. *Cell Rep.* **10**, 266–279

(2015).
82. Houstis, N., *et al.* Reactive oxygen species have a causal role in multiple forms of insulin resistance. *Nature* **440**, 944–948 (2006).
83. Rives, C. *et al.* Oxidative Stress in NAFLD: Role of Nutrients and Food Contaminants. *Biomolecules* vol. 10 (2020).
84. Rani, V., *et al.* Oxidative stress and metabolic disorders: Pathogenesis and therapeutic strategies. *Life Sci.* **148**, 183–193 (2016).
85. Grosso, G. *et al.* Anti-Inflammatory Nutrients and Obesity-Associated Metabolic-Inflammation: State of the Art and Future Direction. *Nutrients* vol. 14 (2022).
86. Liu, L. *et al.* Effect of chlorogenic acid on lipid metabolism in 3T3-L1 cells induced by oxidative stress. *Food Biosci.* **51**, 102330 (2023).
87. Rohm, T. V, *et al.* Inflammation in obesity, diabetes, and related disorders. *Immunity* **55**, 31–55 (2022).
88. Murphy, M. P. *et al.* Guidelines for measuring reactive oxygen species and oxidative damage in cells and in vivo. *Nat. Metab.* **4**, 651–662 (2022).
89. Padayatty, S. J. *et al.* Vitamin C: the known and the unknown and Goldilocks. *Oral Dis.* **22**, 463–493 (2016).
90. Han, R.-M., *et al.* Reaction Dynamics of Flavonoids and Carotenoids as Antioxidants. *Molecules* vol. 17 2140–2160 (2012).
91. Giustarini, D., *et al.* How to Increase Cellular Glutathione. *Antioxidants* vol. 12 (2023).
92. Halliwell, B. Understanding mechanisms of antioxidant action in health and disease. *Nat. Rev. Mol. Cell Biol.* **25**, 13–33 (2024).
93. Hassanpour, S. H. *et al.* Review of the antioxidant potential of flavonoids as a subgroup of polyphenols and partial substitute for synthetic antioxidants. *Avicenna J. phytomedicine* **13**, 354–376 (2023).
94. Sahoo, D. K. *et al.* Oxidative stress, hormones, and effects of natural antioxidants on intestinal inflammation in inflammatory bowel disease. *Front. Endocrinol. (Lausanne).* **14**, (2023).
95. Marino, P. *et al.* Potential Role of Natural Antioxidant Products in Oncological Diseases. *Antioxidants* vol. 12 (2023).
96. Rahaman, M. S. *et al.* Environmental arsenic exposure and its contribution to human diseases, toxicity mechanism and management. *Environ. Pollut.* **289**, 117940 (2021).
97. Ji, X. *et al.* Synthetic Antioxidants as Contaminants of Emerging Concern in Indoor Environments: Knowns and Unknowns. *Environ. Sci. Technol.* **57**, 21550–21557 (2023).
98. Goshtasbi, H. *et al.* Harnessing microalgae as sustainable cellular factories for biopharmaceutical production. *Algal Res.* **74**, 103237 (2023).
99. Mapelli-Brahm, P. *et al.* Microalgae, Seaweeds and Aquatic Bacteria, Archaea, and Yeasts: Sources of Carotenoids with Potential Antioxidant and Anti-Inflammatory Health-Promoting Actions in the Sustainability Era. *Marine Drugs* vol. 21 (2023).
100. Liberti, D. *et al.* Shedding Light on the Hidden Benefit of *Porphyridium cruentum* Culture. 1–12 (2023).

CHAPTER 02

Advancing knowledge on *Porphyridium cruentum:*
a new frontier in lipid accumulation management

CHAPTER 03

Unlocking the anti-adipogenic potential of carotenoids from *Galdieria phlegrea*

CHAPTER 04

Unveiling the potential of *Pseudococcomyxa simplex*:
a stepwise extraction for cosmetic applications

Applied Microbiology and Biotechnology

(2024) 108:390
https://doi.org/10.1007/s00253-024-13229-9

UNVEILING THE POTENTIAL OF *PSEUDOCOCCOMYXA SIMPLEX*: A STEPWISE EXTRACTION FOR COSMETIC APPLICATIONS

Paola Imbimbo[1]; **Enrica Giustino[1]**; Alfonso Ferrara[1]; Gerardo Alvarez-Rivera[2]; Hassan Annaz[3]; Elena Ibanez[2]; Maria Chiara Di Meo[4]; Armando Zarrelli[1]; Daria Maria Monti[1*]

[1] Department of Chemical Sciences, University of Naples Federico II, Via Cinthia 4, 80126 Naples, Italy
[2] Laboratory of Foodomics, Institute of Food Science Research, CIAL, CSIC, Nicolas Cabrera 9, 28049 Madrid, Spain
[3] College of Agriculture and Environmental Science, AgroBioSciences Program, University Mohammed VI Polytechnic, Ben Guerir, Morocco
[4] Department of Sciences and Technologies (DST), University of Sannio, 82100 Benevento, BN, Italy

Abstract

Microalgae are gaining attention as they are considered green fabrics able to synthesize many bioactive metabolites, with unique biological activities. However, their use at an industrial scale is still a challenge because of the high costs related to upstream and downstream processes. Here, a biorefinery approach was proposed, starting from the biomass of the green microalga *Pseudococcomyxa simplex* for the extraction of two classes of molecules with a potential use in the cosmetic industry. Carotenoids were extracted first by an ultrasound-assisted extraction, and then, from the residual biomass, lipids were obtained by a conventional extraction. The chemical characterization of the ethanol extract indicated lutein, a biosynthetic derivative of α-carotene, as the most abundant carotenoid. The extract was found to be fully biocompatible on a cell-based model, active as antioxidant and with an in vitro anti-aging property. In particular, the lutein-enriched fraction was able to activate Nrf2 pathway, which plays a key role also in aging process. Finally, lipids were isolated from the residual biomass and the isolated fatty acids fraction was composed by palmitic and stearic acids. These molecules, fully biocompatible, can find application as emulsifiers and softener agents in cosmetic formulations. Thus, an untapped microalgal species can represent a sustainable source for cosmeceutical formulations.

4.1 Introduction

Cosmetic is one of the most remunerative industrial sectors in the world, constantly growing since 2004. It has been estimated that, in 2028, the revenues of the global cosmetic market will be nearly 129 billion USD. In particular, the beauty market is dominated by skincare, which is expected to reach 221.38 billion UDS by 2030 with a CAGR of 4.79% (https://straitsresearch.com/report/facial-skincare-products-market, accessed on 14 March 2024). Nowadays, consumers prefer to use natural cosmetics that are produced from natural sources that can be considered safe for humans and environment. This trend inversion is due not only to the growing environmental consciousness of the consumers, but also to their awareness of health issues that can occur by using synthetic compounds, such as hyperactivity, allergic reactions, or other side effects[1]. Thus, different cosmetic companies are using biotechnology to ensure quality, efficacy, and safety of the natural products[2]. Among natural sources, microalgae have gained attention as they are considered green fabrics able to synthesize a plethora of bioactive metabolites, endowed with unique biological activities[3]. Moreover, they are perceived as vegan, natural and healthy by consumers. To date, only a few strains have been exploited for cosmetic purposes, such as *Spirulina*, *Dunaliella*, *Chlorella,* and *Haematococcus*[4]. Despite the considerable potential of microalgae, some issues still limit their full industrialization, such as high upstream and downstream costs[5]. To make the use of microalgae sustainable and feasible, the biorefinery approach has been proposed as the technology is able to implement the circular economy and lowers the overall process costs[6]. Carotenoids are pigments which can be used in different fields, such as the food and pharmaceutical industry, and recently, due to the potent antioxidant activity, they have attracted interest to be used as active ingredients in cosmetic formulations. Currently, the market is dominated by astaxanthin, β-carotene, zeaxanthin, lutein, and lycopene[7]. Lipids, and more in general oils, are one of the major components in cosmetic cream formulations[8]. Based on their nature, they can be used for different purposes, such as softener agents, emulsifiers, detergents and skin lighteners[9]. Fatty acids are used in cosmetics as emollients to improve the skin-hydration, and as emulsifiers, since they can act as thickening agents. It has been reported that the ideal length of the carbon chain for fatty acids-based emulsion is 16-18, which correspond to palmitic and stearic acid[10]. Fatty acids are also physiological skin components that ensure the maintenance of skin barrier functions[11]. In this paper we proposed a biorefinery approach starting from the biomass of the green microalga

Pseudococcomyxa simplex for the extraction of two classes of molecules with a potential use in cosmetic industry. Carotenoids were extracted as the first class of molecules by an ultrasound assisted extraction coupled to maceration, and then, from the residual biomass, lipids were obtained by a conventional extraction. Finally, a chemical and biological characterization of both classes of molecules have been carried out to investigate a possible use of these molecules in cosmetic field.

4.2 Materials and Methods

4.2.1 Reagents

All the reagents, unless differently specified, were purchased from Sigma-Aldrich (Milan, Italy).

4.2.2 Microalgae strain and cultivation

Pseudococcomyxa simplex (ACUF 127) was provided by the Algal Collection of the University Federico II (ACUF, www.acuf.net). The cultivation was carried out in bubble column photobioreactors in Bold Basal Medium (BBM) at 24 ± 2 °C with a constant light intensity of 100 PARs [($\mu mol_{photons}/m^2$)/s]. The culture was mixed by bubbling air through a sintered glass tube placed at the bottom of each reactor. Algal growth was monitored by measuring the absorbance at 730 nm.

The dry weight determination was carried out *via* conversion between the Optical Density (O.D.) and the biomass dry weight at the end of the exponential growth phase. The conversion factor was: 1 O.D. corresponded to 0.22 mg dry weight. The biomass concentration achieved at the end of the exponential growth phase was 0.7 $g_{D.W.}$/L.

4.2.3 Pigments extraction and characterization

Pigments were extracted using ethanol as solvent, as previously reported[12]. Briefly, 200 mg of dry weight (D.W.) of alga were suspended in 4 mL of pure ethanol and disrupted by ultrasonication (40% amplitude, 4 min on ice, Bandelin SONOPULS HD 3200, tip MS73). The volume was adjusted to 20 mL and the mixture was shaken for 24 h at 250 rpm at 4 °C in the dark. Pigments were recovered in the supernatants by centrifugation at 5000 *g* for 10 min and then ethanol was removed under N_2 stream. The extraction yield was determined gravimetrically.

Carotenoids and pigments identification was performed by HPLC-DAD-APCI-QTOF-MS/MS. The analysis of the extracts was carried out in an Agilent 1290 UHPLC system (Ultrahigh Performance Liquid Chromatography) equipped with a diode-array detector (DAD), coupled to an Agilent 6540 quadrupole-time-of-flight mass spectrometer (q-TOF MS) equipped with an atmospheric pressure chemical ionization (APCI) source. A Thermo Fisher Scientific Accucore C30 column (2.6 µm, 4.6 x 50 mm) was used at 30 ºC. Separation was achieved using a 12 min gradient program from 100% mobile phase A (90% Methanol, 7% MTBE, 3% water) and 0% mobile phase B (90% MTBE, 10% Methanol) to 0% mobile phase A and 100% mobile phase B, and kept constant for 1.5 min before returning to the initial conditions within 1.5 min. The total run time was 15 min at a flow rate of 0.8 mL/min. The mass spectrometer was operated in positive ionization mode (APCI+), with gas temperature at 300 ºC; drying gas at 8 L/min; vaporizer temperature at 350 ºC; nebulizer pressure at 40 Psi; capillary voltage at 3500 V; corona+: 4 µA; fragmentor voltage at 110 V and skimmer voltage at 45 V. The MS and auto MS/MS modes were set to acquire *m/z* values ranging between 25-1500, at a scan rate of 10 spectra per second. Auto MS/MS mode was operated at two collision-induced dissociation energies: 20 and 40 eV and selecting 4 precursor ions per cycle at a threshold of 200 counts.

4.2.4 Lipids extraction and characterization

Lipids were recovered by using the original Bligh and Dyer protocol[13]. Extractions were carried out on 300 mg of both freeze-dried biomass and residual freeze-dried biomass (i.e., after pigment extraction) using chloroform, methanol, and water in a ratio 2:2:1 (v/v/v) for 1 h at room temperature. At the end of the extraction, the hydrophobic phase was recovered by centrifugation and the extract was dried under N_2 stream. The lipid extract was then fractionated in three different lipid classes (i.e. neutral lipids, fatty acids, and phospholipids) by performing a solid phase extraction (SPE) as previously described[14]. The recovered fatty acids were first derivatized by transforming them into the corresponding methyl esters and then identified and quantified by GC−MS analysis[15].

4.2.5 Biological characterization

4.2.5.1 In vitro anti-aging assays

The *in vitro* anti-aging activity was evaluated by anti-tyrosinase and anti-elastase assays, as described by Mahdi et al. [16]. Kojic acid was used as commercial inhibitor. Values are reported as Inhibitory Concentration (IC_{50}), which represents the concentration of molecule able to inhibit the 50% of the enzyme activity and expressed as mg/mL.

4.2.5.2 Cell culture and biocompatibility of ethanol extract

Immortalized human keratinocytes (HaCaT) were from Innoprot (Biscay, Spain) and immortalized murine fibroblasts (BALB/c-3T3) were from ATCC (VA, USA). Cells were cultured in Dulbecco's modified Eagle's medium (DMEM), supplemented with 10% foetal bovine serum (HyClone), 2 mM *L*-glutamine, and antibiotics, under a 5% CO_2 humidified atmosphere at 37 °C. The biocompatibility of either ethanol extract or FAs was tested. HaCaT cells were seeded in 96-well plate at a density of 2.5×10^3 cells per well, whereas BALB/c-3T3 at a density of 3×10^3 cells per well. HaCaT cells were incubated with increasing concentration (from 0.5 to 100 µg/mL) of both ethanol extract and FAs for 24 and 48 h, whereas BALB/c-3T3 only with ethanol extract. At the end of the incubation, cell viability was assessed by the MTT assay, as previously reported [3]. Cell viability was expressed as the percentage of viable cells in the presence of the extract compared to the controls, represented by untreated cells and cells supplemented with identical volumes of DMSO.

4.2.5.3 Sodium arsenite stress induction and biochemical analyses

HaCaT cells were pre-treated with 90 µg/mL of ethanol extract for 2 h. Then, cells were stressed with 300 µM sodium arsenite ($NaAsO_2$) for 1 h as previously described[17]. Immediately after $NaAsO_2$ stress induction, intracellular ROS levels were determined by DCFDA assay, as previously reported[12], whereas intracellular glutathione (GSH) levels were measured by performing 5,5′-dithiobis-(2-nitrobenzoic acid) (DTNB) assay, as reported by[18].

4.2.5.4 Western blot analysis

90 min after stress induction, HaCaT cells were detached by trypsin and lysate in lysis buffer (0.1 M Tris HCl pH 7.4, 0.3 M NaCl and

0.5% NP40), supplemented with protease and phosphatase inhibitors. After 30 min incubation on ice, lysates were centrifuged at 14,000 *g* for 30 min at 4 °C. Supernatants were collected and protein concentration was determined by the Bradford assay. 80 µg of proteins were separated by SDS-PAGE and analyzed by Western blotting using specific antibodies: anti-phospho-p38, anti-phospho-MAPKAPK-2 from Cell Signalling (Danvers, MA, USA); anti-Nrf2 from Bioss Antibodies (Woburn, MA, USA); anti-HO-1 from Bethyl laboratories INC. (Montgomery, TX, USA), anti-B-23 and anti-β-actin. Band detection and densitometric analyses were performed using a ChemiDoc (Biorad, Hercules, CA, USA), according to the manufacturer's instruction.

4.2.6 Statistical analyses

Samples were tested in three independent analyses, each carried out in triplicate. Results are presented as mean of results obtained after three independent experiments (mean ± SD) and compared by one-way ANOVA according to the Bonferroni's method (post hoc) using Graphpad Prism for Windows, version 6.01.

4.3 Results

4.3.1 Pigments extraction and characterization

The proposed biorefinery strategy consists in the extraction of two different classes of molecules, pigments and lipids, starting from *P. simplex* biomass. The order of the extraction was chosen by following two different criteria: the polarity of the target molecules, to ensure that the extraction solvent would not affect the quality of the residual biomass, and the market value of the molecules to be extracted. To obtain pigments, the biomass was harvested, freeze-dried, and treated as described in Materials and Methods section. At the end of the extraction, the mixture was centrifuged, the supernatant dried under N_2 stream, and cells debris were dried and stored for further extraction. The yield of the ethanol extract was 26 ± 3%. To investigate the composition of the ethanol extract, a profiling analysis using a chromatographic HPLC-DAD system hyphenated to a QTOF-MS analyser was used to obtain complementary structural information. UV-vis profiles and HRMS/MS data acquired in positive ionization mode (APCI+), were jointly analysed to increase structural elucidation capacity. The UHPLC-DAD chromatographic profile, shown in **Figure 1**, revealed the presence of 7 major carotenoids and 6 chlorophylls/chlorophyll derivatives, tentatively identified according to

their maximum absorption wavelength (λ_{max}), molecular ion (*m/z*), and main MS/MS fragments obtained by LC-APCI(+)-MS/MS analysis. Structural information of the annotated pigments is summarized in **Table S1**.

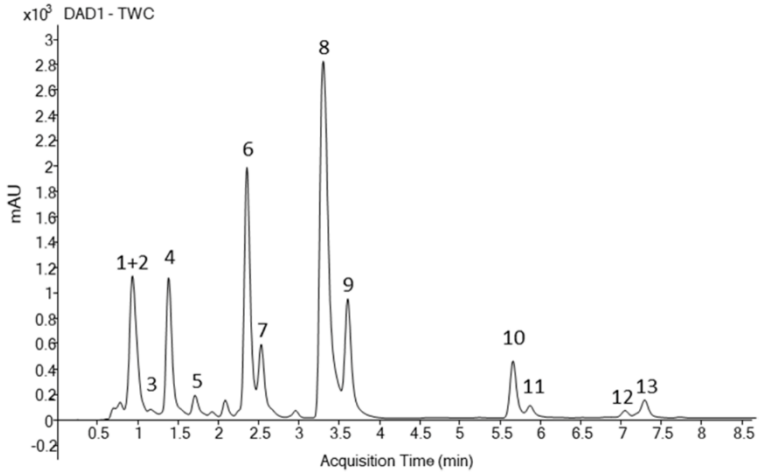

Figure 1. Representative LC-DAD chromatogram of pigments extracted from *P. simplex*. The TWC (total wavelength chromatogram), in the range 190 to 640 nm, is reported. Peaks identification is reported in **Table S1.**

From their calculated molecular formulae, chromatographic peaks 1 to 5 were annotated as compounds belonging to the xanthophylls (oxygen-containing carotenoids), whereas compounds 12 and 13 were classified as carotenes (hydrocarbon carotenoids). The nitrogen-containing pigments (peaks 6 to 11) were classified as chlorophylls and chlorophyll derivatives. Concentration values were estimated for the identified carotenoids following a semi-quantitative approach using β-carotene as reference standard (**Table 1**). Carotenoids 1-5, 12 and 13 showed three typical maximum absorption wavelengths ranging from 400 to 475 nm in their UV-vis spectra. Compounds 1 and 2 are two major carotenoids in *P. simplex*, that coelute under the same peak and show molecular ions at *m/z* 567.4196 ($C_{40}H_{54}O_2$) and *m/z* 601.4251 ($C_{40}H_{56}O_4$), respectively. Compound 3 with *m/z* 585.4302 ($C_{40}H_{56}O_3$) shares similar UV-vis absorption profile to compound 2. The first compound was annotated as a didehydro-carotenediol (e.g., diatoxanthin/monadoxanthin), whereas the second and the third were annotated as neoxanthin and the third one as mutatoxanthin-type, respectively; two biosynthetically related epoxycarotenoids and β-carotene derivatives. Peak 4 (*m/z* 569.4353, $C_{40}H_{56}O_2$) was unambiguously annotated as lutein, the most abundant

carotenoid identified in the ethanol extract of *P. simplex*, whereas peak 5 (*m/z* 551.4247, $C_{40}H_{54}O$) was tentatively identified as crocoxanthin. Both compounds 4 and 5 are biosynthetic derivatives of α-carotene. Additionally, two non-oxygenated carotenoid isomers (peaks 12 and 13) were identified as α- and β-carotene (*m/z* 537.4455, $C_{40}H_{56}$) and exhibited a higher retention time, in agreement with their higher lipophilicity. Chlorophylls and their derivatives exhibit two major absorption bands in the visible range, corresponding to the cyclic tetrapyrrole (porphyrin) skeleton, at around 420-460 nm and above 650 nm. Due to operational restrictions, only the first band could be measured in this work. In agreement with λ_{max} values in literature[19], compounds 6-7 and 8-9 were annotated as chlorophyll *b* and chlorophyll *a* isomers, corresponding to molecular ions at *m/z* 907.5218 ($C_{55}H_{70}MgN_4O_6$) and *m/z* 893.5426 ($C_{55}H_{72}MgN_4O_5$), respectively. Two additional chlorophyll derivatives, lacking the central Mg-atom, were annotated as pheophytin *a* isomer (compounds 10-11). These demetallized forms are less polar than the corresponding chlorophylls, showing higher retention time in reverse phase columns. The most abundant fragment ions in MS/MS spectra of chlorophyll and its derivatives usually correspond to the fragmentation with the loss of the phytyl chain $[M-278]^+$.

Table 1. Concentration values ($mg/g_{extract}$) of carotenoids identified in the ethanol extracts of *P. simplex.*

Peak Nº	Compound	Concentration ($mg/g_{extract}$)
1+2	Diatoxanthin/Monadoxanthin/ Neoxanthin	30 ± 1
3	Mutatoxanthin-type	2.5 ± 0.2
4	Lutein	30 ± 1
5	Crocoxanthin	6 ± 1
12	α-Carotene	1.6 ± 0.3
13	β-Carotene	4.6 ± 0.1

4.3.2 Lipid extraction and characterization

Lipids were extracted as the second class of molecules by an organic-solvent extraction. The extraction was carried out on the residual biomass (i.e., biomass recovered after pigment extraction) after a drying step. In a parallel experiment, lipids were extracted also from the raw biomass, as benchmark, to verify if the lipids extraction could be affected by the previous pigments extraction. As shown in **Figure 2a**, the yield of the hydrophobic fraction obtained from the residual biomass was 7 ± 1% (grey bar). This value represents a 3-fold decrease compared to the extraction yield of the raw biomass (black bar, 24 ± 3%), thus suggesting that lipids extraction was significantly affected from the pigments extraction. To understand the composition of the isolated lipids, a Solid Phase Extraction (SPE) was carried out to isolate the three lipid classes: neutral lipids, fatty acids, and phospholipids. As shown in **Figure 2b**, no significant alteration in neutral lipids was observed, whereas phospholipids significantly decreased (from 28% to 13%). However, it is interesting to notice a significant increase in relative fatty acid content in the extract obtained from the residual biomass (24 ± 1%) in comparison with the one obtained from the raw one (7 ± 2%).

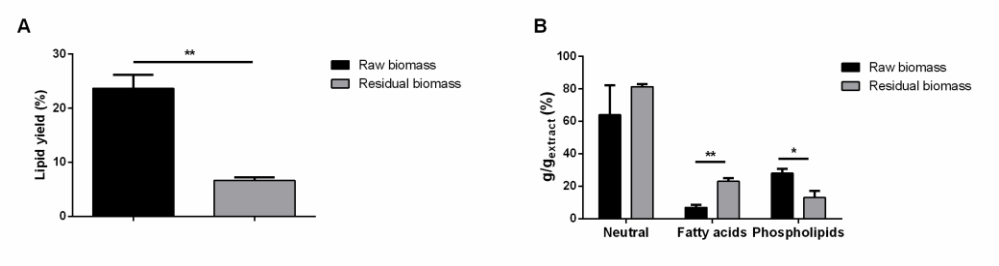

Figure 2. Lipids extraction and fractionation. a: Yields of lipids extracted from *P. simplex* and reported as % with respect to dry weight biomass; **b:** Yield of neutral lipids, fatty acids and phospholipids obtained upon SPE and reported as % with respect of dry weight extract. Black bars refer to raw biomass; gray bars refer to the residual biomass after pigments extraction. Results are reported as means ± SD of at least three independent experiments. * Indicates $p < 0.05$; ** indicates $p < 0.001$. The lines above the bars indicate the samples compared for statistical analysis.

Finally, a gas-chromatography analysis was performed on fatty acids fraction obtained from raw and residual biomass. The results, reported in **Table 2**, suggest that *P. simplex* biomass is enriched in saturated fatty acids (SFA), particularly palmitic and stearic acids. Notably, when fatty acids were recovered from the residual biomass,

the total SFA content increased, to such an extent that the extract appears to be composed only of palmitic and stearic acids.

Table 2. Fatty acids composition by Gas chromatography analysis on samples obtained from Raw and Residual biomass after pigment extraction. Saturated fatty acids (SFA), monounsaturated fatty acids (MUFA), and polyunsaturated fatty acids (PUFA) are reported as relative percentages.

	Fatty Acids	Raw biomass (%)	Residual biomass (%)
SFA			
14:0	Myristic	0.56 ± 0.08	0.4 ± 0.1
16:0	Palmitic	30.0 ± 0.8	62 ± 2
18:0	Stearic	15 ± 1	37 ± 2
24:0	Lignoceric	0.13 ± 0.04	0.02 ± 0.01
MUFA			
16:1n7t	*Trans* Palmitoleic	0.04 ± 0.01	0.09 ± 0.01
16:1n7	Palmitoleic	0.20 ± 0.02	0.05 ± 0.04
18:1n9t	*Trans* Oleic	0.13 ± 0.05	0.04 ± 0.01
18:1n9	Oleic	12 ± 1	0.30 ± 0.08
20:ln9	Eicosenoic	0.09 ± 0.01	0.11 ± 0.03
24:ln9	Nervonic	0.03 ± 0.03	0.010 ± 0.001
PUFA			
18:2n6t	*Trans* Linoleic	0.21 ± 0.08	0.06 ± 0.04
18:2n6	Linoleic	20 ± 1	0.24 ± 0.06
18:3n6	γ-Linoleic	21.0 ± 0.8	0.10 ± 0.03
18:3n3	α-Linoleic	0.06 ± 0.01	0.07 ± 0.04
20:2n6	Eicosadienoic	0.73 ± 0.17	0.03 ± 0.03
20:3n6	Dihomo γ-Linoleic	0.03 ± 0.01	0.20 ± 0.02
20:4n6	Arachidonic (AA)	0.06 ± 0.03	0.02 ± 0.01
20:5n3	Eicosapentaenoic (EPA)	0.02 ± 0.01	0.04 ± 0.02
22:4n6	Docosatetraenoic	0.06 ± 0.04	0.010 ± 0.001
22:5n6	Docosapentaenoic-n6	0.05 ± 0.04	0.01 ± 0.01
22:5n3	Docosapentaenoic-n3	N.D.	0.01 ± 0.01
22:6n3	Docosahexaenoic (DHA)	N.D.	0.010 ± 0.001

4.3.3 Biological characterization

4.3.3.1 In vitro anti-aging activity

Skin aging is a complex mechanism which depends on endogenous and exogenous factors, such as physiological aging and the continuous exposure to stress factors[20]. Thus, there is a direct link between aging and oxidative stress. Different enzymes are involved in skin aging, such as tyrosinase and elastase. The first is involved in the early steps of melanogenesis, whereas the second is involved in elastin degradation, a protein that plays a key role in the maintenance of the elasticity of the overall skin tone[21]. The inhibition of these two enzymes can be a way to slow down skin aging, so that a possible inhibitor effect of *P. simplex* carotenoids extract was evaluated *in vitro*. The carotenoids extract was able to inhibit both enzymes, but with a lower extent with respect to kojic acid, a commercial inhibitor. The amount of extract needed to inhibit 50% of the enzyme activity (IC_{50}) was calculated and reported in **Table 3**.

Table 3. Anti-tyrosinase and anti-elastase activity of *P. simplex* carotenoids extract. Values are reported as IC_{50} (mg/mL). Data shown are means ± S.D. of three independent experiments.

Assay	Kojic acid IC_{50} (mg/mL)	*P. simplex* extract IC_{50} (mg/mL)
Anti-tyrosinase	0.072 ± 0.003	0.48 ± 0.05
Anti-elastase	0.116 ± 0.005	0.55 ± 0.04

4.3.3.2 Effect of carotenoid extract on cell viability

The biocompatibility of the carotenoid extract was evaluated on immortalized human keratinocytes (HaCaT), and on immortalized murine fibroblasts (BALB/c-3T3) by dose- and time-dependent test. Cell viability was assessed by the tetrazolium salt colorimetric (MTT) assay, and cell viability was expressed as the percentage of viable cells in the presence of the extract compared to that of control samples. As shown in **Figure 3**, extract was fully biocompatible on both HaCaT (**Figure 3a**) and BALB/c-3T3 cells (**Figure 3b**), as no reduction in cell viability was observed at any of the experimental conditions tested.

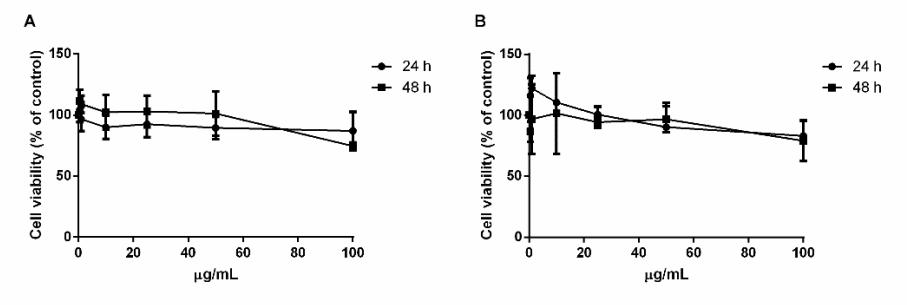

Figure 3. Cell viability of carotenoids extract on eukaryotic cells. HaCaT cells (**A**) and BALB/c-3T3 (**B**) incubated for 24 h (black circles) or 48 h (black squares) with increasing concentrations (0.5-100 µg/mL) of the extract. Cell viability is expressed as a percentage of viable cells in the presence of carotenoids with respect to control cells grown in the absence of the extract. Data shown are means ± S.D. of three independent experiments.

4.3.3.3 Protective effect of carotenoid extract against sodium arsenite-induced oxidative stress

It is known that carotenoids are excellent antioxidants. Thus, their protective effect was tested on a cell-based system, in which cells were stressed with sodium arsenite. Humans are constantly exposed to this contaminant *via* ingestion, inhalation, and also skin absorption[22], with severe health problems, such as cancer, cardiovascular disease, diabetes and skin diseases[23]. All these conditions are triggered by oxidative stress[24]. Thus, HaCaT cell were treated as described in Materials and Methods section, and immediately after $NaAsO_2$-stress induction, intracellular ROS levels were measured by using the fluorescent probe 2',7'-Dichlorofluorescin diacetate (H_2-DCFDA). As shown in **Figure 4a**, in the absence of oxidative stress, no alteration in ROS production was observed when cells were treated with the carotenoid extract, whereas a significant increase in intracellular ROS levels was observed when cells were stressed with $NaAsO_2$. Interestingly, when cells were pre-incubated with ethanol extract prior to stress exposure, an inhibition in ROS production was observed. The protective effect against oxidative stress was confirmed by analyzing the intracellular glutathione levels, a molecule which is normally oxidized during oxidative stress. The intracellular GSH levels were assessed using the 5,5'-Dithiobis-2-nitrobenzoic acid (DTNB) assay. As shown in **Figure 4b**, the exposure of the cells to $NaAsO_2$ resulted in a significant GSH depletion. Nevertheless, the pre-treatment with carotenoids resulted in the inhibition of GSH depletion, thus confirming

the protective effect of the extract against $NaAsO_2$-induced oxidative stress.

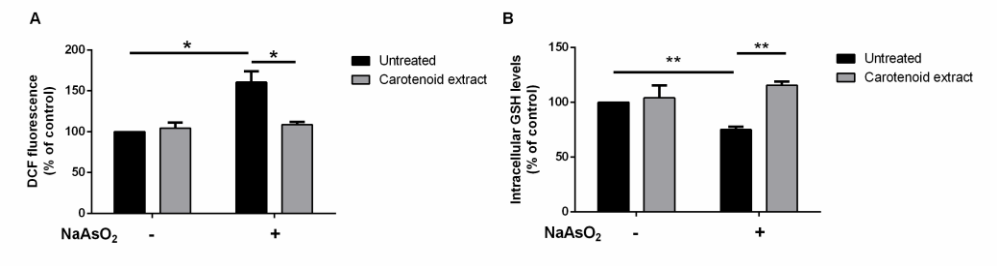

Figure 4. Effect of carotenoid extract on stressed HaCaT cells. Cells were incubated with 90 µg/mL of *P. simplex* carotenoid extract for 2 h in the absence (-) or in the presence (+) of oxidative stress induced by incubating cells with 300 µM $NaAsO_2$ for 1 h. **a**: intracellular ROS levels measured by DCFDA assay; **b**: intracellular GSH levels measured by DTNB assay. Values are expressed as fold increase with respect to untreated cells. Data shown are means ± S.D. of three independent experiments. * Indicates $p < 0.05$; ** indicates $p < 0.001$. Lines above the bars indicate the samples compared for statistical analysis.

4.3.3.4 Activation of mitogen-activated protein kinases (MAPK) mediated by carotenoid extract

Oxidative stress usually results in the activation of MAP (mitogen-activated protein) kinases pathway. Following oxidative stress insult, p38 is phosphorylated and this causes, in turn, the phosphorylation of its direct target, MAPKAPK-2. Thus, Western blotting analyses were performed to evaluate the protective effect of carotenoids extracted from *P. simplex* biomass. As shown in **Figure 5**, the carotenoid extract was able to inhibit the phosphorylation of both p38 and MAPKAPK-2. A complete inhibition in the phosphorylation of p38 and MAPKAPK-2 levels was observed when cells were pre-treated with the extract prior to be stressed.

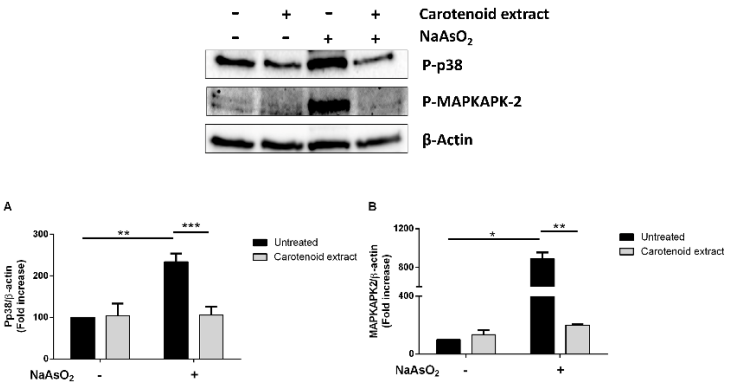

Figure 5. Effect of carotenoid extract on the activation of mitogen-activated protein kinase (MAPK) cascade upon $NaAsO_2$ stress induction. HaCaT cells were treated as described in Materials and Methods section. Phosphorylation levels of p38 and MAPKAPK-2 were analyzed by Western blotting. β-actin was used as an internal standard. The relative densitometric analysis of P-p38 (A) and P-MAPKAPK-2 (B) levels is reported. Black bars refer to control cells in the absence (-) or in the presence (+) of sodium arsenite; light grey bars refer to cells incubated with 90 µg/mL of carotenoids. Data shown are the means ± S.D. of three independent experiments. * Indicates $p < 0.05$, ** indicates $p < 0.01$, *** indicates $p < 0.001$. Lines above the bars indicate the samples compared for statistical analysis.

4.3.3.5 Protection against oxidative stress via the activation of Nrf2 pathway

The nuclear factor E2-related factor 2 (Nrf2) plays a pivotal role in cellular responses to oxidative stress[25], as it regulates the expression of antioxidant enzymes and maintains the redox homeostasis[26]. Under physiological conditions, Nrf2 is in the cytosol, associated to the kelch-like ECH-associated protein 1 (KEAP1). In the presence of external stimuli, such as oxidative stress or low exposure to antioxidants, Nrf2 dissociates from KEAP1 and rapidly translocates into the nucleus where it binds the antioxidant responsive elements (ARE) sequences, thus initiating the transcription of over 200 genes involved in the antioxidant response, among which heme oxygenase 1 (HO-1)[27]. For this reason, the effect of carotenoid extract in the activation of Nrf2 pathway was analyzed. HaCaT cells were treated with 90 µg/mL of carotenoid extract for 10 or 20 min and then lysates were analyzed by Western blot analysis, using Nrf2 antibody. As shown in **Figure 6a**, a significant increase in nuclear Nrf2 levels was observed upon 10 min incubation. To corroborate this result, HO-1 levels were also analyzed by Western blot, upon 20- and 30-min incubation. As shown in **Figure**

6b, a significant increase in HO-1 levels was observed after 20 min incubation.

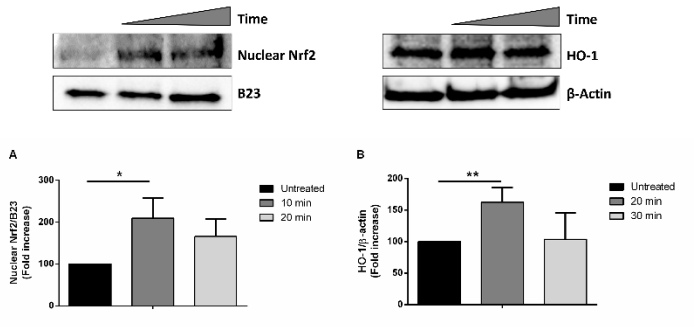

Figure 6. Effect of carotenoid extract on Nrf2 activation. HaCaT cells were incubated with 90 μg/mL of ethanol extract for different length of times. (**a**) Western blot analysis of nuclear Nrf2 of untreated cells (black bars), after 10 min (dark grey bar) and 20 min (light grey bar) incubation. (**b**) Western blot analysis of cytosolic HO-1 of untreated cells (black bars), after 20 min (dark grey bar) and 30 min (light grey bar) incubation. Anti-B23 antibody was used as internal standard for nuclear lysate, whereas anti-β-actin antibody was used for cytosol. Images were quantified by densitometric analysis. Data shown are means ± S.D. of three independent experiments. * Indicates $p < 0.05$ with respect to control cells.

4.3.3.6 Biocompatibility of FAs

Finally, the biocompatibility of palmitic and stearic acids was tested on HaCaT cells. In particular, the FAs obtained at the end of the biorefinery were analyzed following the same procedure used above. As shown in **Figure 7**, no effect on cell viability was observed at any of the experimental conditions under test, thus indicating the safeness of the isolated FAs.

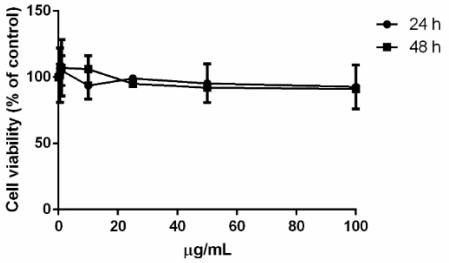

Figure 7. Biocompatibility of isolated FAs on human keratinocytes. HaCaT cells were incubated for 24 h (black circles) or 48 h (black squares) with increasing concentrations (0.5-100 μg/mL) of FAs isolated from the residual biomass of *P. simplex*. Cell viability is expressed as a percentage of viable cells in the presence of the extracts under test with respect to control cells grown in the absence of the FAs. Data shown are means ± S.D. of three independent experiments.

4.4 Discussion

In the last years, the use of natural molecules to be used in cosmeceutical field is emerging and the biotech industries are focusing their attention on safe, sustainable, and economical natural sources. The blue biotechnology, based on the use of aquatic resources as raw materials, is meeting consumer demands for natural active molecules to be used in cosmetics and cosmeceuticals. In this context, microalgae represent a versatile reservoir of active molecules with many potential applications, ranging from antioxidants[14], anticancer[28] to anti-aging[29], as its biomass contains an array of valuable metabolites, such as proteins, lipids, polysaccharides pigments and vitamins, all known for their antioxidant, anti-aging and moisturizing activities. However, several drawbacks hinder microalgae large-scale use, which eventually lead to an increase in the overall costs[5,30]. A possible solution to lower the costs is the biorefinery approach: a stepwise extraction of more than one product to reduce the environmental footprint[31]. This should be combined to eco-friendly extraction techniques to obtain biologically active and safe extracts, in terms of negligible cytotoxicity.

Here, an unexplored green microalga strain has been used to isolate different classes of molecules with biological activity. Starting from *Pseudococcomyxa simplex* biomass, carotenoids were extracted as first using a green approach. It is well-known that carotenoids can exert a potent antioxidant activity, thus protecting skin cells from stress agents and improving the skin appearance[32]. Lutein, the most abundant one, is a high added carotenoid with reported anticancer, antibacterial, anti-neurodegenerative and anti-inflammatory activities[33], sold at 455,000 €/g. The obtained extract shows a strong antioxidant activity and can activate the Nrf2 pathway, which has been primarily identified as a key player in the antioxidant response. The activation of Nrf2 pathway is involved in the modulation of skin pigmentation, in wound healing and in the overall protection of the skin from the environmental stresses, so that the use of Nrf2 modulators is considered a useful tool in dermo-cosmetic applications. Recent studies linked the pivotal role of Nrf2 to other key pathways, such as anti-inflammatory and skin-aging[34]. Wrinkles, loss of elasticity, hyper-pigmentation, dryness are classical symptoms of skin-aging, mainly due to the activity of key enzymes, such as those involved in elastin degradation or in the early steps of melanogenesis[35]. In particular, melanin overproduction can cause different dermatological problems, such as hyperpigmentation, which can finally lead to melanoma[36]. Our data strongly support the connection between antioxidants, Nrf2 activation and skin-aging, as the

extract shows an inhibitory effect towards tyrosinase and elastase enzymes. Our results are in line with those reported in literature on carotenoids extracted from different strains, such as astaxanthin[37,38], lutein[39] and β-carotene[40]. Accordingly, microalgae extracts are currently being formulated into skin-care products for providing anti-aging, moisturizing, antioxidant, and anti-irritant benefits[33]. The lipids isolated from the residual biomass belong to saturated fatty acids, a neglected class of lipids which are now more considered, as they can find application as antibacterial molecules, in cosmetics and in drug delivery[41]. Lipid yield obtained from the raw biomass (24%) is in agreement with literature[42], whereas lipid yield from the residual biomass is almost three times lower, probably because of the first extraction with ethanol. However, from the residual biomass, a pure class of fatty acids is obtained by a single purification step. We can hypothesize that lipid yield is affected by the first extraction solvent: the more hydrophobic solvent is used for the first extraction, the lower is the lipid yield obtained from the residual biomass. According to this hypothesis, when an aqueous buffer is used as first extraction solvent, an increase in the lipid yield is observed, as all the lipophilic molecules cannot be extracted by a polar solvent. Moreover, if lipid recovery is preceded by an ethanol extraction, the lipid content decreases, as some class of lipids (those with a lower hydrophobicity) can be co-extracted by ethanol[14,41] and an increase in SFA content is observed[41]. In cosmetics, fatty acids can be used as oily raw materials, as emulsifiers and as softeners because they can deposit between desquamating cells[9]. The isolated fatty acids were fully biocompatible, thus suggesting a possible role in cosmetics. The main objective of cosmetic formulations is to use extracts endowed with anti-oxidant, anti-aging and moisturizing potential, so that microalgae fulfill these requirements. They also represent a sustainable vegan alternative to replace potentially harmful chemicals, traditionally used in skin care products. Algae molecules can protect from aging, UV, and oxidative stress, but only few strains are commercialized. Currently, molecules or extracts from *Chlorella vulgaris*, *Haematococcus pluvialis*, *Dunaliella salina*, *Nannochloropsis oculata* and *Phaeodactylum tricornutum* are normally employed, so that the exploration of untapped species is now mandatory. This study represents a milestone but also a starting point for process improvement. Indeed, biomass concentration, advances in extraction technologies, formulation strategies and a detailed cost analysis are expected to accelerate the adoption of *P. simplex* in the cosmetics industry.

4.5 References

1. Tang, D. Y. Y. *et al.* Potential utilization of bioproducts from microalgae for the quality enhancement of natural products. *Bioresour. Technol.* **304**, 122997 (2020).
2. Bouzroud, S. *et al.* Biotechnological Approaches to Producing Natural Antioxidants: Anti-Ageing and Skin Longevity Prospects. *Int. J. Mol. Sci.* **24**, (2023).
3. Liberti, D. *et al.* Shedding Light on the Hidden Benefit of *Porphyridium cruentum* Culture. *Antioxidants 2023, Vol. 12, Page 337* **12**, 337 (2023).
4. Yarkent, Ç., Gürlek, C. & Oncel, S. S. Potential of microalgal compounds in trending natural cosmetics: A review. *Sustain. Chem. Pharm.* **17**, 100304 (2020).
5. Imbimbo, P., *et al*. Towards green extraction methods from microalgae learning from the classics. *Appl. Microbiol. Biotechnol.* **104**, 9067–9077 (2020).
6. Igbokwe, V. C., *et al.* Biochemical biorefinery: A low-cost and non-waste concept for promoting sustainable circular bioeconomy. *J. Environ. Manage.* **305**, 114333 (2022).
7. Sathasivam, R. *et al.* A review of the biological activities of microalgal carotenoids and their potential use in healthcare and cosmetic industries. *Mar. Drugs* **16**, (2018).
8. Franco, A. *et al.* Lipids from Insects in Cosmetics and for Personal Care Products. *Insects* **13**, (2022).
9. De Luca, M. *et al.* Lipids from microalgae for cosmetic applications. *Cosmetics* **8**, (2021).
10. Cochran, S. *et al.* Fatty Acids, Fatty Alcohols, Synthetic Esters and Glycerin Applications in the Cosmetic Industry BT - Lipids and Skin Health. in (ed. Pappas, A.) 311–319 (Springer International Publishing, 2015).
11. Knox, S. *et al.* Skin lipids in health and disease: A review. *Chem. Phys. Lipids* **236**, 105055 (2021).
12. Imbimbo, P. *et al.* An Alternative Exploitation of *Synechocystis sp.* PCC6803 : A Cascade Approach for the Recovery of High Added-Value Products. 1–12 (2023).
13. Bligh, E. G. *et al.* A rapid method of total lipid extraction and purification. *Can. J. Biochem. Physiol.* **37**, 911–917 (1959).
14. Imbimbo, P. *et al.* A cascade extraction of active phycocyanin and fatty acids from *Galdieria phlegrea*. *Appl. Microbiol. Biotechnol.* **103**, 9455–9464 (2019).
15. Crescenzo, R. *et al.* Fat Quality Influences the Obesogenic Effect of High Fat Diets. *Nutrients* **7**, 9475–9491 (2015).
16. Mahdi, I. *et al.* Chemical profiling and dermatological and anti-aging properties of *Syzygium jambos L.* (Alston): evidence from molecular docking, molecular dynamics, and in vitro experiments. *Front. Mol. Biosci.* **10**, 1–18 (2024).
17. Sobeh, M. *et al.* Isolation of Myricitrin and 3,5-di-O-Methyl Gossypetin from Syzygium samarangense and Evaluation of their Involvement in Protecting Keratinocytes against Oxidative Stress via Activation of the Nrf-2 Pathway. *Molecules* **24**, (2019).
18. Laezza, C. *et al.* Use of yeast extract to elicit a pulp-derived callus cultures from Annurca apple and potentiate its biological activity. *J. Funct. Foods* **112**, 105988 (2024).

19. Almela, L., *et al.* High-performance liquid chromatographic screening of chlorophyll derivatives produced during fruit storage. *J. Chromatogr. A* **870**, 483–489 (2000).
20. Gu, Y., *et al.* Biomarkers, oxidative stress and autophagy in skin aging. *Ageing Res. Rev.* **59**, 101036 (2020).
21. Panwar, P. *et al.* Expression of elastolytic cathepsins in human skin and their involvement in age-dependent elastin degradation. *Biochim. Biophys. Acta - Gen. Subj.* **1864**, 129544 (2020).
22. Ozturk, M. *et al.* Arsenic and Human Health: Genotoxicity, Epigenomic Effects, and Cancer Signaling. *Biol. Trace Elem. Res.* **200**, 988–1001 (2022).
23. Rahaman, M. S. *et al.* Environmental arsenic exposure and its contribution to human diseases, toxicity mechanism and management. *Environ. Pollut.* **289**, 117940 (2021).
24. Sharifi-Rad, M. *et al.* Lifestyle, Oxidative Stress, and Antioxidants: Back and Forth in the Pathophysiology of Chronic Diseases. *Front. Physiol.* **11**, (2020).
25. Li, W. *et al.* Molecular mechanisms of Nrf2-mediated antioxidant response. *Mol. Carcinog.* **48**, 91–104 (2009).
26. Mansouri, A. *et al.* Antioxidant Effects of Statins by Modulating Nrf2 and Nrf2/HO-1 Signaling in Different Diseases. *J. Clin. Med.* **11**, 1–21 (2022).
27. Mallard, A. R., *et al.* Nuclear factor (erythroid-derived 2)-like 2 (Nrf2) and exercise. *Free Radic. Biol. Med.* **160**, 471–479 (2020).
28. Ferraro, G. *et al.* A thermophilic C-phycocyanin with unprecedented biophysical and biochemical properties. *Int. J. Biol. Macromol.* **150**, (2020).
29. Khemiri, S., *et al.* Bioprospecting of microalgae for a potential use as enzyme inhibitors, anti-ageing and prebiotic agents. *Biocatal. Agric. Biotechnol.* **51**, 102759 (2023).
30. Abdur Razzak, S. *et al.* Microalgae cultivation in photobioreactors: Sustainable solutions for a greener future. *Green Chem. Eng.* (2023).
31. Chanana, I., *et al.* Advancements in Microalgal Biorefinery Technologies and Their Economic Analysis and Positioning in Energy Resource Market. *Fermentation* **9**, (2023).
32. Mussagy, C. U. *et al.* Emerging role of bio-based solvents mixtures to increase the solubility and recovery of carotenoids from processed carrot wastes for potential skin care application. *Ind. Crops Prod.* **205**, 117436 (2023).
33. Desai, S. S. *et al.* Biotechnological Advances in Cosmetic Industry. in *Sustainable Production Innovations* 103–135 (Wiley, 2024).
34. Frantz, M. C., *et al.* Nrf2 in dermo-cosmetic: From scientific knowledge to skin care products. *BioFactors* **49**, 32–61 (2023).
35. Shin, S. H., *et al.* Skin aging from mechanisms to interventions: focusing on dermal aging. *Front. Physiol.* **14**, 1–10 (2023).
36. Bayrakçeken Güven, Z., *et al.* Anti-tyrosinase and antimelanogenic effect of cinnamic acid derivatives from *Prunus mahaleb L*.: Phenolic composition, isolation, identification and inhibitory activity. *J. Ethnopharmacol.* **310**, 116378 (2023).
37. Dutta, S., *et al.* A comprehensive review on astaxanthin sources, structure, biochemistry and applications in the cosmetic industry. *Algal Res.* **74**, 103168 (2023).
38. Mourelle, M. L., *et al.* The potential use of marine microalgae and cyanobacteria in cosmetics and thalassotherapy. *Cosmetics* **4**, (2017).
39. Jiang, R. *et al.* Protective effects of microalgal carotenoids against glycosylation-induced collagen degradation in skin. *J. Funct. Foods* **113**,

106014 (2024).
40. Yeager, D. G. *et al.* What's New in Photoprotection: A Review of New Concepts and Controversies. *Dermatol. Clin.* **37**, 149–157 (2019).
41. Liberti, D. *et al.* Inside out *Porphyridium cruentum*: Beyond the Conventional Biorefinery Concept. *ACS Sustain. Chem. Eng.* (2022).
42. Santhakumaran, P., *et al.* Biomass yield and biochemical profile of fourteen species of fast-growing green algae from eutrophic bloomed freshwaters of Kerala, South India. *Biomass and Bioenergy* **119**, 155–165 (2018).

CHAPTER 05

Exploring the anti-adipogenic properties of carotenoids from *Pseudococcomyxa simplex*

CHAPTER 06

Microalgae flocculation: assessment of extraction yields and biological activity

International Journal of Molecular Sciences

(2024) 25(19):10238
https://doi.org/10.3390/ijms251910238

MICROALGAE FLOCCULATION: ASSESSMENT OF EXTRACTION YIELDS AND BIOLOGICAL ACTIVITY

Paola Imbimbo[1,^], Alfonso Ferrara[1,^], **Enrica Giustino[1]**, Davide Liberti[2]; Daria Maria Monti [1,*]

[1] Department of Chemical Sciences, University of Naples Federico II, Via Cinthia 4, 80126 Naples, Italy;
[2] Centre of Marine Sciences, University of Algarve, Campus de Gambelas, 8005-139 Faro, Portugal

Abstract

Downstream costs represent one of the main obstacles to microalgae widespread. The development of an economical, easily scaling-up strategy could reduce the overall process costs. Here, different flocculants were tested on different microalgae strains and a cyanobacterium. Results indicate that flocculation could be an alternative to centrifugation, as $CaCl_2$ induced a complete flocculation of green and red marine strains (96 ± 4 % and 87.0 ± 0.5 %, respectively), whereas Chitosan was the only agent able to induce flocculation on the cyanobacterium (46 ± 1 %). As for the thermoacidophilic red microalga, 100% flocculation was achieved only by increasing the pH. Carotenoids were extracted from the flocculated biomass and the strategy improved by using the wet biomass. Results indicate that flocculation does not affect carotenoid yield, which is at least the same than that obtained upon centrifugation and extraction from the wet biomass. Then, for the first time, the biological activity of the extracts obtained from the flocculated biomasses was evaluated. Results indicated that only the green microalga extract showed an increased antioxidant activity. In conclusion, this work highlights that a general downstream procedure cannot be developed for microalgae strains but should be rationally tailored.

6.1 Introduction

In the last years, microalgae biomass has been deeply explored as a sustainable alternative to conventional feedstocks, mainly for the presence of a wide array of bioactive molecules. Indeed, carotenoids,

polyunsaturated fatty acids and proteins are all endowed with beneficial properties for human health[1,2]. However, despite microalgae enormous potential, a large scale production is still limited by the high cultivation, harvesting and processes costs[3,4]. It has been estimated that the harvesting step could represent up to 30 % of the overall downstream costs[5,6], making the optimization of an efficient and economic harvesting procedure is still a challenge. Indeed, the selection of the right technology to harvest the biomass could be a turning point into microalgae exploitation cost-effective at large scale.

The main drawbacks related to microalgae harvesting are due to cell size, to their overall negative charge, as well as to their low density; for all these reasons, microalgae cells require an economically expensive and energetically intensive dewatering step. To date, the most used harvesting procedures are sedimentation, centrifugation, filtration, flocculation and flotation[7–9]. Each procedure presents different advantages and drawbacks and usually the choice of the technique is based on the market value of the molecule to be isolated. Among all the harvesting techniques, filtration and centrifugation are the most effective in terms of biomass recovery[10,11], but require a high energy input. In the case of filtration, the frequent replacement of filters makes the technique prohibitive at an industrial scale[12,13]. Sedimentation, on the other hand, is an easy and low-cost procedure, but the efficiency strictly depends on culture density, thus making this procedure time-consuming[14]. Flotation and flocculation are the most promising techniques for microalgae biomass harvesting as they are cheap, easy, fast, and scalable. Despite the potential, flotation has a limited efficiency due to the interaction between cells and air bubbles in the culture medium, as the collapsing of the bubbles could result in flocs breaking[15]. To overcome this limitation, the flotation could be performed in the presence of surfactants, but this would increase the overall costs[13]. On the other hand, flocculation is considered the most cost-effective method, as it requires low energy consumption, is suitable with algal scaling-up systems, and the costs are mainly related to the flocculating agent chosen[16]. Flocculants based on metal salts (such as $AlCl_2$, $AlCl_3$, $FeCl_3$, $Al_2(SO_4)_3$, $Fe_2(SO_4)_3$ are generally used for their low-costs and are commonly used for biofuel production or wastewater treatments, without considering the effects of flocculants on biomass quality and impact on the environment [6,17,18]. However, due to their non-biodegradable nature, these flocculants may irreversibly affect water reuse. Thus, organic flocculants, such as chitosan and starch, have been proposed as green alternatives. Flocculation can be achieved also by increasing the pH of the culture medium (autoflocculation), avoiding

the use of flocculants, with low energy consumption[18]. Recently, new approaches emerged, based on magnetic particles, but their economic feasibility and biocompatibility still need to be evaluated[19]. Besides harvesting, the extraction of biologically active molecules from the biomass represents another challenge to be overcome to fully exploit microalgae potential[20]. Conventional extractions usually require large amounts of organic solvents, which are considered not eco-friendly, require long times, give low yields and they are generally used on a dried biomass, with a consequent increase in the final costs[21–23]. Recently, some green extraction techniques were developed, such as pressurized/supercritical liquid extractions, ultrasound- or microwave-assisted extractions. However, these procedures still present some drawbacks, such as scaling-up, energy consumption, quality and selectivity of the extractions, cost validation, and long extraction times[24,25]. Interestingly, many papers have been published to provide alternatives for harvesting the biomass, but literature is quiescent on the effects that the harvesting methods may have on the quality of the biomass and thus on the extracted molecules. Here, different alternatives, of eco-friendly and cost-effective flocculation procedures were provided, by taking into account different microalgae strains and flocculants. Moreover, evidence of the effect of flocculants on the subsequent carotenoids extractions was provided. The extraction step was improved, avoiding the use of a dried biomass and using a GRAS solvent, and the whole procedure was validated by assaying the in vitro antioxidant activity of carotenoids.

6.2 Materials and Methods

6.2.1 Reagents and chemicals

Solvents and reagents, unless differently specified, were from Sigma-Aldrich (St Louis, MO, USA).

6.2.2 Microalgae strains and culture conditions

Porphyridium cruentum (CCALA 415) was acquired from Culture Collection of Autotrophic Organism (CCALA, Centre for Phycology, Institute of Botany of the AS CR, Dukelská 135, TŘEBOŇ CZ-379 82, Czech Republic), and grown in Porphyridium Medium. *Galdieria phlegrea* (ACUF 009), *Pseudococcomyxa simplex* (ACUF 127) and *Synechococcus bigranulatus* (ACUF 680) were kindly provided by Algal

Collection of the University Federico II (ACUF, University of Naples Federico II, Department of Biology, Naples, Italy, www.acuf.net) and grown in Allen medium, BBM and BG11, respectively. Microalgae strains were grown in bubble column photobioreactors at temperatures, and light intensity [Photosynthetic Active Radiations (PAR) ($\mu mol_{photons}/m^2/s$), as previously described[26–29]. Briefly, cells were cultured as follows: *P. cruentum* at 25°C and 13 PAR; *G. phlegrea* at 37 °C and 200 PAR; P. simplex at 24°C and 100 PAR and S. bigranulatus at 39°C and 300 PAR. Each culture was mixed by bubbling air through a sintered glass tube placed at the bottom of each reactor. Algal growth was daily monitored by measuring the absorbance at 730 nm.

6.2.3 Flocculation

At the end of cultivation, different concentrations of high molecular weight chitosan (CS), calcium chloride (CC), sodium glutamate (SG), and sodium hydroxide (to increase the pH) were added to each strain. In particular, CS was tested at 0.1, 0.15 and 0.2 g/L; CC at 2, 3, and 4 g/L on *P. cruentum, G. phlegrea* and *S. bigranulatus*, whereas on *P. simplex* CC was tested at 0.3, 0.4, 0.5 g/L. Autoflocculation was induced by adjusting pH at 10 and 12 for *P. cruentum*, and at 12 and 13 for the other strains. Flocculation was carried out at the pH measured at the end of cell growth (7 for P. cruentum, 1.5 for *G. phlegrea*, 8 for *S. bigranulatus* and *P. simplex*). After adding the flocculating agent, each culture was stirred for 30 seconds at 1000 rpm and then the O.D. of the solution was measured at 730 nm. Time-course experiments were performed by measuring the O.D. immediately (0 min), and after 10 and 20 minutes from stirring. Flocculation efficiency was calculated as percentage (%) using the formula:

$$\text{Flocculation effiency } (\%) = \left(1 - \frac{\text{O. D. sample}}{\text{O. D. culture}} \times 100\right)$$

where O.D. sample is the O.D. measured after the treatment and O.D. culture is the value measured before any treatment[30].

6.2.4 Pigments extraction and yields determination

Pigments extractions were performed using a GRAS solvent, ethanol, as reported by Aremu, with some modifications[31]. Briefly, for each extraction, independently from the harvesting procedure followed,

the equivalent of 200 mg of dry weight (D.W.) was used for extractions. The biomass was suspended in 4 mL of pure ethanol and disrupted by ultrasonication (40 % amplitude, 4 min on ice, Bandelin SONOPULS HD 3200, tip MS73). The final volume was adjusted to 20 mL and the mixture was shaken for 24 h at 250 rpm in a dark room at 4 °C. The mixture was then centrifuged at 5000 g for 10 min and the supernatant was stored at – 20 °C and dried under N_2 stream at 30 °C. The extraction yields were determined gravimetrically and expressed using the formula:

$$\text{Extraction yield } (\%) = \frac{\text{mg}_{\text{extract}}}{\text{mg}_{\text{biomass dry weight}}} \times 100$$

6.2.5 ABTS assay

The in vitro antioxidant activity of each extract was evaluated by the 2,2'-azinobis-(3-ethylbenzothiazoiline-6-sulfonic acid) ABTS assay, according to Imbimbo[32]. Results are expressed as IC_{50} (µg/mL), i.e., the concentration required to scavenge 50% of free radical ABTS.

6.2.6 Statistical analyses

Samples were tested in three independent analyses, each carried out in triplicate. Results are presented as mean of results obtained after three independent experiments (mean ± S.D.) and compared by one-way ANOVA according to the Bonferroni's method (post hoc) using Graphpad Prism for Windows, version 6.01.

6.3 Results

6.3.1 Flocculation

To get a general understanding of the procedure, different microalgae strains were analyzed: two Rhodophyta (*Porphyridium cruentum* and *Galdieria phlegrea*), a Chlorophyta (*Pseudococcomyxa simplex*) and a Cyanobacterium (*Synechococcus bigranulatus*). Different flocculants, based on their mechanism of action, were tested on each strain: a carbohydrate, chitosan, known to induce flocculation through a bridging mechanism; two salts, calcium chloride and sodium glutamate, which should induce charge neutralization, and the increase of the pH of the cell culture which causes flocculation through a sweeping mechanism. Flocculants were added to the culture, as

described in Materials and Methods section. For each experimental procedure, the culture was collected when the cell concentration reached 7 ± 0.1 O.D./mL and each flocculant was added to the culture medium at three different concentrations (or pH values). Solutions were stirred and analyzed immediately (0 min). To verify the effects of incubation time on flocculation efficiency, longer incubations (10 and 20 min) were done before reading the absorbance of the culture. Samples were analyzed spectrophotometrically, by reading the absorbance at 730 nm. Each sample was compared to untreated cell culture.

6.3.1.1 *Chitosan*

Chitosan (CS) was tested at 0.1, 0.15 and 0.2 g/L. Results are reported in **Figure 1**. In the case of *P. cruentum* culture, a direct correlation between the concentration of polymer added and flocculation efficiency was observed: from 66 % of flocs immediately formed (0.1 g/L of CS), up to 90 % with 0.15 g/L, and 100 % flocculation in the presence of the highest concentration tested (0.2 g/L). *P. cruentum* was completely flocculated in the presence of any CS concentration tested after 10 or 20 min. On the other hand, the other red microalga analyzed, *G. phlegrea*, did not flocculate at any time of any tested CS concentration. CS induced an immediate 84 % flocculation in the green microalga *P. simplex*, independently from the amount of polymer added to the culture. *P. simplex* completely flocculated after 10 or 20 min incubation, independently from the CS concentration. Similar results were obtained with *S. bigranulatus* culture, even if at a lower extent, as only 40% flocculation was observed independently from the concentration of CS used. It is interesting to notice that no significant increase in the efficiency of the process was observed upon 10 or 20 min incubation.

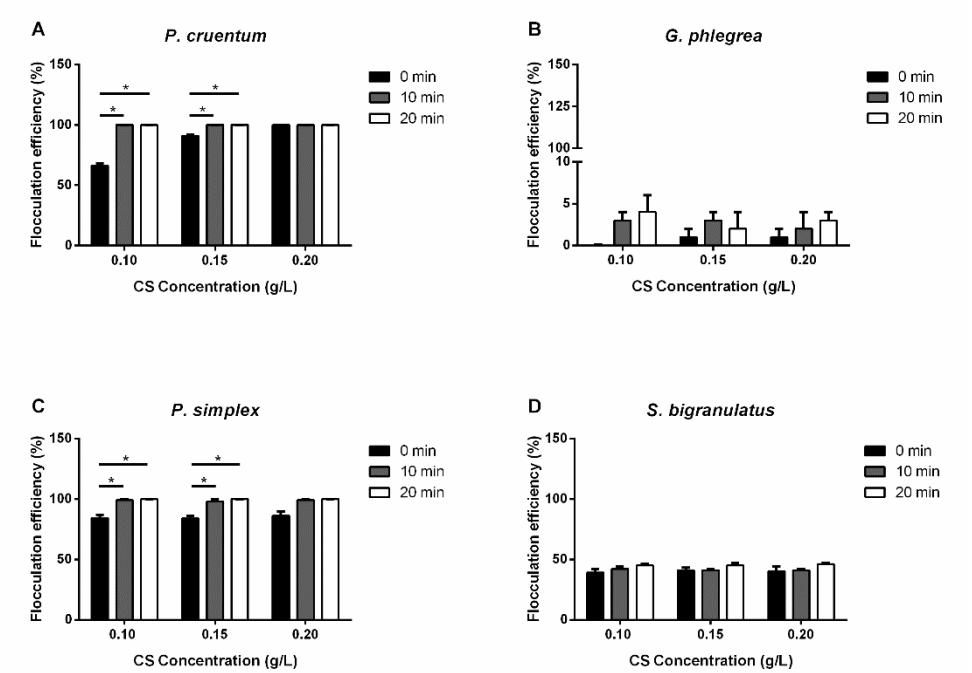

Figure 1. Flocculation efficiency (%) of chitosan (CS). Effect of different CS concentrations on flocculation efficiency of microalgae strains analyzed immediately (0 min, black bars), after 10 min (grey bars) and after 20 min (white bars) from stirring. **A**, *P. cruentum*; **B**, *G. phlegrea*; **C**, *P. simplex*; **D**, *S. bigranulatus* upon different flocculation times. Data are obtained by mean of three independent experiments (mean ± S.D.). * $p < 0.05$. The lines above the bars indicate the two samples compared for statistical analysis.

6.3.1.2 *Calcium Chloride and Sodium Glutamate*

The same set of experiments was done by using two salts, sodium glutamate (SG) and calcium chloride (CC). SG was tested as a possible cost-effective alternative to polyglutamic acid, normally used in the cosmeceutical industry[33]. When SG was tested, no effect was observed at any concentration used on any strain, independently from the incubation time used (data not shown). Different was the case of CC. As shown in **Figure 2**, the red microalga *P. cruentum* showed a time- and concentration-dependent flocculation efficiency, reaching about 90% flocculation at the highest CC concentration tested. CC was unable to induce flocculation on the other red microalga (*G. phlegrea*), at any analyzed experimental condition. *P. simplex* flocs were observed after 10 min incubation, with a 90 % flocculation efficiency, but independently from the concentration of salt used. No flocculation was observed for *S. bigranulatus* at any analyzed condition.

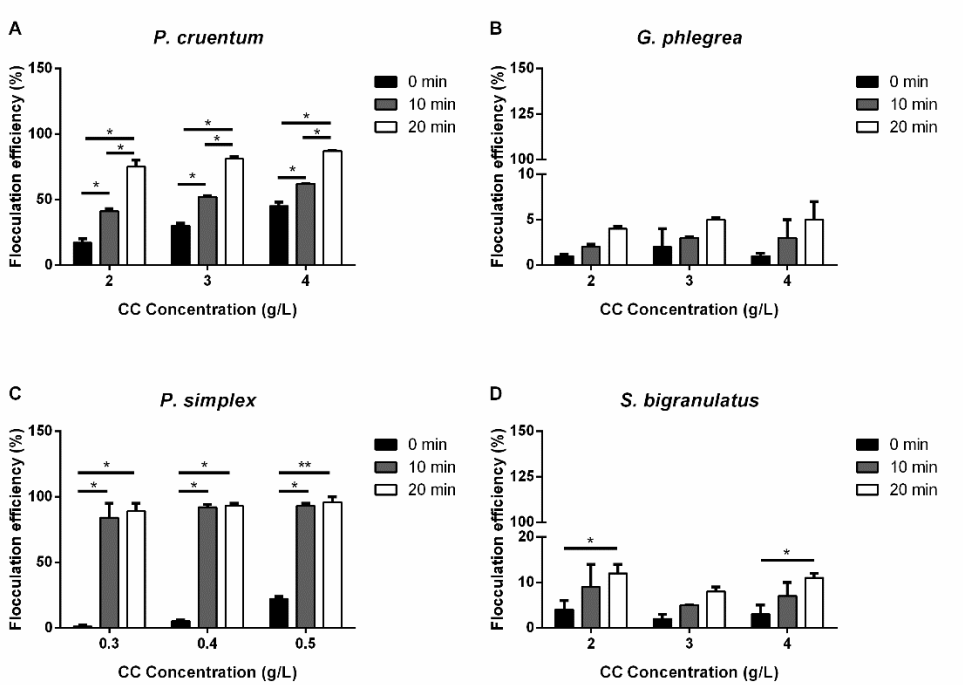

Figure 2. Flocculation efficiency (%) of calcium chloride (CC). Effect of different CC concentrations on flocculation efficiency of microalgae strains analyzed immediately (0 min, black bars), after 10 min (grey bars) and after 20 min (white bars) from stirring. **A**, *P. cruentum*; **B**, *G. phlegrea*; **C**, *P. simplex*; **D**, *S. bigranulatus* upon different flocculation times. Data are obtained by mean of three independent experiments (mean ± S.D.). * $p < 0.05$, ** $p < 0.005$. The lines above the bars indicate the two samples compared for statistical analysis.

6.3.1.3 *pH-mediated flocculation*

Finally, pH increase was tested to analyze autoflocculation. Sodium hydroxide was used to increase the pH of the culture medium, and two pH values were tested for each strain, as indicated in **Figure 3**. Interestingly, with the exception of *S. bigranulatus* culture, increasing pH values induced biomass flocculation on all the tested strains. In particular, the increase of the pH value from 7 to 10 immediately induced more than 90 % of flocculation in *P. cruentum* culture. This value reached 100 % after 10 min incubation. When the pH value was increased from 7 to 12, an immediate and complete flocculation was observed. In the case of *G. phlegrea* culture, the flocculation efficiency was complete after 10 min incubation. Surprisingly, when the pH of the culture was increased to 13, a complete and immediate flocculation occurred, but a bleaching phenomenon in the biomass happened.

Different results were observed for *P. simplex*, in which the switch of the pH value from 8 to 12 induced about 80 % flocculation after 20 min incubation, whereas the increase of the pH to 13 speeded up the process, and the biomass was totally and immediately flocculated. *S. bigranulatus*, instead, showed a small flocculation efficiency over time at pH 12 (from 1 to 38 %) and up to 51 % after 20 min at pH 13.

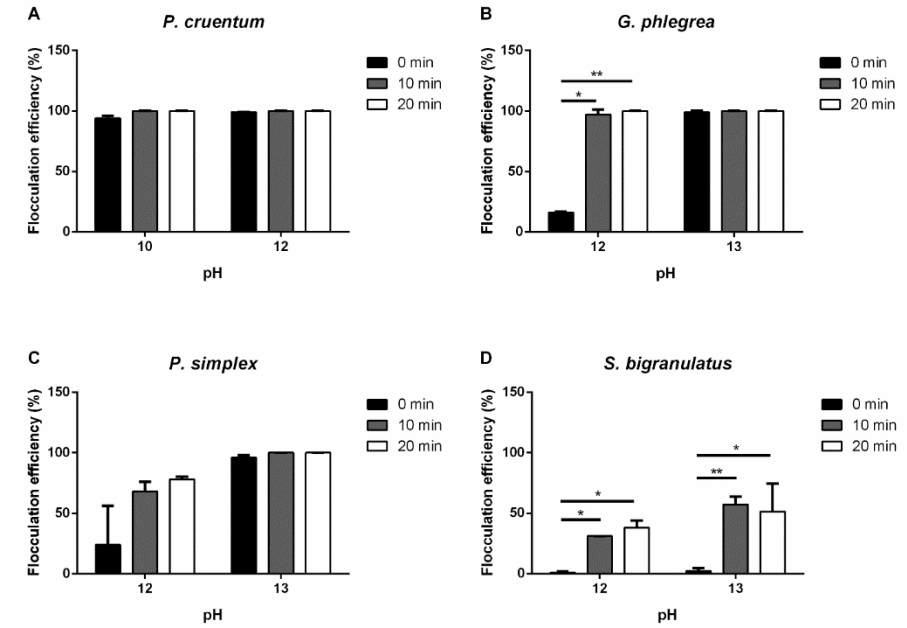

Figure 3. **Flocculation efficiency (%) after pH increase.** Effect of pH on flocculation efficiency of microalgae strains analyzed immediately (0 min, black bars), after 10 min (grey bars) and after 20 min (white bars) from stirring. **A**, *P. cruentum*; **B**, *G. phlegrea*; **C**, *P. simplex*; **D**, *S. bigranulatus* upon different flocculation times. Data are obtained by means of three independent experiments (mean ± S.D.). * $p < 0.05$, ** $p < 0.005$. The lines above the bars indicate the two samples compared for statistical analysis.

Thus, according to literature, a high variability of flocculation is observed among microalgae strains, so that each strain represents a different case study[34]. Based on the overall results, for each strain the best flocculation condition was chosen and reported in **Table 1**. In the case of *P. cruentum*, despite CS provided the best results, the choice fell on CC, as the latter is a valid and economic alternative (about 1,000 vs 44 €/kg, from Sigma-Aldrich).

Table 1. Summary of the selected flocculation conditions for each strain.

Strain	Flocculation condition	Flocculation efficiency 20 min
P. cruentum	4.0 g/L CC	87.0 ± 0.5
G. phlegrea	pH 12	100.0 ± 0.1
	pH 13	100.0 ± 0.1
P. simplex	0.5 g/L CC	96 ± 4
S. bigranulatus	0.2 g/L CS	46 ± 1

6.3.2 Pigment extraction

In order to verify if flocculation has any effect on the subsequent pigments extraction, in terms of yield and activity, each strain was flocculated based on the selected conditions, and pigments were extracted from the resulting wet biomass. Pigments were extracted by using ethanol as a solvent, as it is GRAS, non-toxic for humans and widely used in many applications. The idea of using the wet biomass is another little step forward for the use and application of microalgae, as the drying step is avoided, thus saving energy, and reducing the overall costs. Each extraction was compared to two benchmarks, i.e., a biomass harvested by centrifugation and extracted bypassing the drying step (named wet biomass) or after lyophilization (named dry biomass). As described in Materials and Methods, for each extraction, the same amount of biomass was used for pigments extraction by resuspending the biomass in 4 mL of pure ethanol and disrupting by ultrasonication. The volume was then diluted 2.5-fold, in order to increase the efficiency of the extraction procedure, by moving forward the equilibrium between the components still bound to the matrix and those already solubilized in the solvent. In the case of *P. cruentum* (**Figure 4A**), the yield of the extract obtained from the biomass flocculated with 4 g/L of CC (light grey bar, 15 %) showed an increase in flocculation efficiency compared to both untreated samples (black bar, 7.5 %, dark grey bar, 8.5 %). No significant differences ($p > 0.05$) were observed between the extract obtained from either dry or wet biomass (black bar and dark grey bar, respectively). *G. phlegrea* pigments extraction was performed either on the biomass obtained upon flocculation at pH 12 and also on the bleached biomass (obtained at pH 13). As shown in **Figure 4B**, the yield of the extract obtained from dry biomass (black bar, 16 %) was significantly higher than the wet

biomass (dark grey bar, 13 %, $p < 0.05$), whereas no significant difference was observed with respect to the flocculated biomass at pH 12 (light grey bar, 16 %, $p > 0.05$). The yield of extraction from the flocculated biomass at pH 12 was significantly higher than the wet one (16 and 13%, respectively, $p < 0.05$). In the case of the extract obtained from flocculated biomass at pH 13 (white bar, 12 %), a significant decrease in the extraction yield was observed with respect to dry biomass and to the biomass flocculated at pH 12 ($p < 0.05$). No differences were observed between the extract obtained from the wet biomass and that obtained after flocculation at pH 13 ($p > 0.05$). The extracts obtained from *P. simplex* biomass (**Figure 4C**) did not show a statistically significant difference among them, suggesting that flocculation does not affect the extraction yields. In **Figure 4D**, the extracts obtained from *S. bigranulatus* biomass are reported. The same yield of extraction (22 %) was obtained in the centrifuged wet biomass (dark grey bar) and the flocculated one (light grey bar), and the values were significantly higher ($p < 0.01$) than the yield obtained from the centrifuged dry biomass (black bar, 12 %).

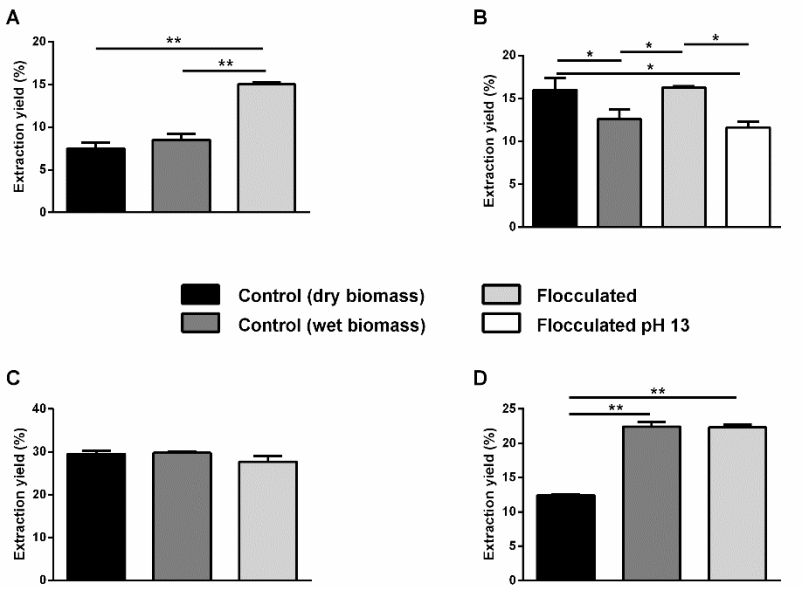

Figure 4. Pigments extraction. Extraction yields (%) are reported as mg of extract with respect to mg of D.W. biomass. Black bars indicate centrifuged dry biomass, dark grey bars indicate centrifuged wet biomass, light grey bars indicate flocculated wet biomass. The white bar is referred to flocculated biomass at pH 13. **A**, *P. cruentum*; **B,** *G. phlegrea*; **C**, *P. simplex*; **D**, *S. bigranulatus*. Results are expressed as the means ± S.D. of three independent experiments. * indicates $p < 0.05$, **

indicates $p < 0.01$. The lines above the bars indicate the two samples compared for statistical analysis.

6.3.3 *In vitro* antioxidant activity

From previous data, it is known that the ethanol extract from *P. cruentum* mainly contains zeaxanthin[27], whereas *S. bigranulatus* extract is enriched in zeaxanthin and xanthophylls[28], *G. phlegrea* contains zeaxanthin and β-carotene[32], and *P. simplex* is enriched in lutein[29]. The ethanol extracts, obtained from either centrifuged or flocculated wet biomasses, were analyzed for their antioxidant capacity by in vitro ABTS assay. The results of the ABTS assay, showed in **Figure 5**, report, for each analyzed condition, the IC_{50} values obtained (i.e., the concentration of extract necessary to inhibit 50% of the free radicals of the $ABTS^{\bullet+}$). In particular, the experiments carried out on the extract obtained from the flocculated biomass of *P. cruentum* revealed a significant increase in the IC_{50} value (187.0 ± 1.1 µg/mL) compared to the extract obtained from centrifuged wet biomass (125.0 ± 1.4 µg/mL, $p < 0.001$). Also in the case of *G. phlegrea* extract, a significant increase ($p < 0.001$) in the IC_{50} value was observed in the flocculated biomass with respect to the benchmark extraction (i.e. centrifuged wet biomass) (93 ± 1 µg/mL and 63 ± 1 µg/mL, respectively), whereas the extract obtained from the biomass flocculated at pH 13 had a IC_{50} value of and of 109 ± 22 µg/mL ($p < 0.05$ compared to the other tested samples). These results suggest that flocculation can negatively affect the antioxidant activity of the extracts. However, the IC_{50} values obtained from *P. simplex* extracts after flocculation showed a significant reduction in comparison to that obtained from the centrifuged biomass (63 ± 1 µg/mL and 93 ± 1 µg/mL, respectively, $p < 0.001$), thus representing an improvement in the antioxidant activity of the extract. Unfortunately, CS showed a small negative effect on *S. bigranulatus* extract, as the IC_{50} values increased from 48 ± 1 to 63 ± 1 µg/mL ($p < 0.01$). It can be hypothesized that the flocculant may interact with the extracted carotenoid, as CC negatively affects the antioxidant activity of *P. cruentum* (enriched in zeaxanthin), but positively affects the antioxidant activity of *P. simplex* (enriched in lutein).

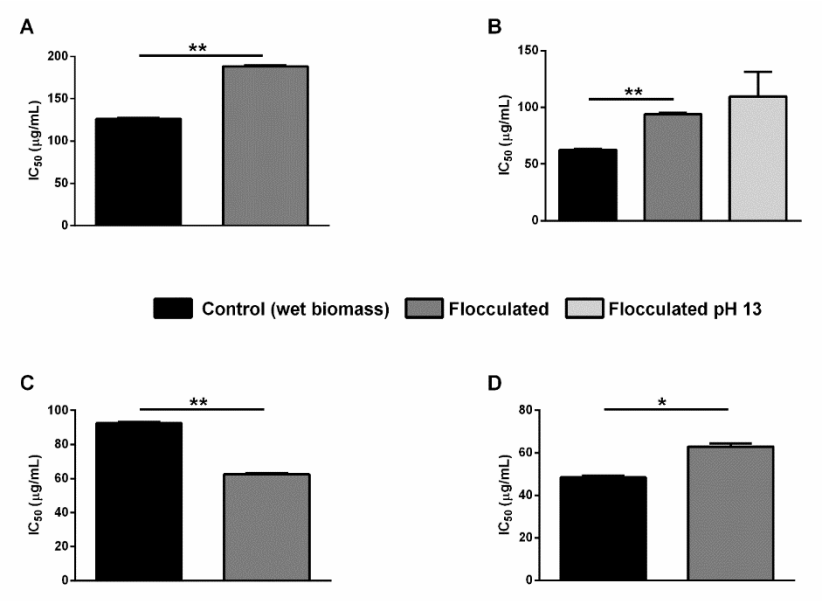

Figure 5. Antioxidant activity of ethanol extracts. Values are expressed as IC_{50} (µg/mL), i.e. the concentration required to scavenge 50% of free radical ABTS. Black bars indicate centrifuged wet biomass, dark grey bars indicate flocculated wet biomass and light grey bar indicates flocculated wet biomass at pH 13. **A**, *P. cruentum*; **B**, *G. phlegrea*; **C**, *P. simplex*; **D**, *S. bigranulatus*. Data are shown as means ± S.D.. Three independent measurements were carried out. * Indicate $p < 0.01$; ** indicate $p < 0.001$ with respect to centrifuged wet biomass. The lines above the bars indicate the two samples compared for statistical analysis.

6.4 Discussion

In the last years, flocculation has been studied as a cost-effective alternative to centrifugation, with the aim to lower the energy consumption and the costs related to the downstream at an industrial level. However, due to the complexity of living systems, such as microalgae and cyanobacteria, it is hard to develop a standardized flocculation procedure that can be effective on different strains[35]. Here, a study on the effect of four flocculants of different nature was carried out on three microalgae strains and one cyanobacterium. Generally speaking, a systematic comparison of different strains could be challenging, as cultivation conditions can differ in some aspects, such as cell concentration or cultivation techniques[34]. For this reason, algae cultures with the same biomass concentrations (7 O.D./mL) were used for all the experiments. Chitosan (CS) was selected as it is a natural and environmentally friendly agent. From a chemical point of view, CS is a polymer obtained from the deacetylation of chitin, and due to its cationic nature, can interact with negatively charged microorganisms.

When the effect of CS was studied on *P. cruentum* culture, a dose-dependence was observed, as 66 % of flocs immediately formed at the lowest concentration tested (0.1 g/L), reaching 100 % flocculation in the presence of the highest concentration tested (0.2 g/L). These results indicate a higher flocculation efficiency compared to those reported by Endrawati and colleagues, who found 67 % flocculation after 10 min of incubation with 0.1 g/L CS and 100 % flocculation only after 40 min[36]**.** In the case of *G. phlegrea*, no flocculation occurred at any of the experimental conditions tested, whereas CS was able to induce 84% flocculation at time 0 in the green microalga *P. simplex*, independently from the concentration used. Similar results were obtained with *S. bigranulatus*, but at a lower extent (40% flocculation efficiency independently from the concentration). Except for *P. cruentum* flocculated in the presence of CS[36], no data are present in the literature on the other analyzed strains. However, it is generally recognized that in CS-induced flocculation, the incubation time, as well as CS concentration can affect the efficiency. As an example, Ahmad and colleagues reported the flocculation of *Chlorella sp.* in the presence of CS, but the authors found a negative correlation between algal coagulation, the amount of CS used, incubation time, and speed rate[37]**.**

Among chemical flocculants, metal ions have been extensively studied for microalgae harvesting, as they are considered highly effective in terms of flocculation efficiency, however, several issues may occur as a possible transfer of the metal ion to microalgae biomass that could turn out to be highly toxic[38]. Aluminum sulfate is one of the most used chemical flocculant, generally used for waste water treatment, but it was not used in this study, as it is toxic and its presence would affect biomass valorization[39]. Alternatively, calcium chloride (CC) is a non-toxic, alkali metal generally used as a food preservative, and therefore could represent a green alternative to metal-based salts, to preserve both the biomass integrity and the environment[40]. Indeed, CC was found to be effective on *P. cruentum* in a time- and concentration-dependent manner, whereas *P. simplex* biomass flocculated after 10 min incubation without a dose-effect dependency. Unfortunately, no effects were observed on *G. phlegrea* and *S. bigranulatus*. Overall, the results obtained on the green microalga are consistent with those reported by Singh et al[40] on *Chlorella pyrenoidosa*. Authors reached almost 98% of flocculation in the presence of ~ 0.3 g/L of CC, but with a longer incubation time then that reported in the present paper. Further analyses are needed to verify its effects on cell morphology. Another unexplored chemical flocculant, sodium glutamate (SG), was tested.

SG is the monomer of the normally used polyglutamic acid (PGA)[41]. PGA works as a bridging agent by its negatively charged glutamic residue, so the inspiring idea was to use the building block to flocculate the biomass, but no positive results were obtained. Autoflocculation occurs when microorganisms self-aggregate when the environmental conditions change. This phenomenon is achieved by neutralizing the negatively charged cell surface, thus creating an alkaline environment (pH > 8.0) that allows cells to aggregate. The variation of pH can be facilitated by adding to microalgae culture a small amount of chemicals, such as NaOH, KOH or $Mg(OH)_2$, thus making this process economically suitable[42]. However, a substantial increase in pH could affect the algae culture and thus the quality of the biomass[12,43]. Here, NaOH was used to increase the pH of the algae culture, and with the exception of *S. bigranulatus*, it was found to be effective on all the other strains. In particular, for *P. cruentum* and *G. phlegrea* a highly efficient flocculation was immediately observed, whereas *P. simplex* completely flocculated upon 10 min incubation. These results are consistent with literature data, as an increase in pH values has been shown to induce autoflocculation, with NaOH the base working at lower concentrations with respect to KOH, $Mg(OH)_2$ and $Al(OH)_2$[18,44]. Despite the promising results, the pH variation in the case of *G. phlegrea* from 1.5 to 13 resulted in a dramatic change in the color of the biomass, suggesting that flocculation could affect not only the quality of the biomass but also the quality of the molecules within it. This evidence is supported by data in literature, which report that pH variations can alter microalgae cell physiology[45]. For this reason, once selected the best flocculation parameter for each strain, a pigment extraction was carried out. Conventionally, extractions are performed on dry biomasses, however, it is known that the drying step is energetically expensive[32]. To further decrease the overall process costs, in this work pigment extractions were carried out on a wet biomass. Results clearly indicate that flocculation does not negatively affect the extraction yields when compared to those obtained starting from a centrifuged biomass, and that the drying step of the biomass can be avoided, with a generally positive impact on the overall downstream costs. Finally, the bioactivity of the extracted molecules was determined in vitro, to deeply understand if the flocculation procedure could affect the bioactivity of the extracted molecules. The ABTS assay revealed that flocculation does not affect the quality of the extracted molecules, with the exception of *P. simplex*, in which the antioxidant activity of the extract obtained from the flocculated biomass improved with respect to that obtained from the centrifuged one (IC_{50} values: 63 µg/mL vs 93 µg/mL). Further

analyses are mandatory to deeply investigate this hypothesis. These results are important as this is the first report in which flocculants have been related to the quality of the extracted molecules. Many papers have been published so far, with a simple relationship between the efficiency of flocculation and biomass morphology[18,38,39]. However, no analysis on the bioactivity of the molecules extracted from flocculated biomass has been reported so far, probably because research has been mainly focused on wastewater treatment or biodiesel production[40–42]. To date, only Taghavijeloudar and colleagues successfully extracted proteins, carbohydrates, and lipids from a *Chlorella sorokiniana* strain, but no data are reported on the biological activity of the obtained molecules[46]. Understanding the domino effect of flocculants on biomass and molecules to be extracted represents a priority for a safe and mindful use of microalgae, which are now considered in a wider perspective, not only for their lipid content, but as a source of green, vegan and sustainable molecules.

6.5 References

1. Siddiqui, A., *et al.* Engineering microalgae through chloroplast transformation to produce high-value industrial products. *Biotechnol. Appl. Biochem.* **67**, 30–40 (2020).
2. Levasseur, W., *et al.* A review of high value-added molecules production by microalgae in light of the classification. *Biotechnol. Adv.* **41**, 107545 (2020).
3. Acién Fernández, F. G., *et al.* Chapter 21 - Costs analysis of microalgae production. in *Biomass, Biofuels, Biochemicals* (eds. Pandey, A., Chang, J.-S., Soccol, C. R., Lee, D.-J. & Chisti, Y. B. T.-B. from A. (Second E.) 551–566 (Elsevier, 2019).
4. Udayan, A., *et al.* Emerging industrial applications of microalgae: challenges and future perspectives. *Syst. Microbiol. Biomanufacturing* **1**, 411–431 (2021).
5. Roy, M. *et al.* A comprehensive review on microalgal harvesting strategies: Current status and future prospects. *Algal Res.* **44**, 101683 (2019).
6. Okoro, V., *et al.* Microalgae cultivation and harvesting: Growth performance and use of flocculants - A review. *Renew. Sustain. Energy Rev.* **115**, 109364 (2019).
7. Fuad, N. *et al.* Mass harvesting of marine microalgae using different techniques. *Food Bioprod. Process.* **112**, 169–184 (2018).
8. Hidayah Mat Yasin, *et al.* The Effect of Microalgae Harvesting on Lipid for Biodiesel Production. *Mater. Today Proc.* **19**, 1582–1590 (2019).
9. Rawat, I., *et al.* Dual role of microalgae: Phycoremediation of domestic wastewater and biomass production for sustainable biofuels production. *Appl. Energy* **88**, 3411–3424 (2011).
10. Barros, A. I., *et al.* Harvesting techniques applied to microalgae: A review. *Renew. Sustain. Energy Rev.* **41**, 1489–1500 (2015).
11. Najjar, Y. S. H. *et al.* Harvesting of microalgae by centrifugation for biodiesel production: A review. *Algal Res.* **51**, 102046 (2020).

12. Min, K. H., *et al.* Recent progress in flocculation, dewatering, and drying technologies for microalgae utilization: Scalable and low-cost harvesting process development. *Bioresource Technology* vol. 344 126404.
13. Kumar, N., *et al.* Microalgae harvesting techniques: updates and recent technological interventions. *Critical Reviews in Biotechnology* vol. 43 342–368.
14. Ortiz, A., *et al.* Optimization and operation of a demonstrative full scale microalgae harvesting unit based on coagulation, flocculation and sedimentation. *Sep. Purif. Technol.* **259**, 118171 (2021).
15. Demir-Yilmaz, I. *et al.* Bubble functionalization in flotation process improve microalgae harvesting. *Chem. Eng. J.* **452**, 139349 (2023).
16. Xu, H. *et al.* A novel biomineralization-inspired flocculation approach for harvesting high quality microalgal biomass: Dual action of cationic polyelectrolytes and nanosilica. *Bioresour. Technol.* **388**, 129739 (2023).
17. Zhang, J. *et al.* A novel method to harvest microalgae via co-culture of filamentous fungi to form cell pellets. *Bioresour. Technol.* **114**, 529–535 (2012).
18. de Morais, E. G. *et al.* Microalgae harvesting for wastewater treatment and resources recovery: A review. *N. Biotechnol.* **78**, 84–94 (2023).
19. Zhang, B. *et al.* Efficient magnetic flocculation for microalgae harvesting using a novel composite flocculant of Fe_3O_4-based starch-grafted-cationic polyacrylamide. *J. Water Process Eng.* **55**, 104121 (2023).
20. Gifuni, I., *et al.* Current Bottlenecks and Challenges of the Microalgal Biorefinery. *Trends Biotechnol.* **37**, 242–252 (2019).
21. Mansour, E. A., *et al.* Efficacy of extraction techniques and solvent polarity on lipid recovery from domestic wastewater microalgae. *Environ. Nanotechnology, Monit. Manag.* **12**, 100271 (2019).
22. Sati, H., *et al.* Microalgal lipid extraction strategies for biodiesel production: A review. *Algal Res.* **38**, 101413 (2019).
23. Sousa, V., *et al.* Microalgae biomass as an alternative source of biocompounds: New insights and future perspectives of extraction methodologies. *Food Res. Int.* **173**, (2023).
24. Pocha, C. K. R., *et al.* Current advances in recovery and biorefinery of fucoxanthin from *Phaeodactylum tricornutum*. *Algal Res.* **65**, 102735 (2022).
25. Chong, J. W. R. *et al.* Bridging artificial intelligence and fucoxanthin for the recovery and quantification from microalgae. *Bioengineered* vol. 14 2244232.
26. Imbimbo, P. *et al.* A cascade extraction of active phycocyanin and fatty acids from *Galdieria phlegrea*. *Appl. Microbiol. Biotechnol.* **103**, 9455–9464 (2019).
27. Liberti, D. *et al.* Inside out *Porphyridium cruentum*: Beyond the Conventional Biorefinery Concept. *ACS Sustain. Chem. Eng.* **11**, 381–389 (2023).
28. D'Elia, L. *et al.* Thermo resistant antioxidants from photoautotrophic microorganisms: screening and characterization. *World J. Microbiol. Biotechnol.* **37**, 1–13 (2021).
29. Imbimbo, P. *et al.* Unveiling the potential of *Pseudococcomyxa simplex*: a stepwise extraction for cosmetic applications. *Appl. Microbiol. Biotechnol.* (2024) doi:10.1007/s00253-024-13229-9.
30. Chua, E. T., *et al.* Effective Harvesting of *Nannochloropsis* Microalgae Using Mushroom Chitosan: A Pilot-Scale Study. *Front. Bioeng. Biotechnol.* **8**, 1–8 (2020).
31. Aremu, A. O. *et al.* Changes in phytochemical content and pharmacological activities of three Chlorella strains grown in different nitrogen conditions. *J. Appl. Phycol.* **28**, 149–159 (2016).

32. Imbimbo, P. *et al.* Green Compressed Fluid Technologies To Extract Antioxidants and Lipids from *Galdieria phlegrea* in a Biorefinery Approach. *ACS Sustain. Chem. Eng.* **8**, 2939–2947 (2020).
33. Elbanna, K., *et al.* Poly (γ) glutamic acid: a unique microbial biopolymer with diverse commercial applicability. *Front. Microbiol.* **15**, 1–22 (2024).
34. Lama, S. *et al.* Flocculation properties of several microalgae and a cyanobacterium species during ferric chloride, chitosan and alkaline flocculation. *Bioresour. Technol.* **220**, 464–470 (2016).
35. Rosmahadi, N. A. *et al.* Assuaging microalgal harvesting woes via attached growth: A critical review to produce sustainable microalgal feedstock. *Sustain.* **13**, 1–24 (2021).
36. Endrawati, H. *et al.* The effect of chitosan concentration on flocculation efficiency microalgae *Porphyridium cruentum* (Rhodhophyta). *IOP Conf. Ser. Earth Environ. Sci.* **919**, (2021).
37. Ahmad, A. L., *et al.* Optimization of microalgae coagulation process using chitosan. *Chem. Eng. J.* **173**, 879–882 (2011).
38. Rossi, S. *et al.* Metal-based flocculation to harvest microalgae: a look beyond separation efficiency. *Sci. Total Environ.* **799**, 149395 (2021).
39. Zhu, L. *et al.* Effects of operating parameters on algae *Chlorella vulgaris* biomass harvesting and lipid extraction using metal sulfates as flocculants. *Biomass and Bioenergy* **132**, 105433 (2020).
40. Singh, H. M., *et al.* Optimization of flocculation efficiency of *Chlorella pyrenoidosa* with CaCl2 using the Box-Behnken design of response surface methodology: A cost effective statistical investigation. *Biomass Convers. Biorefinery* **14**, 3261–3273 (2024).
41. Pugazhendhi, A. *et al.* A review on chemical mechanism of microalgae flocculation via polymers. *Biotechnol. Reports* **21**, e00302 (2019).
42. Babakhani, P., *et al.* The shift in carbon source induces pH increase and autoflocculation in microalgal suspensions facilitating multi-approach biomass harvesting. *Biomass Convers. Biorefinery* (2022).
43. Chen, C. Y., *et al.* Perspectives on cultivation strategies and photobioreactor designs for photo-fermentative hydrogen production. *Bioresour. Technol.* **102**, 8484–8492 (2011).
44. Vandamme, D., *et al.* Flocculation of *Chlorella vulgaris* induced by high pH: Role of magnesium and calcium and practical implications. *Bioresour. Technol.* **105**, 114–119 (2012).
45. Kuzhiumparambil, U. *et al.* Effects of harvesting on morphological and biochemical characteristics of microalgal biomass harvested by polyacrylamide addition, pH-induced flocculation, and centrifugation. *Bioresour. Technol.* **359**, 127433 (2022).
46. Taghavijeloudar, M., *et al.* A rapid, efficient and eco-friendly approach for simultaneous biomass harvesting and bioproducts extraction from microalgae: Dual flocculation between cationic surfactants and bio-polymer. *Sci. Total Environ.* **854**, 158717 (2023).

CHAPTER 07

GENERAL DISCUSSION

7.1 *General discussion*

The present PhD project aimed to define the role of antioxidant molecules isolated from microalgae for cosmeceutical and nutraceutical applications.

The results obtained in this study have highlighted several key aspects of the industrial-scale use of microalgae. Specifically, while their remarkable heterogeneity is the key feature for their application across diverse industrial sectors, it also presents the main challenge in defining a standardized process that is independent of the species analyzed. Indeed, the valorization criteria for all the algal cultures here presented were specifically tailored to meet the requirements of each case. A similar trend was observed in the optimization of the flocculation system, where, after evaluating various approaches, the optimal conditions were customized for each microalga. Overall, the biorefinery systems explored in this project proved to be essential for obtaining high-value-added molecules, using a minimal number of unit operations, all performed with eco-friendly, low-environmental-impact techniques. This approach preserved both the quality of the molecules and the biomass, ensuring the efficiency of subsequent extractions. All biomasses were effectively valorized, with *P. cruentum* serving as a clear example. The exhausted medium at the end of cultivation is no longer considered a waste to display, but a rich source of highly valuable molecules, sulfated exopolysaccharides, with proven biological activity.

Furthermore, the studies on *Galdieria phlegrea* revealed an additional important aspect: the biorefinery process itself can serve as a strategy for obtaining active extracts, while making the process economically feasible. Indeed, only the carotenoids extracted in cascade exhibited biological activity, suggesting the presence of toxic contaminants in the extract obtained from fresh biomass. However, these contaminants appeared to be removed during the first extraction step, in which another high-value-added molecule (i.e., phycocyanin[1]) was isolated.

Another fundamental aspect of using a biorefinery approach, often not sufficiently emphasized, lies in the ability to extract, from the same biomass, molecules with different biological and physico-chemical characteristics that can be combined. In this regard, we can consider *Porphyridium cruentum*, from which both sulfated exopolysaccharides (s-EPSs) and phycoerythrin were extracted. As previously mentioned, s-EPSs are high-value molecules due to their specific biological activities, such as antioxidant, anti-inflammatory, and wound healing

properties[2]. Although s-EPSs from *P. cruentum*, and EPS in general, have been poorly studied for their effects on lipid metabolism regulation, with only a few *in vivo* studies on EPS from lactic acid bacteria, they are well known for their rheological[3–5]. Their primary role in protecting marine microalgal cells from osmotic stress induced by high saline concentrations, is retained also when isolated and tested for different purposes. Indeed, s-EPSs from microalgae exhibit distinctive gelling, moisturizing, and soothing characteristics, making them ideal as carriers in cream formulations, cosmetic additives, and thickening agents, while preserving their biological activities. When these properties are combined with the extraction of phycoerythrin from the same biomass, whose biological characteristics are well-documented in the literature[6–8], the theoretical idea arises that these two molecules could be combined to create a finished cosmeceutical product, by exploiting a single microalga. This theoretical application becomes even more plausible when considering the data presented in this work on lipid metabolism, hepatic steatosis, and cellular differentiation systems, for which both molecules were found to be active, although affecting on different aspects. It is, therefore, reasonable to speculate that their combination could enhance their individual potential, resulting in an innovative yet entirely natural therapeutic product.

Although microalgae represent a promising tool for therapeutic and natural agents, their use in the treatment of lipid metabolism-related issues is still insufficiently explored. This limitation is primarily due to the lack of applied research in the field and the limited number of microalgae recognized as safe and approved for industrial use. In this regard, the study conducted on *Pseudococcomyxa simplex* plays a crucial role in demonstrating the limitations of these regulations. This green microalga, belonging to the *Chlorophyaceae* family, was first studied in the late 20th century during the active research period on microalgae, primarily to determine its correct taxonomic classification[9]. Aside from these works, only one recent study mentions *P. simplex* in the context of optimizing growth under different conditions, comparing it with other chlorophytes, though without yielding significant results[10]. The study conducted on this microalga, instead, yielded surprising findings. The molecules extracted were all characterized and found to be enriched in pigments of exceptionally high commercial value. The carotenoid profile produced by *P. simplex* mainly consists of lutein and neoxanthin, both high added carotenoids with reported anticancer, antibacterial, anti-neurodegenerative and anti-inflammatory activities[11], sold at 455,000 €/g and 694,000 €/g, respectively. Moreover, the

obtained extract demonstrated a remarkable array of biological activities, including anti-aging effects, antioxidant activity through Nrf2 pathway activation, and anti-adipogenic activity by inhibiting the differentiation pathway. The second class of molecules extracted, lipids, showed a predominance of stearic and palmitic acid. Despite their generally negative reputation, these fatty acids – while lacking the beneficial properties of polyunsaturated fatty acids (PUFAs) – have a growing market as emollients in cosmetic formulations. Furthermore, these lipids were found to be biocompatible with immortalized human keratinocytes, supporting the hypothesis of their potential use in the cosmetic industry.

In conclusion, this PhD project has highlighted the significant potential of microalgae as an innovative source of antioxidant molecules, active in various cellular mechanisms related to the improvement of oxidative stress, such as cellular aging and lipid metabolism disorders. Microalgae thus emerge as tools that are both preventive, due to their high capacity to inhibit lipid accumulation in adipose tissue, and therapeutic, with applications in the cosmeceutical and nutraceutical fields, suggesting real potential applications for the compounds analyzed. Furthermore, the research emphasized the importance of using biorefinery systems, not only to reduce process costs but also to obtain molecules with enhanced biological activities, as shown in the case of *Galdieria phlegrea*.

The integrated biorefinery approach, coupled with the optimization of harvesting and extraction processes, provides concrete solutions to reduce production costs and improve the overall sustainability of the process. However, although the results are highly encouraging, the transition from laboratory research to industrial-scale production requires further efforts, not only in terms of technological innovation but also in addressing the regulatory and commercial challenges associated with the use of microalgae. Indeed, industrial applications based exclusively on microalgae are still relatively limited, even though major cosmetic companies are launching microalgae-based products, such as sunscreens and moisturizers, onto the market. Only through the integration of these solutions can we hope to fully realize the potential of microalgae, creating a sustainable future that combines scientific innovation with effective industrial applications, significantly contributing to human health and the mitigation of climate change.

7.2 *References*

1. Imbimbo, P. *et al.* A cascade extraction of active phycocyanin and fatty acids from *Galdieria phlegrea*. *Appl. Microbiol. Biotechnol.* **103**, 9455–9464 (2019).
2. De Jesus Raposo, M. F., *et al.* Bioactivity and applications of sulphated polysaccharides from marine microalgae. *Marine Drugs* vol. 11 233–252 (2013).
3. Zhuang, D. *et al.* Application progress of bioactive compounds in microalgae on pharmaceutical and cosmetics. *Chemosphere* **291**, 132932 (2022).
4. Bernal, P. *et al.* Promising biotechnological applications of antibiofilm exopolysaccharides. *Microb. Biotechnol.* **5**, 670–673 (2012).
5. Zhang, Z. *et al.* Isolated exopolysaccharides from *Lactobacillus rhamnosus* GG alleviated adipogenesis mediated by TLR2 in mice. *Sci. Rep.* **6**, 1–14 (2016).
6. Liberti, D. *et al.* Shedding Light on the Hidden Benefit of *Porphyridium cruentum* Culture. 1–12 (2023).
7. Liberti, D. *et al.* Inside out *Porphyridium cruentum*: Beyond the Conventional Biorefinery Concept. *ACS Sustain. Chem. Eng.* (2022).
8. Imchen, T. *et al.* Marine algae colorants: Antioxidant, anti-diabetic properties and applications in food industry. *Algal Res.* **69**, 102898 (2023).
9. Broady, P. A. The morphology, distribution and ecology of *Pseudococcomyxa simplex* (Mainx) Fott (Chlorophyta, Chlorellaceae), a widespread terrestrial Antarctic alga. *Polar Biol.* **7**, 25–30 (1987).
10. Robles, M. *et al.* Mixotrophic growth of a highly acidic habitat microalga for production of valuable fatty acids. *J. Appl. Phycol.* **36**, 2489–2502 (2024).
11. Desai, S. S., *et al.* Biotechnological Advances in Cosmetic Industry. in *Sustainable Production Innovations* 103–135 (Wiley, 2024).

APPENDIX

List of scientific publications

I- Giustino, E., Imbimbo, P., Trepiana, J., Portillo, M.P., Monti, D. M. (2024). Advancing knowledge on *Porphyridium cruentum*: a new frontier in lipid accumulation management. **Submitted to** *Oxidative Medicine and Cellular Longevity* **(Chapter 2)**.

II- Giustino, E., Imbimbo, P., Trepiana, J., Portillo, M.P., Monti, D. M. (2024). Unlocking the antiadipogenic potential of carotenoids from *Galdieria phlegrea*. **Submitted to** *Applied Microbiology and Biotecnology* **(Chapter 3).**

III- Imbimbo, P., Ferrara, A., **Giustino, E.**, Liberti, D., Monti, D. M. (2024). Microalgae flocculation: assessment of extraction yields and biological activity. International Journal of Molecular Sciences. (2024) 25(19):10238. https://doi.org/10.3390/ijms251910238. **(Chapter 6)**

IV- Imbimbo, P., **Giustino, E.**, Ferrara, A., Alvarez-Rivera, G., Annaz, H., Ibanez, E., Di Meo, M.C., Zarrelli, A., Monti, D. M. (2024). Unveiling the potential of *Pseudococcomyxa simplex*: a stepwise extraction for cosmetic applications. Applied Microbiology and Biotechnology, 108(1), 390. https://doi.org/10.1007/s00253-024-13229-9. **(Chapter 4)**

V- Liberti, D., Imbimbo, P., **Giustino, E.**, D'Elia, L., Ferraro, G., Casillo, A., Illiano, A., Pinto, G., Di Meo, M. C., Alvarez, G., Corsaro, M. M., Amoresano, A., Zarrelli, A., Ibáñez, E., Merlino, A., Monti, D. M. (2022). Inside out *Porphyridium cruentum*: Beyond the conventional biorefinery concept. *ACS Sustainable Chemistry & Engineering*, *11*(1), 381-389. https://doi.org/10.1021/acssuschemeng.2c05869.

VI- Liberti, D., Imbimbo, P., **Giustino, E.**, D'Elia, L., Silva, M., Barreira, L., Monti, D. M. (2023). Shedding light on the hidden benefit of *Porphyridium cruentum* culture. *Antioxidants*, *12*(2), 337. https://doi.org/10.3390/antiox12020337.

List of scientific communication

- Imbimbo, P., Ferrara, A., **Giustino, E.**, Liberti, D., Monti, D. M.: Microalgae flocculation: assessment of extraction yields and biological activity. Congresso AISAM 2024 (Firenze, October 16-18th, 2024).

- **Giustino, E.**, Imbimbo, P., Trepiana, J., Portillo, M.P., Monti, D. M.: Unlocking the antiadipogenic potential of carotenoids from *Galdieria phlegrea*. Congresso AISAM 2024 (**Oral communication**. Firenze, October 16-18th, 2024).

- **Giustino, E.**, Imbimbo, P., Ferrara, A., Monti, D. M.: *Unveiling the microalgae potential: bioproducts and application.* Workshop Euskampus *"Usefulness of dietary bioactive compounds and probiotics in health promotion"* (**Oral communication**. Vitoria-Gasteiz, November 9th, 2023).

- **Giustino, E.**, Schiavone, G., Schibeci, M.: *Shell to Sell: cracking the surface of shrimps shell potential*. National Bioeconomy Day. (Napoli, May 25th, 2023).

- **Giustino, E.,** Imbimbo, P., Monti, D.M.: *Microalgae and Pigments: not only bright colors.* III Workshop AISAM Giovani; (Verona, June 29th-30th, 2022).

- **Giustino, E.,** Imbimbo, P., Rossi, M., Monti, D. M.: *When Microalgae Application Meets Innovation.* Meeting of the Campania SIB Section (Napoli, October 26th, 2022).

- Liberti, D., Imbimbo, P., **Giustino, E.**, D'Elia, L., Ferraro, G., Casillo, A., Illiano, A., Pinto, G., Di Meo, M. C., Alvarez, G., Corsaro, M. M., Amoresano, A., Zarrelli, A., Ibáñez, E., Merlino, A., Monti, D. M. *Inside out Porphyridium cruentum: Beyond the conventional biorefinery concept.* Meeting of the Campania SIB Section (Napoli, October 26th, 2022).

- **Giustino, E.,** Imbimbo, P., Rossi, M., Monti, D. M.: *When Microalgae Application Meets Innovation.* 3rd AISAM National Congress (Napoli, October 16-18th, 2022).

- Liberti, D., Imbimbo, P., **Giustino, E.**, D'Elia, L., Ferraro, G., Casillo, A., Illiano, A., Pinto, G., Di Meo, M. C., Alvarez, G., Corsaro, M. M., Amoresano, A., Zarrelli, A., Ibáñez, E., Merlino, A., Monti, D. M.: *Inside out Porphyridium cruentum: Beyond the conventional biorefinery concept.* 3rd AISAM National Congress (Napoli, October 16-18th, 2022).

Scientific activities in foreign laboratory: From September 26th, 2023 to April 30th 2024, in the research group of Prof. Maria Puy Portillo. Obesity and Nutrition group, Department of Pharmacy of the University of the Basque Country, Vitoria-Gasteiz (Spain).

ACS Sustainable Chemistry & Engineering

pubs.acs.org/journal/ascecg

Research Article

Inside out *Porphyridium cruentum*: Beyond the Conventional Biorefinery Concept

Davide Liberti, Paola Imbimbo, Enrica Giustino, Luigi D'Elia, Giarita Ferraro, Angela Casillo, Anna Illiano, Gabriella Pinto, Maria Chiara Di Meo, Gerardo Alvarez-Rivera, Maria Michela Corsaro, Angela Amoresano, Armando Zarrelli, Elena Ibáñez, Antonello Merlino, and Daria Maria Monti*

Cite This: https://doi.org/10.1021/acssuschemeng.2c05869

Read Online

ACCESS | Metrics & More | Article Recommendations | Supporting Information

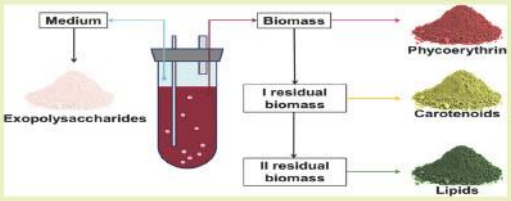

ABSTRACT: Here, an unprecedented biorefinery approach has been designed to recover high-added value bioproducts starting from the culture of*Porphyridium cruentum*. This unicellular marine red alga can secrete and accumulate high-value compounds that can find applications in a wide variety of industrial fields. 300 ± 67 mg/L of exopolysaccharides were obtained from cell culture medium; phycoerythrin was efficiently extracted (40% of total extract) and isolated by single chromatography, with a purity grade that allowed the crystal structure determination at 1.60 Å; a twofold increase in β-carotene yield was obtained from the residual biomass; the final residual biomass was found to be enriched in saturated fatty acids. Thus, for the first time, a complete exploitation of*P. cruentum*culture was set up.

KEYWORDS: *microalgae, cascade approach, high-added-value molecules, phycoerythrin, sulfated exopolysaccharides*

INTRODUCTION

Microalgae capture carbon dioxide during their growth to perform photosynthesis. This implies the production of oxygen and the reduction of carbon dioxide emissions.[1] It is noteworthy that microalgae are used as a reliable source of food and high-added value products.[2] Microalgae can be considered perfect candidates for their use in biorefinery approaches,[3] as they can grow in lands which do not compete with food production, and with a higher growth rate with respect to conventional crops. From a theoretical point of view, a biorefinery is a combination of multiple integrated processes able to convert the biomass into a variety of high-added value products, in an economical and environmentally sustainable approach.[4] This is in line with the principles of circular economy, fostered by international organizations and promoted by European Union (https://eur-lex.europa.eu/legal-content/EN/ALL/?uri=CELEX%3A52015DC0614). Unfortunately, in the microalgae field, a real biorefinery has been demonstrated only for few strains,[5] and most of the present literature is focused on the extraction of one or two classes of molecules, thus suggesting that the process is not economically feasible.

Porphyridium cruentum is a red marine microalga, reservoir of potentially high-added value molecules, such as carotenoids, sulfated exopolysaccharides (EPSs), B-phycoerythrin (PE), and lipids.[6−9] Carotenoids are well-known antioxidants, also able to counteract many disorders, from type 2 diabetes, to degenerative diseases or cancer.[10] Sulfated EPSs have a chemical structure which confer them peculiar rheological properties[11] and many biological activities,[12] such as antimicrobial, anti-inflammatory,[13] hypocholesterolemic,[14] antiviral activities,[15] and skin protective activity.[16] PE, the main protein found in*P. cruentum*, has a good market value for different reasons: (i) in biomedical and molecular applications for its natural fluorescence; (ii) as a natural red-colored protein to be used as a dye for food and cosmetics, and (iii) in the

Received: September 30, 2022
Revised: November 10, 2022

pharmaceutical industry thanks to its antioxidant activity.[17] Finally, recent literature exploited the use of saturated fatty acids as antimicrobial agents and as drug delivery systems.[18,19]

Thus, taking advantage of the chemical composition of*P. cruentum*, here we propose a real biorefinery. For the first time, not only the biomass but also the exhausted medium was fully exploited to recover: EPSs from the medium and PE, carotenoids and lipids from the biomass. Molecules were extracted sequentially, starting from the most valuable one, without affecting the activity of the molecules in the residual biomass.

MATERIALS AND METHODS

Reagents. All chemicals, solvents, and reagents, unless differently specified, were from Sigma-Aldrich (St Louis, MO, USA).

Microalgal Strain and Dry Weight Determination. *Porphyridium cruentum* strain was acquired from Culture Collection of Autotrophic Organism (CCALA, Centre for Phycology, Institute of Botany of the AS CR, Dukelská 135, TŘEBOŇ CZ-379 82, Czech Republic). Preculture (50 mL, 0.09 ± 0.01 O.D./mL) of *P. cruentum* was inoculated in *Porphyridium* medium[20] in a 1 L bubble column photobioreactor (working volume 800 mL) in a room with constant temperature (25 ± 1 °C) and light (fluorescent lamps with an intensity of 13 ± 1 PAR $\left[\frac{\mu mol_{photons}}{m^2/s}\right]$) in autotrophic conditions, without CO_2. The culture was mixed by bubbling through a sintered glass tube placed at the bottom of each culture tube. Algal growth was monitored by measuring the absorbance at 730 nm. The O.D. values were converted into biomass amount by correlating O.D. and dry cell weight.

Exopolysaccharide Isolation and Quantization. To process a high volume of medium, the latter was concentrated 10 times by lyophilization, prior to addition of pure ethanol (1:2 v/v); EPSs were then recovered by centrifugation (12,000 *g*, 30 min, 4 °C), collected and lyophilized. Total carbohydrates were quantified by the phenol–sulfuric acid method, according to Geresh et al.,[21] with some modifications, as reported in Gallego.[4] A reference curve was obtained by using glucose (0.03–1.0 mg/mL).

Determination of Monosaccharide Composition. Lyophilized EPSs (2 mg) were solubilized with 1 mL of HCl/CH_3OH (1.25 M) for 16 h at 80 °C.[22] Then, the sample was dried and acetylated with 25 μL of acetic anhydride and 25 μL of pyridine and kept at 100 °C for 30 min. The mixture was analyzed by gas chromatography–mass spectrometry (GC–MS) by using an Agilent Technologies instrument (GC 7820A, MS 5977B), equipped with a HP-5MS 30 m, 0.25 mm, 0.25 μm capillary column. The following temperature program was used to analyze acetylated methyl glycosides: 140 °C for 3 min, 140 °C → 240 °C at 3 °C/min.

Total Carbon, Hydrogen, Nitrogen, and Sulfur. The determination of total carbon (C), hydrogen (H), nitrogen (N), and sulfur (S) in EPSs recovered from *P. cruentum* medium was carried out by performing total combustion, using the FlashSmart Elemental Analyzer, according to Álvarez-Gómez and colleagues.[23] Elements (C, H, N, S) were expressed as % with respect to the sample's total weight.

Protein Extraction and Quantification. Fresh biomass was harvested by centrifugation at 1200*g* for 30 min at room temperature and resuspended at 10 $mg_{D.W.}$/mL in PBS pH 7.4. Cell disruption was done by: (i) maceration; (ii) freeze and thaw; (iii) French Press, and (iv) sonication. For the maceration, the biomass was kept at 4 °C in agitation for 24 h. For the freeze and thaw method, the biomass was frozen (−80 °C) and then thawed (37 °C) for five cycles. For the French Press, two cycles were performed at a pressure of 2 kbar. The ultrasound method was performed by operating with MS73 tip at 40% amplitude of the instrument (Bandelin Sonoplus HD 3200) for different lengths of time, from 4 to 20 min, (30″ on, 30″ off), on ice. At the end of each step, samples were centrifuged at 5000 *g* at 4 °C for 30 min, proteins were recovered in the supernatant, total proteins were determined by BCA Protein Assay Kit (Thermo Scientific) and then SDS-PAGE analysis followed by Coomassie staining was performed. Phycobiliprotein concentration was determined by the Bennet and Bogorad equations:[24]

$$C_{PC} = \frac{[Abs_{615nm} - (0.474 \times Abs_{652})]}{5.34} \quad (1)$$

$$C_{Apc} = \frac{[Abs_{652nm} - (0.208 \times Abs_{620nm})]}{5.09} \quad (2)$$

$$C_{Pe} = \frac{[Abs_{562nm} - (2.41 \times C_{Pc}) - (0.849 \times C_{Apc})]}{9.62} \quad (3)$$

The reported wavelengths (562, 615, and 652 nm) correspond to the maximum of absorption of phycoerythrin, phycocyanin, and allophycocyanin, respectively.

Phycoerythrin Purification. PE purification was performed by comparing three techniques: anion-exchange chromatography, gel filtration, and ultrafiltration. Anion-exchange chromatography was carried out by using a Nuvia-Q resin equilibrated with PBS pH 7.4, and elution was performed using 0.25 M NaCl. Gel filtration was performed by using a Sephadex G-75 equilibrated in PBS pH 7.4. Ultrafiltration was carried out with a 10 kDa molecular weight cut-off membrane, and the process was performed at 4 °C. The fractions obtained by anion-exchange and gel filtration, as well as the retentate obtained by ultrafiltration, were collected and analyzed by SDS-PAGE followed by Coomassie staining and PE purity grade was calculated by measuring the ratio Abs_{562nm}/Abs_{280nm}.

Crystallization, Data Collection, Structure Solution, and Refinement of Phycoerythrin. PE crystals were grown by the hanging drop vapor diffusion method[25] using a drop containing 10 mg/mL PE in 0.25 M ammonium sulfate, 25 mM potassium phosphate at pH 5.0, equilibrated with a reservoir containing 0.5 M ammonium sulfate, and 50 mM potassium phosphate at pH 5.0. Red crystals were visible after 1 week (Figure S1, Supporting Information).

The crystals were soaked in a cryoprotectant solution containing 30% (v/v) glycerol in the reservoir solution and cooled at −173 °C. Starting from one crystal, a high-resolution data set was collected at the XRD2 beamline at the Elettra synchrotron in Trieste, Italy, at −173 °C. Data were processed and scaled using Autoproc.[26] The crystal was trigonal, space group R3, with unit cell parameters $a = b = 186.59$ Å, $c = 59.19$ Å, $\alpha = \beta = 90°$, and $\gamma = 120°$. For data collection statistics, see Table S1 (Supporting Information). The structure of PE was solved by molecular replacement using PHASER,[27] and the PE structure deposited in the Protein Data Bank under the accession 3VS8,[28] as a starting model. The structure shows the presence of two ($\alpha\beta$) dimers in the asymmetric unit. Visual inspection and model improvements were carried out using Coot.[29] Refinements were carried out using Refmac 5.0.[30] *R* factor and *R* free values were used to optimize the refinement strategy. The final model, which has good geometries and refinement statistics (Table S1, Supporting Information), was deposited in the Protein Data Bank under the accession code 8B4N. Pymol (www.pymol.org) was used to obtain molecular-graphics figures.

In Situ Digestion. A single PE crystal was solubilized in water and analyzed by SDS-PAGE. For in-gel hydrolysis, SDS-PAGE bands were excised from the gel lane, destained by consecutive cycles of 0.1 M NH_4HCO_3 at pH 8.0 and acetonitrile (ACN), followed by reduction (10 mM DTT in 100 mM NH_4HCO_3, 45 min, at 56 °C) and alkylation (55 mM IAM in 100 mM NH_4HCO_3, 30 min, at room temperature). The gel pieces were washed with 0.1 M NH_4HCO_3 of pH 8.0 and ACN and subjected to the enzymatic hydrolysis by covering them with 40 μL sequencing grade modified trypsin (10 ng/μL trypsin; 10 mM NH_4HCO_3) overnight at 37 °C. Peptide mixtures were eluted, vacuum-dried, and resuspended in 2% ACN acidified with 0.1% HCOOH. Tryptic peptide mixtures were analyzed by MALDI-TOF (AB SCIEX, Milan, Italy) to reveal the amino acid sequence of the three phycoerythrin chains.

https://doi.org/10.1021/acssuschemeng.2c05869
ACS Sustainable Chem. Eng. XXXX, XXX, XXX−XXX

Mass Spectrometry Analyses. Matrix-assisted laser desorption/ionization (MALDI) mass spectrometry (MS) experiments were performed on a 5800 MALDI-TOF-TOF ABSciex equipped with a nitrogen laser (337 nm) (AB SCIEX, Milan, Italy). Starting from each band, aliquots of peptide mixture (0.5 μL) were mixed (1:1, v/v) with alphacyano hydroxycinnamic acid (10 mg/mL) in acetonitrile: 55 mM citric acid (70:30) solution. Calibration was done by using a calibration mixture from AB SCIEX (Monoisotopic $(M + nH)^{n+}$: 904.46 Da des-Arg-Bradykinin, 1296.68 Da Angiotensin I, 1570.67 Da Glu-Fibrinopeptide B, 2093.08 Da ACTH (clip 1–17), 2465.19 Da ACTH (clip 18–39), 3657.92 Da ACTH (clip 7–38)). Peptides were identified by MS spectra, acquired using a mass (m/z) range of 400–4000 Da. Peptide mass fingerprinting was performed by MS digest of homologue phycoerythrin sequences. MALDI MS experiments were performed on a 5800 MALDI-TOF-TOF ABSciex equipped with a nitrogen laser (337 nm) (AB SCIEX, Milan, Italy). The instrument operated with an accelerating voltage of 20 kV, a grid voltage at 66% of the source voltage, and a delay time at 200 ns. Laser power was set to 3500 V for the spectra acquisition. Each spectrum represents the sum of 10,000 laser pulses from randomly chosen positions on the same target place. The data were reported as monoisotopic masses.

Carotenoid Extraction and Characterization. Carotenoids were extracted from the dry biomass, either raw or after protein extraction. Extractions were performed in ethanol, as reported by Aremu, with some modifications.[31] Briefly, for each extraction, 200 mg of freeze-dried biomass was suspended in pure ethanol (4 mL) and sonicated (40% amplitude, 4 min on ice, Bandelin Sonoplus HD 3200, tip MS73). The mixture volume was then adjusted to 20 mL and shaken for 24 h at 250 rpm in a dark room at 4 °C. The supernatant was collected by centrifugation at 12,000g for 10 min, dried under nitrogen stream, and then stored at −20 °C. Carotenoid identification was performed by HPLC-DAD-APCI-QTOF-MS/MS, whereas quantization was done by calibration curves obtained by using commercial zeaxanthin and β-carotene, according to a method previously described,[5] with some modifications. The analysis of the extracts was carried out in an Agilent 1290 UHPLC system (Ultrahigh Performance Liquid Chromatography) equipped with a diode-array detector (DAD), coupled to an Agilent 6540 quadrupole-time-of-flight mass spectrometer (q-TOF MS) equipped with an atmospheric pressure chemical ionization (APCI) source, all from Agilent Technologies (Santa Clara, CA, USA). Extracts were solubilized in ethanol (5 mg/mL), filtered through 0.45 μm nylon filters, and then analyzed under positive ionization mode, using the following parameters: capillary voltage, 3.5 kV; drying temperature, 350 °C; vaporizer temperature, 400 °C; drying gas flow rate, 8 L/min; nebulizer gas pressure, 40 psi; corona current (which sets the discharge amperage for the APCI source), 4000 nA. The mass spectrometer was operated in MS and tandem MS modes for the structural analysis of all compounds. The MS and Auto MS/MS modes were set to acquire m/z values ranging between 50 and 1100 and 50 and 800, respectively, at a scan rate of 5 spectra per second.

Lipids Extraction and Characterization. Lipids were extracted on the dried biomass. Both the raw and the two residual biomasses (I and II residual biomass) were dried at 60 °C for 24 h. Lipids were obtained as reported by Bligh and Dyer.[32] Nitrogen flux was used to dry, recover, and weigh lipids. Lipid fractionation was performed by solubilizing them in chloroform and using a commercial prepacked column containing a stationary phase made of Florisil. Neutral lipids were eluted with chloroform:methanol (2:1, v/v), fatty acids with 2% acetic acid in diethyl-ether, whereas phospholipids were eluted with 100% methanol. The recovered fatty acids were then characterized by GC–MS, as previously reported.[33]

Statistical Analyses. Results are reported as mean of results obtained after three independent experiments (mean ± SD) and compared by one-way analysis of variance according to Bonferroni's method (post hoc) using Graphpad Prism for Windows, version 6.01.

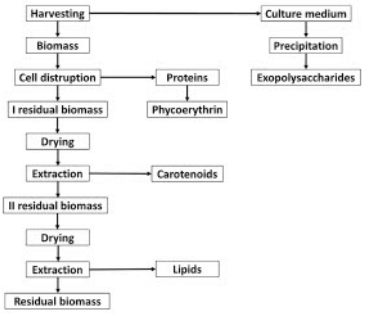

Figure 1. Schematic representation of the applied process.

RESULTS AND DISCUSSION

Exopolysaccharide Recovery and Characterization. Figure 1 reports the extraction strategy used to recover different molecules from *P. cruentum*. At the end of cell growth, medium, generally regarded as waste, was collected and polysaccharides were isolated by precipitation using ethanol or 2-propanol. The EPS content was measured by the phenol–sulfuric acid method and no difference between the two applied solvents was observed (ethanol yield 0.100 ± 0.020 and 2-propanol 0.116 ± 0.020 mg/mL); thus ethanol was selected because of its wide range of applications.[34] The EPS yield was found to be 300 ± 67 mg/L of culture medium, which corresponds to an EPS yield of 0.53 $g/g_{d.w.biomass}$. The monosaccharide composition was achieved by GC–MS analysis, after derivatization as acetylated methyl glycosides (AMGs). The GC–MS chromatogram disclosed the presence of mainly xylose (Xyl), galactose (Gal), and glucose (Glc). Finally, traces of rhamnose (Rha), glucuronic acid (GlcA), and glucosamine (GlcN) were detected (Figure 2).

Because the EPSs from *P. cruentum* are known to be sulfated, the elemental composition analysis was performed. Results, reported in Table 1, indicate that the % of sulfur present in the sample is similar to that reported in the literature (7.4% ± 0.2%).[35,36] No proteins were detected.

Biomass Exploitation. *Phycoerythrin Extraction Optimization.* To extract PE, different extraction procedures were evaluated, as described in Materials and Methods. Total protein concentration was determined by colorimetric assay (BCA), whereas PE, phycocyanin (PC), and allophycocyanin (APC) concentrations were obtained using the Bennet and Bogorad equations (reported in the Material and Methods section). As shown in Table 2, the amount of PE was similar in all the analyzed samples, whereas PC and APC were found to be most abundant only in the extract obtained by French Press. Indeed, the presence of APC and PC in the French Press extract halved the purity grade of the extract with respect to those obtained for the other three extracts.

Supernatants were also analyzed by SDS-PAGE followed by Coomassie staining (Figure S2A, Supporting Information) and UVA light exposure, taking advantage of chromophores present in PE (Figure S2B, Supporting Information). The analyses revealed two major bands, whose molecular weights corresponded to α and β subunits (17 kDa) and γ subunit (30

https://doi.org/10.1021/acssuschemeng.2c05869
ACS Sustainable Chem. Eng. XXXX, XXX, XXX−XXX

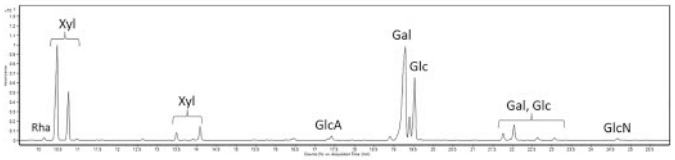

Figure 2. GC–MS chromatogram of the AMG of *P. cruentum* exopolysaccharides recovered from the culture medium. In the graph, the relative ion current abundance is reported as a function of retention time (min).

Table 1. Elemental Composition and Protein Content of EPS[a]

O (%)	N (%)	H (%)	C (%)	S (%)	protein content (mg/mL)
76.0 ± 2.4	1.1 ± 0.6	2.6 ± 0.4	13.1 ± 1.3	7.4 ± 0.2	N.D.

[a]Elements were measured by an elemental analyzer. Oxygen % was calculated by subtracting the % of the other elements from 100%. % are expressed as mg of each element/mg of analyzed EPS. Protein content was measured by colorimetric assay.

Table 2. Total Protein and Phycobiliprotein Concentration, Extraction Yield, and Phycoerythrin Purity Grade Obtained for Each Extraction Protocol[a]

	maceration	sonication	freeze and thaw	French press
protein yield (%)	44 ± 5	35 ± 4	35 ± 3	37 ± 6
PE yield (%)	1.8 ± 0.1	1.8 ± 0.8	1.8 ± 0.5	1.4 ± 0.7
PE purity grade (Abs_{562nm}/Abs_{280nm})	0.8 ± 0.1	0.9 ± 0.1	1.1 ± 0.1	0.4 ± 0.2
PC yield (%)	0.14 ± 0.02	0.48 ± 0.1	0.21 ± 0.1	1.4 ± 0.5
APC yield (%)	0.13 ± 0.1	0.2 ± 0.1	0.5 ± 0.02	1.1 ± 0.2

[a]Total protein concentration was obtained by BCA assay and total PE, PC, and APC concentration by Bennett and Bogorad equations. Yields are expressed as $g_{protein}/g_{d.w.biomass}$. The PE purity grade was calculated from the Abs_{562nm}/Abs_{280nm} ratio.

kDa) of PE, in each lane. Results suggested ultrasound as the most promising method. As biomass storage is a crucial step in industrial-scale processes, also from a logistically point of view,[37] extractions were performed by ultrasound on either fresh or frozen biomass (stored at −80 °C) for different lengths of time (from 4 to 20 min). At the end of each extraction, the disrupted biomass was analyzed by SDS-PAGE (Figure S2C,D, Supporting Information). Supernatants obtained after 20 min extraction seemed to be the best choice for fresh biomass, as 4 min extraction allowed to recover a PE content of 1.8% (Table 2) with a purity grade of 0.9 (Table 2), whereas 20 min of sonication on fresh biomass allowed to recover a PE content of 3.0 ± 0.4% with a purity grade of 1.5 ± 0.3. These extraction values are higher with respect to those obtained, after 20 min of sonication, from the frozen biomass: PE content of 2.2 ± 0.2 to 3.0 ± 0.4% for frozen and fresh biomass, respectively, and a PE purity grade of 1.0 ± 0.2 and 1.5 ± 0.3 for frozen and fresh biomass, respectively.

Phycoerythrin Purification and Structure Determination. PE purification was performed by comparing three techniques: anion-exchange chromatography, gel filtration, and ultrafiltration. The results of the different techniques are reported in the Supporting Information (Figure S2E–G, Supporting Information). Only the size-exclusion chromatography allowed obtaining pure PE; in particular, this purification step allowed to recover about 80% of PE and to reach a purity grade of 4.0. It is known that a purity grade ≥4.0 indicates a protein to be used in analytical grade.[38] According to the overall results, this approach allowed obtaining high-purity grade PE by only one step extraction and purification. To the best of our knowledge, this is the first time that PE was extracted and purified with such a purity grade by using only a single purification step.[39−42] To determine the protein identity and purity, PE was crystallized, and its X-ray structure was determined at 1.60 Å resolution. The X-ray structure is constituted by 5990 atoms, including five phycoerythrobilin (PEB) chromophores for each $\alpha\beta$ dimer, one methylated Asn in position β72 (Figure 3A) for each β subunit, two sulfate ions, and 324 water molecules and refines to *R* factor/*R*free values of 0.222/0.256. The structure confirms the formation of the $(\alpha\beta)_3$ hexamer (Figure 3C,D) but does not allow to identify the exact location of the γ subunit (Figure 3E). Similar results were obtained in previous studies[43,44] and were attributed to rotational disorder of the γ subunit within the protein crystal and to the finding that the electron density of this subunit is averaged out by the threefold crystallographic symmetry. The α subunit contains 164 residues, the β subunit 177 residues. The overall structure of the protein is very similar to that previously reported and deposited in the Protein Data Bank under accession code 3V58, obtained from crystals grown under different experimental conditions, but at the same pH. After superposition, the 164 CA atoms of the α subunit have a root-mean-square (r.m.s.) deviation of 0.146 Å, and the 177 CA atoms of β subunit have an r.m.s. deviation of 0.142 Å. Each $\alpha\beta$ dimer has five PEBs in position α82, α139, β61, β82, and β158. The first PEB, which adopts two alternate conformations in our structure, is covalently attached to the side chain of Cys82 of the α subunit by ring A. The second PEB is bound to Cys139 of the same subunit. The other three PEBs are found in the β subunit. They are bound to the side chains of Cys61, Cys82, and Cys158. The stereochemistry of the chromophores and their interaction with protein residues are basically identical to that observed in the starting model[28] and previously described. An example of the well-defined electron density maps of the

https://doi.org/10.1021/acssuschemeng.2c05869
ACS Sustainable Chem. Eng. XXXX, XXX, XXX−XXX

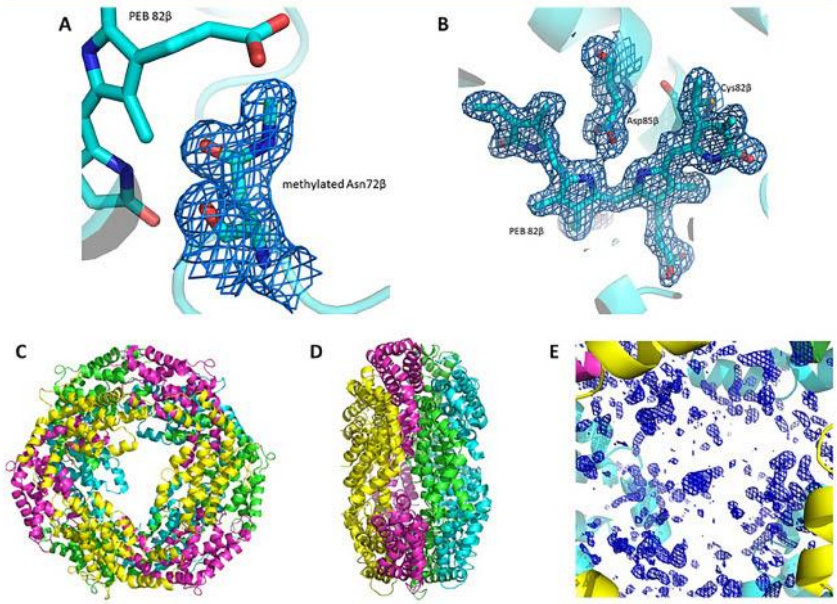

Figure 3. PE crystal structure. (A) 2Fo-Fc electron density map (1.0σ) of the methylated Asn72β in the structure of PE. (B) 2Fo-Fc electron density maps contoured at 1.0σ of one of the five PEB chromophores found in the structure of PE. (C) $(\alpha\beta)_3$ hexamer shown from the upper view and the lateral view (D). Electron density of the central cavity is shown in panel E. This segment of electron density should contain information on the location of the γ subunit.

chromophores is reported in Figure 3B. To verify the presence of a γ subunit, PE crystals were dissolved and analyzed by UV−vis absorption spectroscopy, SDS-PAGE analyses, and mass spectrometry. The UV−vis absorption spectrum (Figure S3A, Supporting Information) showed a peculiar shoulder at 498 nm, ascribed to the phycourobilin chromophore of the γ subunit. SDS-PAGE analysis (Figure S3B, Supporting Information) showed the presence of two molecular species, whose molecular mass was compatible with α and β subunits (double bands at about 17 kDa) and with the γ subunit (30 kDa). In situ digestion was performed on the bands and the peptide mixtures were analyzed by MALDI-TOF; peptide mass fingerprinting was performed by MS digest of homologue phycoerythrin sequences. The assignment of each mass spectrometry signal allowed highlighting the peptide sequence along the entire protein sequence. As shown in Figure 4,BA, the MS analysis of lower band enabled tracing the peptide sequence (labeled in bold and underlined) for the α and β chains, displaying a sequence coverage of 64 and 61%, respectively. The MS analysis of the higher band, on the other hand, revealed that the signals were attributed to two γ-chains with comparable sequence coverage (59.3 and 43.5%), as shown in Figure 4C,D. The presence of the two γ subunits has been previously found in the structure of the entire phycobilisome solved by electron microscopy (PDB code 6KGX).[45] The heptameric structures of PE, with the two different γ subunits, extracted from PDB code 6KGX are reported in Figure 5, with the same orientation.

Carotenoid Extraction and Characterization. Carotenoid extraction was performed by using a conventional method on both residual biomass (herein referred as I residual biomass) and on the raw one, used as benchmark (as reported in the Materials and Methods section). HPLC analyses (Figure 6) revealed that zeaxanthin and β-carotene were the major pigments present in the two extracts. Quantification analyses for the two carotenoids are reported in Table 3 and indicate that all the zeaxanthin isoforms present in the I residual biomass represented about 55% of those present in the raw biomass, whereas β-carotene isoform recovery was about 210% with respect to the raw biomass. It is important to point out that the carotenoids yield obtained from the I residual biomass was comparable to the one obtained by innovative green extractions performed on the residual biomass of the same species,[4] thus suggesting the feasibility of the proposed process.

Lipid Extraction and Characterization. According to the strategy described in Figure 1, lipid extraction represented the last class of the proposed process, after a drying step. To verify

https://doi.org/10.1021/acssuschemeng.2c05869
ACS Sustainable Chem. Eng. XXXX, XXX, XXX−XXX

Figure 4. α, β, and γ chain sequences of *P. cruentum* detected by MALDI-TOF analysis. (A) α chain sequence displaying the different peptides (bold and underlined) compared to P11392 (PHEA_PORPP) sequence on UniProt. (B) β chain sequence displaying the different peptides (bold and underlined) compared to P11393 (PHEB_PORPP) sequence on UniProt. (C) γ chain sequence displaying the different peptides (bold and underlined) compared to A0A5J4YX19 (PHEB_PORPP) sequence on UniProt. (D) γ chain sequence displaying the different peptides (bold and underlined) compared to A0A5J4YZM7 (PHEB_PORPP) sequence on UniProt.

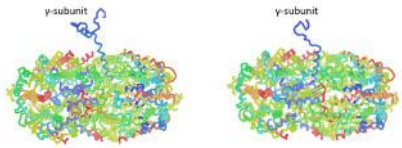

Figure 5. Heptameric $(\alpha\beta)_3\gamma$ structures observed in the phycobilisome from *P. cruentum*.

if the previous extractions could affect lipid composition, control experiments were performed by determining the composition of the lipid fraction obtained after PE extraction (I residual biomass) and after PE and carotenoid extraction (II residual biomass). The extractions were performed according to Bligh and Dyer,[32] followed by a solid phase extraction (SPE). As shown in Table 4, a 14% yield of total lipids was obtained from the raw biomass, whereas about 29% were extracted from the I residual biomass (i.e., after protein extraction). Nevertheless, when lipids were extracted from the II residual biomass (i.e., after protein and carotenoid extractions), the yield (14.1%) was comparable to those calculated for the raw biomass. Interestingly, the gas chromatography analysis of the fatty acid fraction revealed a clear trend: while polyunsaturated fatty acids (PUFAs) decreased during the cascade extractions (from 26 to 14 to 4%), a clear increase in the yield of saturated fatty acids (SFAs) was observed (from 72 to 76 to 93%). SFAs are considered now as an interesting new class of molecules, thanks to their chemical stability, responsible for their well-defined melting points and biocompatibility. Thus, they have been proposed as new materials for drug-controlled release or simply as antibacterial molecules.[18,19]

CONCLUSIONS

The strategy proposed in Figure 1 was found to be effective, because an innovative and reliable strategy was set up to sequentially recover high-added-value products from *P. cruentum* culture. In particular, (i) *P. cruentum* culture is completely employed to recover intra- and extracellular class of high-added-value molecules; (ii) the yield of each extracted class of molecules is similar to those obtained when extractions are performed to recover single class of molecules; and (iii) according to the biorefinery principles, all the class of molecules have been recovered starting from the one with the highest market value. Simultaneous microalgae culture valorization and carbon capture can contribute to the sustainable expansion of the microalgae market.

ASSOCIATED CONTENT

Supporting Information

The Supporting Information is available free of charge at https://pubs.acs.org/doi/10.1021/acssuschemeng.2c05869.

Crystallographic data; PE extraction and purification analyses; carotenoid identification (PDF)

https://doi.org/10.1021/acssuschemeng.2c05869
ACS Sustainable Chem. Eng. XXXX, XXX, XXX−XXX

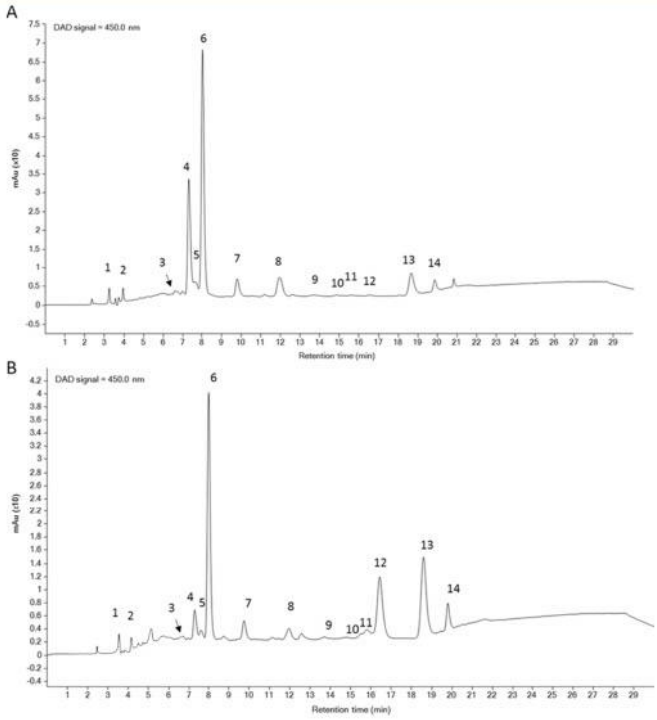

Figure 6. Representative HPLC–DAD chromatograms of carotenoids extracted from *P. cruentum* biomass. (A) Raw biomass; (B) I residual biomass (after PE extraction). Peak numbers and their identification are reported in Table S2, Supporting Information.

Table 3. Comparison between Zeaxanthin, β-Carotene, and Their Isomers in the Raw and I Residual Extracts

peak number	retention time (min)	peak identification	raw biomass ($mg/g_{extract}$)	I residual biomass ($mg/g_{extract}$)
5	7.668	zeaxanthin isomer I	1.03	0.64
6	8.057	zeaxanthin	21.37	11.79
7	9.826	zeaxanthin isomer II	2.84	1.69
13	18.701	β-carotene	0.20	0.44
14	18.892	β-carotene isomer	0.04	0.07

Table 4. Total Lipid Yields[a]

	lipid yield (%)	neutral lipids (%)	phospholipids (%)	fatty acids (%)	PUFA (%)	SFA (%)
raw biomass	14.0 ± 2.6	11.2 ± 1.5	12.0 ± 4.0	3.7 ± 0.3	25.8 ± 4.6	71.7 ± 13.6
I residual biomass	28.8 ± 1.5	10.2 ± 0.3	10.6 ± 0.3	2.5 ± 0.2	14.4 ± 1.9	76.3 ± 5.8
II residual biomass	14.1 ± 0.4	9.1 ± 0.6	3.8 ± 0.4	1.6 ± 0.2	4.3 ± 0.8	92.8 ± 7.2

[a]Lipids mean yields are reported as the percentage of the ratio between each lipidic class after SPE and dried raw biomass.

https://doi.org/10.1021/acssuschemeng.2c05869
ACS Sustainable Chem. Eng. XXXX, XXX, XXX−XXX

AUTHOR INFORMATION

Corresponding Author

Daria Maria Monti − *Department of Chemical Sciences, University of Naples Federico II, Naples 80126, Italy;* orcid.org/0000-0002-1136-0576; Email: mdmonti@unina.it

Authors

Davide Liberti − *Department of Chemical Sciences, University of Naples Federico II, Naples 80126, Italy;* orcid.org/0000-0003-1255-5030

Paola Imbimbo − *Department of Chemical Sciences, University of Naples Federico II, Naples 80126, Italy*

Enrica Giustino − *Department of Chemical Sciences, University of Naples Federico II, Naples 80126, Italy*

Luigi D'Elia − *Department of Chemical Sciences, University of Naples Federico II, Naples 80126, Italy;* orcid.org/0000-0002-6557-1715

Giarita Ferraro − *Department of Chemical Sciences, University of Naples Federico II, Naples 80126, Italy*

Angela Casillo − *Department of Chemical Sciences, University of Naples Federico II, Naples 80126, Italy*

Anna Illiano − *Department of Chemical Sciences, University of Naples Federico II, Naples 80126, Italy;* orcid.org/0000-0003-1491-8966

Gabriella Pinto − *Department of Chemical Sciences, University of Naples Federico II, Naples 80126, Italy;* orcid.org/0000-0001-9169-3452

Maria Chiara Di Meo − *Department of Sciences and Technologies (DST), University of Sannio, Benevento 82100, Italy*

Gerardo Alvarez-Rivera − *Laboratory of Foodomics, Institute of Food Science Research, CIAL, CSIC, Madrid 28049, Spain;* orcid.org/0000-0003-1657-8141

Maria Michela Corsaro − *Department of Chemical Sciences, University of Naples Federico II, Naples 80126, Italy;* orcid.org/0000-0002-6834-8682

Angela Amoresano − *Department of Chemical Sciences, University of Naples Federico II, Naples 80126, Italy*

Armando Zarrelli − *Department of Chemical Sciences, University of Naples Federico II, Naples 80126, Italy;* orcid.org/0000-0001-7866-821X

Elena Ibáñez − *Laboratory of Foodomics, Institute of Food Science Research, CIAL, CSIC, Madrid 28049, Spain*

Antonello Merlino − *Department of Chemical Sciences, University of Naples Federico II, Naples 80126, Italy;* orcid.org/0000-0002-1045-7720

Complete contact information is available at: https://pubs.acs.org/10.1021/acssuschemeng.2c05869

Author Contributions

D.L. and D.M.M. designed the concept and supervised the experiments. D.L., P.I., E.G., and L.D.E. performed the experimental work with microalgae. G.F. grew the crystals of PE and performed the X-ray diffraction data collection and data processing. A.M. solved and refined the structure of PE. A.C. and M.M.C. analyzed EPSs. A.I., G.P., and A.A. analyzed PE sequence. M.C.D.M. and A.Z. analyzed lipid composition. G.A.-R. and E.I. analyzed carotenoids. D.L. P.I, E.G., and D.M.M. wrote the manuscript. Both G.F. and A.M. analyzed the structure and wrote the crystallographic sections of the paper. All authors have read and agreed to the published version of the manuscript.

Notes

The authors declare no competing financial interest.

ACKNOWLEDGMENTS

P.I. would like to acknowledge ALGAE4IBD project (FROM NATURE TO BEDSIDE-ALGAE BASED BIO COMPOUND FOR PREVENTION) funded by the European Union's Horizon 2020 Research and Innovation program under grant agreement N° 101000501. This work was supported by the Ministry of Science and Innovation of Spain (Grant No. PID2020-113050RB-I00). G.A.-R. would like to acknowledge the Ministry of Science and Innovation (MICINN) for his 'Juan de la Cierva-Incorporación' postdoctoral grant IJC2019-041482-I. A.M. and G.F. thank Elettra Synchrotron of Trieste staff for their help during X-ray diffraction data collection.

REFERENCES

(1) Zhang, S.; Liu, Z. Advances in the Biological Fixation of Carbon Dioxide by Microalgae. *J. Chem. Technol. Biotechnol.* **2021**, *96*, 1475−1495.

(2) Bhalamurugan, G. L.; Valerie, O.; Mark, L. Valuable Bioproducts Obtained from Microalgal Biomass and Their Commercial Applications: A Review. *Environ. Eng. Res.* **2018**, *23*, 229−241.

(3) Yen, H. W.; Hu, I. C.; Chen, C. Y.; Ho, S. H.; Lee, D. J.; Chang, J. S. Microalgae-Based Biorefinery - From Biofuels to Natural Products. *Bioresour. Technol.* **2013**, *135*, 166−174.

(4) Gallego, R.; Martínez, M.; Cifuentes, A.; Ibáñez, E.; Herrero, M. Development of a Green Downstream Process for the Valorization of *Porphyridium Cruentum* Biomass. *Molecules* **2019**, *24*, 1564.

(5) Imbimbo, P.; Bueno, M.; D'Elia, L.; Pollio, A.; Ibañez, E.; Olivieri, G.; Monti, D. M. Green Compressed Fluid Technologies To Extract Antioxidants and Lipids from *Galdieria Phlegrea* in a Biorefinery Approach. *ACS Sustainable Chem. Eng.* **2020**, *8*, 2939−2947.

(6) Feller, R.; Matos, Â. P.; Mazzutti, S.; Moecke, E. H. S.; Tres, M. V.; Derner, R. B.; Oliveira, J. V.; Junior, A. F. Polyunsaturated ω-3 and ω-6 Fatty Acids, Total Carotenoids and Antioxidant Activity of Three Marine Microalgae Extracts Obtained by Supercritical CO_2 and Subcritical N-Butane. *J. Supercrit. Fluids* **2018**, *133*, 437−443.

(7) Di Lena, G.; Casini, I.; Lucarini, M.; Lombardi-Boccia, G. Carotenoid Profiling of Five Microalgae Species from Large-Scale Production. *Food Res. Int.* **2019**, *120*, 810−818.

(8) Rebolloso Fuentes, M. M.; Acién Fernández, G. G.; Sánchez Pérez, J. A.; Guil Guerrero, J. L. Biomass Nutrient Profiles of the Microalga *Porphyridium Cruentum*. *Food Chem.* **2000**, *70*, 345−353.

(9) Gaignard, C.; Gargouch, N.; Dubessay, P.; Delattre, C.; Pierre, G.; Laroche, C.; Fendri, I.; Abdelkafi, S.; Michaud, P. New Horizons in Culture and Valorization of Red Microalgae. *Biotechnol. Adv.* **2019**, *37*, 193−222.

(10) Rodriguez-Concepcion, M.; Avalos, J.; Bonet, M. L.; Boronat, A.; Gomez-Gomez, L.; Hornero-Mendez, D.; Limon, M. C.; Meléndez-Martínez, A. J.; Olmedilla-Alonso, B.; Palou, A.; Ribot, J.; Rodrigo, M. J.; Zacarias, L.; Zhu, C. A Global Perspective on Carotenoids: Metabolism, Biotechnology, and Benefits for Nutrition and Health. *Prog. Lipid Res.* **2018**, *70*, 62−93.

(11) Xiao, R.; Zheng, Y. Overview of Microalgal Extracellular Polymeric Substances (EPS) and Their Applications. *Biotechnol. Adv.* **2016**, *34*, 1225−1244.

(12) De Jesus Raposo, M. F.; De Morais, R. M. S. C.; De Morais, A. M. M. B. Bioactivity and Applications of Sulphated Polysaccharides from Marine Microalgae. *Mar. Drugs* **2013**, *11*, 233−252.

(13) Mišurcová, L.; Škrovánková, S.; Samek, D.; Ambrožová, J.; Machů, L. Health Benefits of Algal Polysaccharides in Human Nutrition. *Adv. Food Nutr. Res.* **2012**, *66*, 75−145.

(14) Dvir, I.; Stark, A. H.; Chayoth, R.; Madar, Z.; Arad, S. M. Hypocholesterolemic Effects of Nutraceuticals Produced from the Red Microalga *Porphyridium Sp.* in Rats. *Nutrients* **2009**, *1*, 156−167.

(15) Huheihel, M.; Ishanu, V.; Tal, J.; Arad, S. Activity of *Porphyridium Sp.* Polysaccharide against Herpes Simplex Viruses *in Vitro* and *in Vivo*. *J. Biochem. Biophys. Methods* **2002**, *50*, 189–200.
(16) Meléndez-Martínez, A. J.; Mapelli-Brahm, P.; Stinco, C. M. The Colourless Carotenoids Phytoene and Phytofluene: From Dietary Sources to Their Usefulness for the Functional Foods and Nutricosmetics Industries. *J. Food Compos. Anal.* **2018**, *67*, 91–103.
(17) Qiu, J.; Madoz-Gurpide, J.; Misek, D. E.; Kuick, R.; Brenner, D. E.; Michailidis, G.; Haab, B. B.; Omenn, G. S.; Hanash, S. Development of Natural Protein Microarrays for Diagnosing Cancer Based on an Antibody Response to Tumor Antigens. *J. Proteome Res.* **2004**, *3*, 261–267.
(18) Yoon, B.; Jackman, J.; Valle-González, E.; Cho, N. J. Antibacterial Free Fatty Acids and Monoglycerides: Biological Activities, Experimental Testing, and Therapeutic Applications. *Int. J. Mol. Sci.* **2018**, *19*, 1114.
(19) Xue, K.; Lv, S.; Zhu, C. Bringing Naturally-Occurring Saturated Fatty Acids into Biomedical Research. *J. Mater. Chem. B* **2021**, *9*, 6973–6987.
(20) Brody, M.; Emerson, R. The Effect of Wavelength and Intensity of Light on the Proportion of Pigments in *Porphyridium Cruentum*. *Am. J. Bot.* **1959**, *46*, 433–440.
(21) Geresh, S.; Adin, I.; Yarmolinsky, E.; Karpasas, M. Characterization of the Extracellular Polysaccharide of *Porphyridium Sp.*: Molecular Weight Determination and Rheological Properties. *Carbohydr. Polym.* **2002**, *50*, 183–189.
(22) Ricciardelli, A.; Casillo, A.; Vergara, A.; Balasco, N.; Corsaro, M. M.; Tutino, M. L.; Parrilli, E. Environmental Conditions Shape the Biofilm of the Antarctic Bacterium *Pseudoalteromonas Haloplanktis* TAC125. *Microbiol. Res.* **2019**, *218*, 66–75.
(23) Álvarez-Gómez, F.; Korbee, N.; Casas-Arrojo, V.; Abdala-Díaz, R. T.; Figueroa, F. L. UV Photoprotection, Cytotoxicity and Immunology Capacity of Red Algae Extracts. *Molecules* **2019**, *24*, 341.
(24) Bennett, A.; Bogobad, L. Complementary chromatic adaptation in a filamentous blue-green alga. *J. Cell Biol.* **1973**, *58*, 419–435.
(25) Russo Krauss, I.; Merlino, A.; Vergara, A.; Sica, F. An Overview of Biological Macromolecule Crystallization. *Int. J. Mol. Sci.* **2013**, *14*, 11643.
(26) Vonrhein, C.; Flensburg, C.; Keller, P.; Sharff, A.; Smart, O.; Paciorek, W.; Womack, T.; Bricogne, G. Data Processing and Analysis with the autoPROC Toolbox. *Acta Crystallogr. Sect. D Biol. Crystallogr.* **2011**, *67*, 293–302.
(27) McCoy, A. J.; Grosse-Kunstleve, R. W.; Adams, P. D.; Winn, M. D.; Storoni, L. C.; Read, R. J. Phaser Crystallographic Software. *J. Appl. Crystallogr.* **2007**, *40*, 658–674.
(28) Camara-Artigas, A.; Bacarizo, J.; Andujar-Sanchez, M.; Ortiz-Salmeron, E.; Mesa-Valle, C.; Cuadri, C.; Martin-Garcia, J. M.; Martinez-Rodriguez, S.; Mazzuca-Sobczuk, T.; Ibañez, M. J.; Allen, J. P. PH-Dependent Structural Conformations of B-Phycoerythrin from *Porphyridium Cruentum*. *FEBS J.* **2012**, *279*, 3680–3691.
(29) Emsley, P.; Cowtan, K. Coot: Model-Building Tools for Molecular Graphics. *Acta Crystallogr. Sect. D Biol. Crystallogr.* **2004**, *60*, 2126–2132.
(30) Murshudov, G. N.; Vagin, A. A.; Dodson, E. J. Refinement of Macromolecular Structures by the Maximum-Likelihood Method. *Acta Crystallogr. Sect. D Biol. Crystallogr.* **1997**, *53*, 240–255.
(31) Aremu, A. O.; Masondo, N. A.; Molnár, Z.; Stirk, W. A.; Ördög, V.; Van Staden, J. Changes in Phytochemical Content and Pharmacological Activities of Three Chlorella Strains Grown in Different Nitrogen Conditions. *J. Appl. Phycol.* **2016**, *28*, 149–159.
(32) Bligh, E. G.; Dyer, W. J. A Rapid Method of Total Lipid Extraction and Purification. *Can. J. Biochem. Physiol.* **1959**, *37*, 911–917.
(33) Imbimbo, P.; Romanucci, V.; Pollio, A.; Fontanarosa, C.; Amoresano, A.; Zarrelli, A.; Olivieri, G.; Monti, D. M. A Cascade Extraction of Active Phycocyanin and Fatty Acids from *Galdieria Phlegrea*. *Appl. Microbiol. Biotechnol.* **2019**, 9455–9464.
(34) Melo, T.; Figueiredo, A. R. P.; da Costa, E.; Couto, D.; Silva, J.; Domingues, M. R.; Domingues, P. Ethanol Extraction of Polar Lipids from *Nannochloropsis Oceanica* for Food, Feed, and Biotechnology Applications Evaluated Using Lipidomic Approaches. *Mar. Drugs* **2021**, *19*, 593.
(35) Bernaerts, T. M. M.; Kyomugasho, C.; Van Looveren, N.; Gheysen, L.; Foubert, I.; Hendrickx, M. E.; Van Loey, A. M. Molecular and Rheological Characterization of Different Cell Wall Fractions of *Porphyridium Cruentum*. *Carbohydr. Polym.* **2018**, *195*, 542–550.
(36) Ben Hlima, H.; Smaoui, S.; Barkallah, M.; Elhadef, K.; Tounsi, L.; Michaud, P.; Fendri, I.; Abdelkafi, S. Sulfated Exopolysaccharides from *Porphyridium Cruentum*: A Useful Strategy to Extend the Shelf Life of Minced Beef Meat. *Int. J. Biol. Macromol.* **2021**, *193*, 1215–1225.
(37) Gruber-Brunhumer, M. R.; Jerney, J.; Zohar, E.; Nussbaumer, M.; Hieger, C.; Bromberger, P.; Bochmann, G.; Jirsa, F.; Schagerl, M.; Obbard, J. P.; Fuchs, W.; Drosg, B. Associated Effects of Storage and Mechanical Pre-Treatments of Microalgae Biomass on Biomethane Yields in Anaerobic Digestion. *Biomass Bioenergy* **2016**, *93*, 259–268.
(38) Fernández-Rojas, B.; Hernández-Juárez, J.; Pedraza-Chaverri, J. Nutraceutical Properties of Phycocyanin. *J. Funct. Foods* **2014**, *11*, 375–392.
(39) Nguyen, H. P. T.; Morançais, M.; Déléris, P.; Fleurence, J.; Nguyen-Le, C. T.; Vo, K. H.; Dumay, J. Purification of R-Phycoerythrin from a Marine Macroalga *Gracilaria Gracilis* by Anion-Exchange Chromatography. *J. Appl. Phycol.* **2020**, *32*, 553–561.
(40) Serucnik, M.; Vicente, F. A.; Brecko, Ž.; Coutinho, J. A. P.; Ventura, S. P. M.; Žnidaršič-Plazl, P. Development of a Microfluidic Platform for R-Phycoerythrin Purification Using an Aqueous Micellar Two-Phase System. *ACS Sustainable Chem. Eng.* **2020**, *8*, 17097–17105.
(41) Vicente, F. A.; Cardoso, I. S.; Martins, M.; Gonçalves, C. V. M.; Dias, A. C. R. V.; Domingues, P.; Coutinho, J. A. P.; Ventura, S. P. M. R-Phycoerythrin Extraction and Purification from Fresh *Gracilaria Sp.* Using Thermo-Responsive Systems. *Green Chem.* **2019**, *21*, 3816–3826.
(42) Ulagesan, S.; Nam, T. J.; Choi, Y. H. Extraction and Purification of R-Phycoerythrin Alpha Subunit from the Marine Red Algae *Pyropia Yezoensis* and Its Biological Activities. *Molecules* **2021**, *26*, 6479.
(43) Ficner, R.; Huber, R. Refined Crystal Structure of Phycoerythrin from *Porphyridium Cruentum* at 0.23-Nm Resolution and Localization of the Gamma Subunit. *Eur. J. Biochem.* **1993**, *218*, 103–106.
(44) Ritter, S.; Hiller, R. G.; Wrench, P. M.; Welte, W.; Diederichs, K. Crystal Structure of a Phycourobilin-Containing Phycoerythrin at 1.90-Å Resolution. *J. Struct. Biol.* **1999**, *126*, 86–97.
(45) Ma, J.; You, X.; Sun, S.; Wang, X.; Qin, S.; Sui, S. F. Structural Basis of Energy Transfer in *Porphyridium Purpureum* Phycobilisome. *Nature* **2020**, *579*, 146–151.

https://doi.org/10.1021/acssuschemeng.2c05869
ACS Sustainable Chem. Eng. XXXX, XXX, XXX−XXX

Supporting information

Table of contents:

Table S1. Data collection and refinement statistics.

Data collection	
Space group	R3
a=b, c (Å)	186.590, 59.190
α=β, γ (°)	90.0, 120.0
Molecules for asymmetric unit	Two αβ dimers
Observed reflections	925709 (44973)
Unique reflections	100909 (5012)
Resolution (Å)	46.65– 1.60 (1.62– 1.60)
Completeness (%)	99.0 (98.3)
Rmerge (%)	0.101 (1.028)
Average I/σ(I)	12.9 (2.2)
Multiplicity	9.2 (9.0)
$CC_{1/2}$	0.997 (0.595)
Refinement	
Resolution (Å)	46.65 -1.60
N° reflections	95441
N° reflections in working set	6986
Rfactor/Rfree	0.223/0.256
N° non-H atoms in the refinement	5990
B-factor overall ($Å^2$)	18.1
Average B-factor	23.93
Ramachandran values (%)	
Most favoured/ Additional allowed	97.19
Outliers	0.62
R.m.s.d. from ideality	
R.m.s.d. bonds (Å)	0.010
R.m.s.d. angles (°)	1.602

Figure S1. PE crystals. Crystals were grown by hanging drop vapor diffusion method using a drop containing 10 mg/mL PE in 0.250 M ammonium sulphate, 0.025 M potassium phosphate at pH 5.0, equilibrated with a reservoir containing 0.500 M ammonium sulphate, 0.050 M potassium phosphate at pH 5.0.

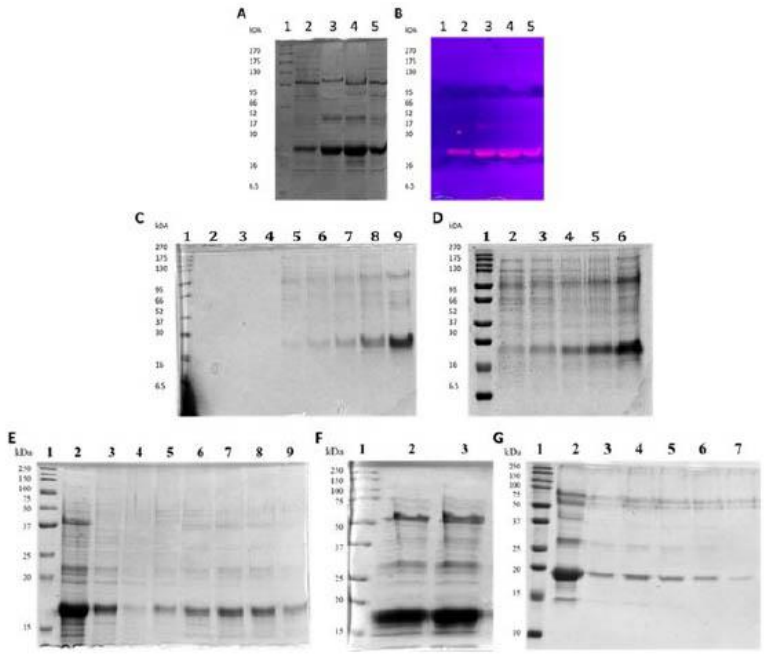

Figure S2. PE extraction and purification. Coomassie stained (**A**) and UVA light exposed unstained (**B**) SDS-PAGE analysis of total proteins extracted with different techniques. Lane 1: protein molecular weight markers; lane 2: Freeze & thaw extract; lane 3: Ultrasound extract; lane 4: Maceration extract; lane 5: French Press extract. 30 µg of total proteins were loaded in each lane. **C, D,** Coomassie staining of SDS-PAGE. Proteins were extracted by ultrasounds for different times. **(C)** fresh biomass and **(D)** frozen biomass. **C:** Lane 1: protein molecular weight markers; lanes 2-4: empty lanes; lanes 5-9: proteins extracted for 4, 8, 12, 16, and 20 minutes, respectively. **D:** Lane 1: protein molecular weight markers; lanes 2-6: proteins extracted for 4, 8, 12, 16, and 20 minutes, respectively. **E-G.** SDS-PAGE analysis of different procedures to isolate PE from *P. cruentum*. **E**: Anion-exchange. Lane 1: molecular weight markers; lane 2: total protein extract, lane 3: unbound; lane 4: washing fraction 1; lane 5: washing fraction 3; lane 6-9: samples eluted by 0.25 M NaCl. **F**: Ultrafiltration. Lane 1: molecular weight markers; lane 2: total protein extract; lane 3: ultrafiltration retentate. **G**: Size exclusion chromatography. Lane 1: molecular weight markers; lane 2: total protein extract; lanes 3-7: samples eluted from gel filtration. In all lanes, 30 µg of total proteins were analyzed.

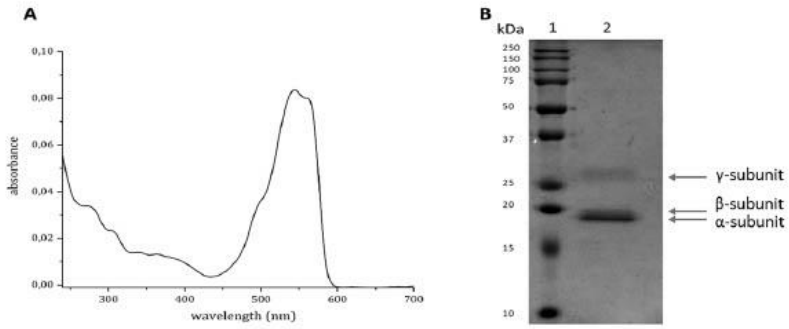

Figure S3. Analyses of PE dissolved crystals. A: UV-vis spectrum obtained from PE dissolved crystals. Spectrum was acquired at 25 °C, in the range 400–700 nm. **B**: SDS-PAGE analyses of PE dissolved crystals. Lane 1: molecular weight markers; lane 2: 20 µL of PE dissolved crystals.

Table S2. Tentatively identified compounds from *P. cruentum* extracts by HPLC-DAD-APCI-QTOF-MS/MS analysis, including peak annotation, high-resolution mass spectrometry features and UV–Vis maxima.

Peak	RT (min)	Identification	Experimental $[M+H]^+$ *m/z*	UV–Vis maxima (nm)	MS/MS product ions
1	3.471	Chlorophyll derivative I	549.4875	340s, 380s, 428	307.1400, 97.1048
2	4.177	Chlorophyll derivative II	549.4871	340s, 380s, 428	305.1354, 255.0720
3	6.658	Phaeophorbid B, methyl ester	623.2851	420	565.2795, 499.2056
4	7.347	Pheophytin derivative	909.5374	340s, 380s, 428	631.2374, 559.2071
5	7.668	Zeaxanthin isomer I	569.4357	422, 446, 474	464.8067, 281.2215, 175.1480
6	8.057	Zeaxanthin	569.4342	420s, 445, 476	423.3309, 338.2549, 175.1480
7	9.826	Zeaxanthin isomer II	569.4365	422, 446, 474	539.4249, 175.1480
8	11.920	3-Acetylpheophytin a	887.5709	410	609.2687, 549.2495
9	13.621	Divinyl pheophytin a	869.5547	410	592.2652, 487.1950
10	14.656	Plastoquinone	749.6235	420	551.3212, 495.2654, 151.0743
11	14.862	Pheophytin b	885.5527	420	607.2536, 503.2403
12	16.500	Pheophytin a	871.5739	420	594.2828, 533.2567
13	18.701	β-Carotene	537.4441	420s, 450, 480	375.2935, 173.1293
14	18.892	β-Carotene isomer	537.4456	420s, 450, 480	261.1637, 146.1004

antioxidants

MDPI

Article

Shedding Light on the Hidden Benefit of *Porphyridium cruentum* Culture

Davide Liberti [1], Paola Imbimbo [1,*], Enrica Giustino [1], Luigi D'Elia [1], Mélanie Silva [2], Luísa Barreira [2] and Daria Maria Monti [1,*]

[1] Department of Chemical Sciences, University of Naples Federico II, Via Cinthia 4, 80126 Naples, Italy
[2] Centre of Marine Sciences, University of Algarve, 8005-139 Faro, Portugal
* Correspondence: paola.imbimbo@unina.it (P.I.); mdmonti@unina.it (D.M.M.)

Abstract: Microalgae can represent a reliable source of natural compounds with different activities. Here, we evaluated the antioxidant and anti-inflammatory activity of sulfated exopolysaccharides (s-EPSs) and phycoerythrin (PE), two molecules naturally produced by the red marine microalga *Porphyridium cruentum* (CCALA415). *In vitro* and cell-based assays were performed to assess the biological activities of these compounds. The s-EPSs, owing to the presence of sulfate groups, showed biocompatibility on immortalized eukaryotic cell lines and a high antioxidant activity on cell-based systems. PE showed powerful antioxidant activity both *in vitro* and on cell-based systems, but purification is mandatory for its safe use. Finally, both molecules showed anti-inflammatory activity comparable to that of ibuprofen and helped tissue regeneration. Thus, the isolated molecules from microalgae represent an excellent source of antioxidants to be used in different fields.

Keywords: microalgae; exopolysaccharides; phycoerythrin; antioxidant activity; anti-inflammatory activity; biocompatibility; wound healing

Citation: Liberti, D.; Imbimbo, P.; Giustino, E.; D'Elia, L.; Silva, M.; Barreira, L.; Monti, D.M. Shedding Light on the Hidden Benefit of *Porphyridium cruentum* Culture. *Antioxidants* **2023**, *12*, 337. https://doi.org/10.3390/antiox12020337

Academic Editors: Antonella D'Anneo and Marianna Lauricella

Received: 9 January 2023
Revised: 25 January 2023
Accepted: 26 January 2023
Published: 31 January 2023

1. Introduction

Microalgae are ubiquitous eukaryotic photosynthetic microorganisms that are able to live in different environments, in single colonies, chains, or groups; depending on the species, their size can vary from a few to hundreds of micrometers [1–3]. The biodiversity of microalgae is mainly due to their unique ability to adapt and grow even under unfavorable growth conditions (e.g., extreme temperatures, variable salinity, and low or high light intensity) and to produce a wide range of interesting chemical compounds with novel structures and biological activities [4,5]. Among the microalgae, the red marine microalga *Porphyridium cruentum* could be pointed to as a commercial source of various high-value bioproducts [1], to be recovered from the same culture, in order to make the whole process economically feasible [6–10]. In particular, *P. cruentum* produces sulfated exopolysaccharides (s-EPSs) that are accumulated in a layer surrounding the cytoplasmic membrane. These exopolysaccharides act as a mucilage, because *P. cruentum* is without a well-defined cell wall [11]. They are composed of glucuronic acid and several major neutral monosaccharides, such as D- and L-Gal, D-Glc, D-Xyl, D-GlcA, and sulfate groups. S-EPSs from *P. cruentum* have antioxidant [12], immunomodulatory, anti-inflammatory, hypocholesterolemic, antimicrobial, and antiviral activity [13,14]. S-EPSs from *P. cruentum* also exhibit specific rheological properties that can be exploited in food applications [12,15]. In addition to exopolysaccharides, *P. cruentum* produces a broad range of colored pigments, including chlorophylls, carotenoids, and phycobilins, which are commercially utilized in the food, pharmaceutical, and cosmetic industries [16]. Amongst them, phycoerythrin (PE) is a light-harvesting protein with a structure of $(\alpha\beta)_6\gamma$ complex and a MW ranging from 240 to 260 kDa. Due to its unique biological properties, PE has gained much attention from the food and pharmaceutical industries and in the molecular biology field [17–22]. Here, starting from our recent results [10], a comprehensive study on the biological activities

of s-EPSs and purified phycoerythrin was carried out in order to verify if the extraction techniques could affect their biological activities.

2. Materials and Methods

2.1. Reagents

All solvents, reagents, and chemicals were purchased from Sigma-Aldrich (St Louis, MO, USA).

2.2. Biocompounds Isolation

S-EPSs and PE were isolated and purified from the culture of *Porphyridium cruentum* (CCALA415) as previously described [10]. Briefly, at the end of cell growth, the culture was centrifuged to recover s-EPSs in the supernatant. The s-EPSs were precipitated by adding pure ethanol (1:2 *v*/*v*) and centrifuging the sample (12,000× *g*, 30 min, and 4 °C). The supernatant was discarded, and the precipitate was freeze-dried. S-EPSs yield was 300 ± 67 g/L, which corresponds to 0.53 $g/g_{d.w.\ biomass}$. In the case of PE, a crude aqueous extract was obtained *via* sonication (40% amplitude; 20 min, 30 s on and 30 s off) from the harvested biomass. PE was then isolated *via* a one-step purification procedure as reported by Liberti, up to a purity grade of 4 [10].

2.3. Eukaryotic Cell Culture and Biocompatibility Assay

Immortalized human keratinocytes (HaCaT, Innoprot, Derio, Spain) and immortalized murine fibroblasts Balb/c-3T3 (ATCC, Virginia, USA) were cultured in 10% foetal bovine serum in Dulbecco's modified Eagle's medium, in the presence of 1% penicillin/streptomycin and 2 mM L-glutamine, in a 5% CO_2 humidified atmosphere at 37 °C. To verify the biocompatibility of the crude extract of s-EPSs and of purified PE, cells were seeded in 96-well plates at a density of 2×10^3/well and, 24 h after seeding, were incubated with increasing concentrations of the extract/compounds (5 to 75 µg/mL for EPS, 5 to 500 µg/mL of total proteins for crude extracts, and 5 nM to 100 nM for purified PE) for 72 h. At the end of the incubation period, cell viability was assessed with the MTT assay. Cell survival is expressed as the percentage of viable cells in the presence of compounds compared with control cells (represented by the average obtained between untreated cells and cells supplemented with the highest concentration of buffer).

2.4. In Vitro Antioxidant Assays

The antioxidant activity of the extract/compounds was tested by measuring their ability to scavenge the free radicals 1,1-diphenyl-2-picrylhydrazyl radical and 2,2′-azinobis-[3-ethylbenzthiazoline-6-sulfonic acid] (DPPH and ABTS, respectively) and to reduce or chelate redox active iron and copper (ferric-reducing antioxidant power (FRAP); iron-chelating activity (ICA), and copper-chelating activity (CCA), respectively). DPPH and FRAP assays were performed following the procedure reported by Rodrigues et al. [23], and ascorbic acid and butylhydroxytoluene (BHT), respectively, were used as positive controls at the same concentrations of the sample under test. The ability of the extract/compounds to scavenge the ABTS radical was assessed as previously reported [24]. The results were compared to a calibration curve obtained using Trolox (6-hydroxy-2,5,7,8-tetramethylchromane-2-carboxylic acid) as the standard. ICA and CCA were determined by measuring the formation of the Fe^{2+}-ferrozine complex and by using pyrocatechol violet, respectively, according to the method reported by Megias [25]. EDTA was used as a standard at a final concentration of 100 µg/mL. S-EPS or purified PE was tested between 0.05 and 120 µg/mL and 0.2 and 270 nM, respectively. The results are expressed as IC_{50}, i.e., the concentration required to scavenge 50% of the free radical or as the highest percentage achieved.

2.5. Determination of Intracellular ROS Levels on Eukaryotic Cell Lines by DCFDA Assay

The protective effect of s-EPSs (from 5 to 75 µg/mL) or purified PE (10 nM) against oxidative stress was measured by determining the intracellular reactive oxygen species (ROS) levels, following the protocol used by Imbimbo [26].

2.6. Determination of Intracellular Glutathione Levels (DTNB Assay) and Lipid Peroxidation Levels (TBARS Assay) on Eukaryotic Cell Lines

Intracellular GSH levels and lipid peroxidation levels were measured by following the procedure described by Petruk [27] using 12 µg/mL of s-EPSs or 10 nM of purified PE.

2.7. Anti-Inflammatory Activity

The anti-inflammatory activity of the compounds was tested by their ability to inhibit cyclooxygenase-2 (COX-2). S-EPS or purified PE was tested at different concentrations (4 and 167 µg/mL for s-EPSs or 10 and 27 nM for purified PE) using a commercial inhibitory screening assay kit, Cayman test kit-560131 (Cayman Chemical Company, Ann Arbor, MI, USA). Ibuprofen was used as a positive control. Results are expressed as a percentage of inhibition of COX-2.

2.8. Wound Healing Assay

Wound healing was assessed with a scratch assay. HaCaT cells were seeded at a cell density of 3×10^5 cells/cm^2 for 24 h, to allow cells to reach about 95% of confluence. Then, cells were washed with PBS, scratched manually with a 200 µL pipet tip, and incubated with 12 µg/mL of s-EPSs or 10 nM of purified PE. The scratch size was monitored at 0 h and 24 h by acquiring images using optical microscopy (Zeiss LSM 710, Zeiss, Germany) at 10× magnification. The width of the wound was measured by using Zen Lite 2.3 software (Zeiss, Germany). Results are expressed as a reduction of the area (fold) compared with untreated cells.

2.9. Statistical Analyses

All the experiments were performed in triplicate. Results are presented as the mean of results obtained after three independent experiments (mean ±SD) and compared by one-way ANOVA according to Bonferroni's method (post hoc) using GraphPad Prism for Windows, version 6.01 (Dotmatics, California, USA).

3. Results

3.1. s-Exopolysaccharides Characterization

3.1.1. s-EPSs Biocompatibility on Cell-Based Model

s-EPSs were tested for their biocompatibility on two eukaryotic immortalized cell lines: HaCaT (human keratinocytes) and Balb/c-3T3 (murine fibroblasts). Twenty-four hours after seeding, cells were incubated with increasing amounts of s-EPSs (from 5 to 75 µg/mL). After 72 h of incubation, cell viability was assessed by the MTT assay; cell survival is expressed as the percentage of viable cells in the presence of s-EPSs compared with that of control samples (i.e., untreated cells). The results in Figure 1 show that, under all the experimental conditions, the s-EPSs were fully biocompatible on both the cell lines analyzed.

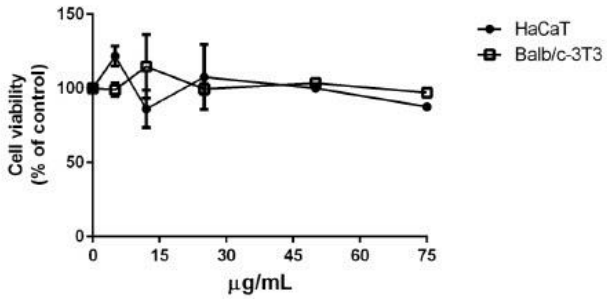

Figure 1. Effect of s-EPSs from *P. cruentum* on cell viability. Dose–response curves of HaCaT (black dots) and Balb/c-3T3 (empty squares) cells after 72 h of incubation with increasing concentrations of exopolysaccharides (5–75 µg/mL). Cell viability is reported as a function of s-EPS concentration.

3.1.2. s-EPSs *In Vitro* Antioxidant Activity

The antioxidant activity of s-EPS was evaluated with different *in vitro* analyses: ABTS, DPPH, FRAP, and iron and copper chelating assays. As shown in Table 1, s-EPSs were not able to scavenge the ABTS and DPPH radicals, whereas a slight but significant activity was observed for the chelation of iron and for ferric ion reduction assays. Both tests are based on the ability to act on iron: the former measures the ability of the compounds under test to bind Fe^{2+}, whereas the latter analyzes the ability to reduce Fe^{3+} to Fe^{2+}. As for the copper chelating assay, the highest activity reached, at the highest concentration tested, was 9 ± 3%, a value much lower than the one obtained by testing the positive control molecule at the same concentration.

Table 1. *In vitro* antioxidant and chelating activity of s-EPSs. Results are expressed as percentage of inhibition. The concentration evaluated is referred to the final concentration of s-EPSs or positive control used in the well.

Test	Concentration (µg/mL)	s-EPSs Activity (%)	C+ Activity (%)
FRAP	120	34 ± 3	97 ± 1
ABTS	25	2 ± 2	98 ± 2
DPPH	50	1 ± 1	52 ± 1
ICA	55	66 ± 3	91 ± 1
CCA	45	9 ± 3	91 ± 2

3.1.3. s-EPSs Antioxidant Activity on a Cell-Based Model

The antioxidant activity of s-EPSs was also evaluated on HaCaT cells. For this purpose, cells were incubated with increasing concentrations of s-EPSs (from 5 to 50 µg/mL) for 2 h, and then oxidative stress was induced by UVA irradiation (100 J/cm^2). Immediately after irradiation, the intracellular ROS levels were measured by using H_2DCFDA as a probe. For each set of experiments, untreated cells were used as a control. As shown in Figure 2, UVA treatment significantly increased the DCF fluorescence (black bars, $p < 0.001$). In the absence of stress, s-EPSs induced a slight but significant increase in the intracellular ROS level (Figure 2, white, dashed grey, and dark grey bars on the left part of the graph). Interestingly, when cells were preincubated with s-EPSs prior to being stressed, only 5 and 12 µg/mL were able to protect the cells from ROS formation (Figure 2, light grey and white bars on the right part of the graph), whereas the higher concentrations had no protective effect. This result is in agreement with those of Giordano et al. [28], as antioxidants act at low

concentrations, whereas, at high concentrations, they may work as pro-oxidants. Based on these results, s-EPSs were used at 12 μg/mL for further experiments.

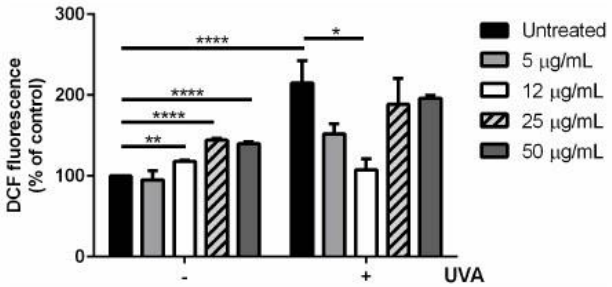

Figure 2. Antioxidant activity of s-EPSs on UVA-stressed HaCaT cells. Intracellular ROS levels were determined with DCFDA assay. Cells were preincubated in the presence of increasing amounts (from 5 to 50 μg/mL) of s-EPSs for 2 h prior to UVA irradiation (100 J/cm^2). Results are expressed as percentages compared with untreated cells. Black bars refer to untreated cells; light grey bars refer to cells incubated with 5 μg/mL of s-EPSs; white bars refer to cells incubated with 12 μg/mL; dashed bars refer to cells incubated with 25 μg/mL; dark grey bars refer to cells incubated with 50 μg/mL of s-EPSs in the absence (−) or presence (+) of UVA stress. Data shown are means ± S.D. of three independent experiments. * indicates $p < 0.05$, ** indicates $p < 0.01$, and **** indicates $p < 0.001$.

To deeply analyze the protective effect of s-EPSs, the intracellular glutathione levels and lipid peroxidation levels were determined with DTNB and TBARS assays, respectively. In the absence of any treatment, a significant decrease ($p < 0.01$) in GSH levels was observed after UVA exposure (Figure 3A), and s-EPSs (grey bars) were able to inhibit GSH oxidation, thus confirming a protective effect against oxidative stress. As for the TBARS assay, a significant increase ($p < 0.05$) in lipid peroxidation levels was observed after UVA treatment (black bars, Figure 3B), but, notably, this effect was inhibited upon pretreatment with s-EPSs (grey bars). Treatment of the cells with exopolysaccharides did not significantly alter either glutathione or lipid peroxidation levels in the absence of UVA treatment (−). Taken together, the results clearly indicate that s-EPSs are able to protect cells from oxidative damage.

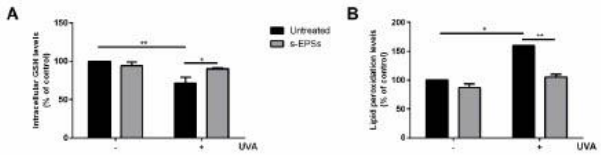

Figure 3. Protective effect of s-EPSs on HaCaT cells. Intracellular GSH levels were determined with a DTNB assay (**A**) and lipid peroxidation levels were determined with a TBARS assay (**B**). Cells were preincubated in the presence of 12 μg/mL of s-EPSs for 2 h prior to UVA irradiation (100 J/cm^2). GSH and lipid peroxidation levels were measured 90 min after UVA irradiation. Black bars refer to untreated cells, and grey bars refer to cells incubated with s-EPSs, in the absence (−) or in the presence (+) of UVA stress. Values are expressed as percentages compared with untreated cells. Data shown are means ± S.D. of three independent experiments. * Indicates $p < 0.05$; ** indicates $p < 0.01$.

3.1.4. *In Vitro* Anti-Inflammatory Activity of s-EPSs

As inflammation is a condition strictly linked to oxidative stress, the anti-inflammatory activity of s-EPSs was measured by evaluating their capacity to inhibit the enzyme COX-2. When inflammation occurs, COX-2 is able to enhance the prostanoid production [29]. As reported in Table 2, surprisingly, s-EPSs showed no significant differences compared with ibuprofen used as positive control when tested at the same concentration, thus suggesting a new role of s-EPSs in inflammation control.

Table 2. *In vitro* s-EPSs anti-inflammatory activity.

	Concentration (μg/mL)	Inhibition (%)
s-EPSs	167	77 ± 8
Ibuprofen	167	99 ± 1

3.2. Phycoerythrin Characterization

3.2.1. Phycoerythrin Biocompatibility on Immortalized Eukaryotic Cells

Following biomass lysis, phycoerythrin (PE) had a purity grade of 1.5 [10]. This value is considered as reagent-grade, thus indicating that the protein can be used as it is for food applications [30]. In order to verify the safety of the protein on eukaryotic cells, an MTT assay was performed by comparing the crude extract with the purified protein (purity grade of four). The results of the MTT assay, reported in Figure 4, clearly show that only pure PE was fully biocompatible with both cell lines (Figure 4B), while the crude extract exerted a dose-dependent toxicity (Figure 4A). These results clearly indicate that PE needs to be purified to a higher purity grade before being used on cell-based models, or, at least, that it cannot be applied when present in the extract at concentrations higher than a certain threshold (100 μg/mL).

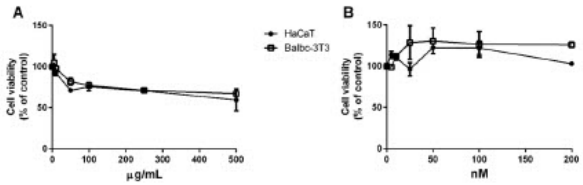

Figure 4. Biocompatibility of total extract (**A**) and purified PE (**B**) on eukaryotic cells. Dose–response curves of HaCaT (black dots) and Balb/c-3T3 cells (empty squares) after 72 h of incubation with increasing concentrations of total extract (**A**) and purified PE (**B**). Cell viability was assessed with an MTT assay and is reported as a function of extract/protein concentration.

3.2.2. *In Vitro* Antioxidant Activity

In vitro analysis of the antioxidant activity of purified PE was carried out with the abovementioned experimental procedures. As reported in Table 3, purified PE was not able to scavenge the DPPH radical or chelate copper ions. However, it demonstrated a high capacity to scavenge the ABTS radical ion and to reduce ferric iron or chelate iron with considerably low IC_{50} values (0.072 ± 0.004 and 0.084 ± 0.012 μM, 0.084 ± 0.004 μM, respectively). Noteworthy, the purified PE IC_{50} values were about 160, 1000, and 600 times lower than the IC_{50} values obtained with the positive control molecules (Trolox, 12 ± 1 μM in the ABTS; BHT, 90 ± 4 μM in the FRAP; and EDTA, 51 ± 3 μM in the ICA).

Table 3. *In vitro* antioxidant and chelating activity of purified PE. Results are expressed as IC_{50} values, μM.

Test	Purified PE	Positive Control
	IC_{50} (μM)	
ABTS	0.072 ± 0.004	12 ± 1
DPPH	>0.27	29 ± 2
FRAP	0.084 ± 0.012	90 ± 4
ICA	0.084 ± 0.004	51 ± 3
CCA	>0.1	63 ± 2

3.2.3. Cell-Based Antioxidant Activity of PE

Starting from the encouraging results obtained *in vitro*, purified PE was tested on the UVA-stressed HaCaT experimental system used for s-EPSs. Cells were treated with 2.5 μg/mL (10 nM) of purified PE for 2 h, and then oxidative stress was induced by UVA irradiation (100 J/cm^2). At the end of irradiation, the intracellular ROS levels were evaluated. As shown in Figure 5, UVA induced a significant increase in intracellular ROS levels (black bars, 200%) compared with untreated cells ($p < 0.001$). When cells were treated with purified PE (grey bars), no increase in intracellular ROS levels was observed. Interestingly, when cells were incubated with purified PE prior to UVA exposure, an inhibition of the intracellular ROS production was observed.

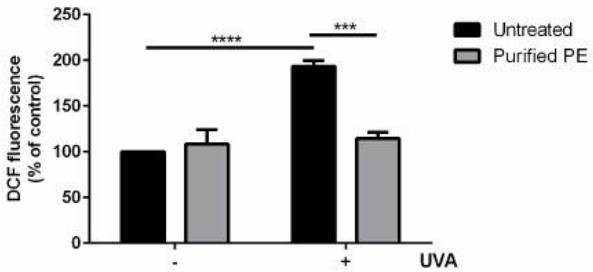

Figure 5. Protective effect of purified PE on UVA-stressed HaCaT cells. Intracellular ROS levels were determined with DCFDA assay. Cells were preincubated in the presence of 10 nM of purified PE (grey bars) for 2 h prior to UVA irradiation (100 J/cm^2). Black bars refer to untreated cells in the absence (–) or in the presence (+) of UVA stress. Values are expressed as percentages compared with untreated cells. Data shown are means ± S.D. of three independent experiments. *** indicates $p < 0.005$; **** indicates $p < 0.001$ with respect to UVA-treated cells.

The effect of purified PE on GSH and lipid peroxidation was also assessed. As shown in Figure 6, PE was able to fully protect cells from oxidative stress, as no alteration in either the GSH levels (Figure 6A) or in the lipid peroxidation levels (Figure 6B) was found when the cells were pretreated with purified PE prior to stress, thus confirming the protective effect of the protein against oxidative stress.

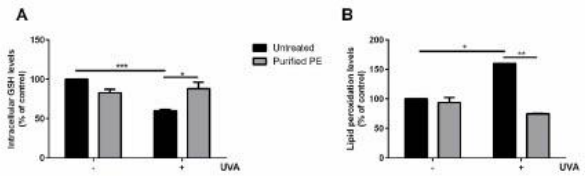

Figure 6. Analysis of intracellular GSH and lipid peroxidation levels on HaCaT cells. Cells were preincubated with 10 nM of purified PE for 2 h before UVA irradiation (100 J/cm^2). (**A**) determination of intracellular GSH levels; (**B**) analysis of lipid peroxidation levels. In both experiments, measurements were recorded 90 min after UVA-induced stress. Values are expressed as a percentage compared with control (i.e., untreated) cells. Data shown are means ± S.D. of three independent experiments. * indicates $p < 0.05$, ** indicates $p < 0.01$, and *** indicates $p < 0.005$.

3.2.4. *In Vitro* PE Anti-Inflammatory Activity

Purified PE was also able to inhibit COX-2 (Table 4) by about 75%, although the level of inhibition attained with ibuprofen 24 nM could not be achieved at any of the analyzed concentrations.

Table 4. COX-2 inhibition by purified PE.

Sample	Concentration (nM)	Inhibition (%)
Phycoerythrin	27	75 ± 8
	10	72 ± 8
Ibuprofen	24	96 ± 1

3.3. Effect of s-EPSs and Purified PE on Wound Healing

Finally, a scratch assay was carried out on HaCaT cells to test the ability of s-EPSs and purified PE to induce cell migration related to wound repairing. The results are reported in Figure 7 and in Table 5. In the absence of any treatment, the cells spontaneously migrated to induce the re-epithelialization. Interestingly, when the cells were treated with either s-EPSs or purified PE, a significant enhancement in the wound closure was observed after 24 h. Indeed, s-EPSs reduced the scratched area by 2.5 ± 0.17-fold and purified PE by 2.4 ± 0.1317-fold compared with untreated cells (1.80 ± 0.02-fold reduction).

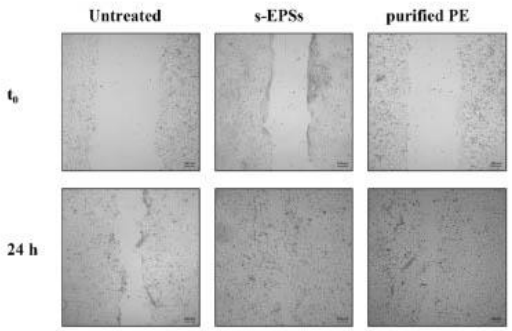

Figure 7. Effect of s-EPSs and purified PE on wound healing. Confluent HaCaT cells were scratched and treated with either 12 µg/mL s-EPSs or 10 nM purified PE for 24 h. Optical microscopy images were acquired at 10× magnification at the beginning (t_0) and end (24 h) of the incubation.

Table 5. Reduction of area (fold) of wound closure upon 24 h of incubation with either s-EPSs or purified PE. Data shown are means ± S.D. of three independent experiments. For each experiment, at least 10 images were acquired. * indicates $p < 0.05$.

Sample	Reduction in Area (Fold)
Untreated	1.80 ± 0.02
s-EPSs	2.50 ± 0.17 *
Purified PE	2.40 ± 0.13 *

* = $p < 0.05$.

4. Discussion

As the use of synthetic molecules is known to be harmful in the long run, the search for new natural compounds endowed with beneficial properties is urgent [31]. In this context, antioxidants from microalgae could represent an excellent alternative, but the costs of microalgae upstream and downstream processes are still too high [32].

We recently set up a cascade approach to recover four classes of molecules from *P. cruentum* culture: s-EPSs, PE, carotenoids, and saturated fatty acids. Among them, here, we evaluated the biological activity of s-EPSs and PE. S-EPSs were chosen as it is generally thought that polysaccharides with a high sulfated content have biological activities [33], such as antioxidant action [34]. It is known that antioxidant molecules can bind metal ions, forming metal–ion complexes. The presence of sulfate groups could increase the metal-binding capacity of the carbohydrates by donating an electron pair or by losing a proton, thus stabilizing the complex [35,36].

In agreement with the findings of Wang et al., we found that s-EPSs had no radical scavenging activity against DPPH, whereas they showed antioxidant activity in the ABTS assay, with IC_{50} values ranging from 6.59 to 8.92 mg/mL [37]. Interestingly, despite the low antioxidant activity observed *in vitro*, s-EPSs were active on a cell-based system at a concentration almost 600 times lower than that measured *in vitro*. This result is in agreement with literature, as it is well known that *in vitro* assays should not be compared with cell-based ones. Indeed, antioxidants provide their function by different mechanisms of action, so that bioavailability, stability, retention, or reactivity of the compound under test in a complex system, such as that of eukaryotic cells, cannot be either mimicked or evaluated *in vitro* [38]. Our results indicated that s-EPSs were able not only to inhibit the intracellular ROS production but also to prevent GSH depletion and lipid peroxidation.

Different is the case of PE, which was found to be a very powerful antioxidant agent *in vitro* and on a cell-based system. The ABTS assay was in line with that observed by Sonani on a PE from a different source (IC_{50} of 72 ± 4 nM vs. 101 nM, respectively) [39], whereas the PE prepared by this author had lower DPPH-scavenging (IC_{50} of 930 nM) and iron-chelating abilities (IC_{50} of 484 nM) than the purified PE prepared in this study. We hypothesize that the higher antioxidant activity measured in our experimental system may rely on the source or strain used. A different source may also affect the biocompatibility results: indeed, we found that only pure PE was biocompatible with eukaryotic cells, strongly suggesting the importance of purification of the protein for all the potential applications. Pure PE protected cells from UVA irradiation at a concentration in the low nanomolar range (10 nM). Generally, antioxidants prevent the generation of free radicals, which can significantly affect some physiological processes, including wound healing. In particular, ROS generation can damage tissues and slow down the regeneration process. The presence of antioxidants should counteract chronic inflammation and at the same time contribute to promoting tissue regeneration [40]. Considering that both s-EPSs and PE were able to inhibit one of the key enzymes in the inflammation process (COX-2) and to induce a significantly faster scratch closure compared with untreated cells, we can conclude that the bioproducts obtained by *P. cruentum* represent an excellent ingredient for new biomaterials, such as medical patches.

5. Conclusions

In this study, s-EPSs and PE, obtained from *P. cruentum* culture by a cascade approach described in a previous work [10], showed a remarkable antioxidant activity in a cell-based system, higher than that obtained by *in vitro* assays, thus suggesting that the reliability of *in vitro* assays has to be overhauled. Moreover, both molecules showed anti-inflammatory characteristics comparable with ibuprofen and a significant ability to promote cell proliferation.

Author Contributions: D.L., P.I. and D.M.M. designed the concept and supervised the experiments. D.L., P.I., E.G. and L.D. performed the experimental work with microalgae. D.L., P.I., E.G. and D.M.M. wrote the manuscript. L.B. supervised M.S. on the in vitro experiments. All authors have read and agreed to the published version of the manuscript.

Funding: This work was carried out with funding from the Portuguese Foundation for Science and Technology (FCT) through UIDB/04326/2020, UIDP/0436/2020, LA/P/0101/2020.

Institutional Review Board Statement: Not applicable.

Informed Consent Statement: Not applicable.

Data Availability Statement: The data presented in this study are available in the article.

Acknowledgments: P.I. would like to acknowledge the ALGAE4IBD project (From Natura to Bedside-Algae Based Bio Compound for Prevention) funded by the European Union's Horizon 2020 Research and Innovation program under grant agreement No. 101000501.

Conflicts of Interest: The authors declare no conflict of interest.

References

1. Mobin, S.; Alam, F. Some Promising Microalgal Species for Commercial Applications: A Review. *Energy Procedia* **2017**, *110*, 510–517. [CrossRef]
2. Alam, F.; Date, A.; Rasjidin, R.; Mobin, S.M.A.; Moria, H.; Baqui, A. Biofuel from Algae: Is It a Viable Alternative? In *Advances in Biofuel Production: Algae and Aquatic Plants*; Apple Academic Press: New York, NY, USA, 2014; pp. 32742–33487.
3. Suganya, T.; Varman, M.; Masjuki, H.H.; Renganathan, S. Macroalgae and Microalgae as a Potential Source for Commercial Applications along with Biofuels Production: A Biorefinery Approach. *Renew. Sustain. Energy Rev.* **2016**, *55*, 909–941. [CrossRef]
4. Herrero, M.; Mendiola, J.A.; Plaza, M.; Ibañez, E. Screening for Bioactive Compounds from Algae. In *Advanced Biofuels and Bioproducts*; Springer: New York, NY, USA, 2013; pp. 833–872.
5. Anbuchezhian, R.; Karuppiah, V.; Li, Z. Prospect of Marine Algae for Production of Industrially Important Chemicals. In *Algal Biorefinery: An Integrated Approach*; Springer: Cham, Switzerland, 2015; pp. 195–217.
6. Feller, R.; Matos, Â.P.; Mazzutti, S.; Moecke, E.H.S.; Tres, M.V.; Derner, R.B.; Oliveira, J.V.; Junior, A.F. Polyunsaturated ω-3 and ω-6 Fatty Acids, Total Carotenoids and Antioxidant Activity of Three Marine Microalgae Extracts Obtained by Supercritical CO_2 and Subcritical n-Butane. *J. Supercrit. Fluids* **2018**, *133*, 437–443. [CrossRef]
7. Di Lena, G.; Casini, I.; Lucarini, M.; Lombardi-Boccia, G. Carotenoid Profiling of Five Microalgae Species from Large-Scale Production. *Food Res. Int.* **2019**, *120*, 810–818. [CrossRef]
8. Rebolloso Fuentes, M.M.; Acién Fernández, G.G.; Sánchez Pérez, J.A.; Guil Guerrero, J.L. Biomass Nutrient Profiles of the Microalga *Porphyridium cruentum*. *Food Chem.* **2000**, *70*, 345–353. [CrossRef]
9. Gaignard, C.; Gargouch, N.; Dubessay, P.; Delattre, C.; Pierre, G.; Laroche, C.; Fendri, I.; Abdelkafi, S.; Michaud, P. New Horizons in Culture and Valorization of Red Microalgae. *Biotechnol. Adv.* **2019**, *37*, 193–222. [CrossRef]
10. Liberti, D.; Imbimbo, P.; Giustino, E.; D'elia, L.; Ferraro, G.; Casillo, A.; Illiano, A.; Pinto, G.; Di Meo, M.C.; Alvarez-Rivera, G.; et al. Inside out *Porphyridium Cruentum*: Beyond the Conventional Biorefinery Concept. *ACS Sustain. Chem. Eng.* **2023**, *11*, 381–389. [CrossRef]
11. Dvir, I.; Stark, A.H.; Chayoth, R.; Madar, Z.; Arad, S.M. Hypocholesterolemic Effects of Nutraceuticals Produced from the Red Microalga *Porphyridium* sp. in Rats. *Nutrients* **2009**, *1*, 156–167. [CrossRef]
12. Ben Hlima, H.; Smaoui, S.; Barkallah, M.; Elhadef, K.; Tounsi, L.; Michaud, P.; Fendri, I.; Abdelkafi, S. Sulfated Exopolysaccharides from *Porphyridium cruentum*: A Useful Strategy to Extend the Shelf Life of Minced Beef Meat. *Int. J. Biol. Macromol.* **2021**, *193*, 1215–1225. [CrossRef]
13. Mišurcová, L.; Škrovánková, S.; Samek, D.; Ambrožová, J.; Machů, L. Health Benefits of Algal Polysaccharides in Human Nutrition. *Adv. Food Nutr. Res.* **2012**, *66*, 75–145.

14. Gallego, R.; Martínez, M.; Cifuentes, A.; Ibáñez, E.; Herrero, M. Development of a Green Downstream Process for the Valorization of *Porphyridium cruentum* Biomass. *Molecules* **2019**, *24*, 1564. [CrossRef]
15. Medina-Cabrera, E.V.; Gansbiller, M.; Rühmann, B.; Schmid, J.; Sieber, V. Rheological Characterization of *Porphyridium sordidum* and *Porphyridium purpureum* Exopolysaccharides. *Carbohydr. Polym.* **2021**, *253*, 117237. [CrossRef]
16. Sudhakar, M.P.; Jagatheesan, A.; Perumal, K.; Arunkumar, K. Methods of Phycobiliprotein Extraction from *Gracilaria crassa* and Its Applications in Food Colourants. *Algal Res.* **2015**, *8*, 115–120. [CrossRef]
17. Kannaujiya, V.K.; Kumar, D.; Pathak, J.; Sinha, R.P. Phycobiliproteins and Their Commercial Significance. In *Cyanobacteria*; Elsevier: Amsterdam, The Netherlands, 2019; pp. 207–216.
18. Hsieh-Lo, M.; Castillo, G.; Ochoa-Becerra, M.A.; Mojica, L. Phycocyanin and Phycoerythrin: Strategies to Improve Production Yield and Chemical Stability. *Algal Res.* **2019**, *42*, 101600. [CrossRef]
19. Manirafasha, E.; Ndikubwimana, T.; Zeng, X.; Lu, Y.; Jing, K. Phycobiliprotein: Potential Microalgae Derived Pharmaceutical and Biological Reagent. *Biochem. Eng. J.* **2016**, *109*, 282–296. [CrossRef]
20. Simovic, A.; Combet, S.; Velickovic, T.C.; Nikolic, M.; Minic, S. Probing the Stability of the Food Colourant R-Phycoerythrin from Dried Nori Flakes. *Food Chem.* **2022**, *374*, 131780. [CrossRef]
21. Ganesan, A.R.; Subramani, K.; Shanmugam, M.; Seedevi, P.; Park, S.; Alfarhan, A.H.; Rajagopal, R.; Balasubramanian, B. A Comparison of Nutritional Value of Underexploited Edible Seaweeds with Recommended Dietary Allowances. *J. King Saud Univ.* **2020**, *32*, 1206–1211. [CrossRef]
22. García, A.B.; Longo, E.; Murillo, M.C.; Bermejo, R. Using a B-Phycoerythrin Extract as a Natural Colorant: Application in Milk-Based Products. *Molecules* **2021**, *26*, 297. [CrossRef]
23. Rodrigues, M.J.; Neves, V.; Martins, A.; Rauter, A.P.; Neng, N.R.; Nogueira, J.M.F.; Varela, J.; Barreira, L.; Custódio, L. In Vitro Antioxidant and Anti-Inflammatory Properties of *Limonium algarvense* Flowers' Infusions and Decoctions: A Comparison with Green Tea (*Camellia sinensis*). *Food Chem.* **2016**, *200*, 322–329. [CrossRef]
24. Re, R.; Pellegrini, N.; Proteggente, A.; Pannala, A.; Yang, M.; Rice-Evans, C. Antioxidant Activity Applying an Improved ABTS Radical Cation Decolorization Assay. *Free Radic. Biol. Med.* **1999**, *26*, 1231–1237. [CrossRef]
25. Megías, C.; Pastor-Cavada, E.; Torres-Fuentes, C.; Girón-Calle, J.; Alaiz, M.; Juan, R.; Pastor, J.; Vioque, J. Chelating, Antioxidant and Antiproliferative Activity of *Vicia sativa* Polyphenol Extracts. *Eur. Food Res. Technol.* **2009**, *230*, 353–359. [CrossRef]
26. Imbimbo, P.; Romanucci, V.; Pollio, A.; Fontanarosa, C.; Amoresano, A.; Zarrelli, A.; Olivieri, G.; Monti, D.M. A Cascade Extraction of Active Phycocyanin and Fatty Acids from *Galdieria phlegrea*. *Appl. Microbiol. Biotechnol.* **2019**, *103*, 9455–9464. [CrossRef] [PubMed]
27. Petruk, G.; Di Lorenzo, F.; Imbimbo, P.; Silipo, A.; Bonina, A.; Rizza, L.; Piccoli, R.; Monti, D.M.; Lanzetta, R. Protective Effect of *Opuntia ficus-indica* L. Cladodes against UVA-Induced Oxidative Stress in Normal Human Keratinocytes. *Bioorg. Med. Chem. Lett.* **2017**, *27*, 5485–5489. [CrossRef] [PubMed]
28. Giordano, M.E.; Caricato, R.; Lionetto, M.G. Concentration Dependence of the Antioxidant and Prooxidant Activity of Trolox in Hela Cells: Involvement in the Induction of Apoptotic Volume Decrease. *Antioxidants* **2020**, *9*, 1058. [CrossRef] [PubMed]
29. Landa, P.; Kokoska, L.; Pribylova, M.; Vanek, T.; Marsik, P. In Vitro Anti-Inflammatory Activity of Carvacrol: Inhibitory Effect on COX-2 Catalyzed Prostaglandin E2 Biosynthesisb. *Arch. Pharm. Res.* **2009**, *32*, 75–78. [CrossRef]
30. Fernández-Rojas, B.; Hernández-Juárez, J.; Pedraza-Chaverri, J. Nutraceutical Properties of Phycocyanin. *J. Funct. Foods* **2014**, *11*, 375–392. [CrossRef]
31. Montégut, L.; de Cabo, R.; Zitvogel, L.; Kroemer, G. Science-Driven Nutritional Interventions for the Prevention and Treatment of Cancer. *Cancer Discov.* **2022**, *12*, 2258–2279. [CrossRef]
32. Coulombier, N.; Jauffrais, T.; Lebouvier, N. Antioxidant Compounds from Microalgae: A Review. *Mar. Drugs* **2021**, *19*, 549. [CrossRef]
33. Wang, Y.; Xing, M.; Cao, Q.; Ji, A.; Liang, H.; Song, S. Biological Activities of Fucoidan and the Factors Mediating Its Therapeutic Effects: A Review of Recent Studies. *Mar. Drugs* **2019**, *17*, 183. [CrossRef]
34. de Souza, M.C.R.; Marques, C.T.; Dore, C.M.G.; da Silva, F.R.F.; Rocha, H.A.O.; Leite, E.L. Antioxidant Activities of Sulfated Polysaccharides from Brown and Red Seaweeds. *J. Appl. Phycol.* **2007**, *19*, 153–160. [CrossRef]
35. Bhunia, B.; Uday, U.S.P.; Oinam, G.; Mondal, A.; Bandyopadhyay, T.K.; Tiwari, O.N. Characterization, Genetic Regulation and Production of Cyanobacterial Exopolysaccharides and Its Applicability for Heavy Metal Removal. *Carbohydr. Polym.* **2018**, *179*, 228–243. [CrossRef]
36. Andrew, M.; Jayaraman, G. Structural Features of Microbial Exopolysaccharides in Relation to Their Antioxidant Activity. *Carbohydr. Res.* **2020**, *487*, 107881. [CrossRef]
37. Wang, W.-N.; Li, Y.; Zhang, Y.; Xiang, W.-Z.; Li, A.-F.; Li, T. Comparison on Characterization and Antioxidant Activity of Exopolysaccharides from Two Porphyridium Strains. *J. Appl. Phycol.* **2021**, *33*, 2983–2994. [CrossRef]
38. López-Alarcón, C.; Denicola, A. Evaluating the Antioxidant Capacity of Natural Products: A Review on Chemical and Cellular-Based Assays. *Anal. Chim. Acta* **2013**, *763*, 1–10. [CrossRef]

39. Sonani, R.R.; Singh, N.K.; Kumar, J.; Thakar, D.; Madamwar, D. Concurrent Purification and Antioxidant Activity of Phycobiliproteins from *Lyngbya* sp. A09DM: An Antioxidant and Anti-Aging Potential of Phycoerythrin in Caenorhabditis Elegans. *Process Biochem.* **2014**, *49*, 1757–1766. [CrossRef]
40. Alvarez, X.; Alves, A.; Ribeiro, M.P.; Lazzari, M.; Coutinho, P.; Otero, A. Biochemical Characterization of *Nostoc* sp. Exopolysaccharides and Evaluation of Potential Use in Wound Healing. *Carbohydr. Polym.* **2021**, *254*, 117303. [CrossRef]

Applied Microbiology and Biotechnology (2024) 108:390
https://doi.org/10.1007/s00253-024-13229-9

BIOTECHNOLOGICAL PRODUCTS AND PROCESS ENGINEERING

Unveiling the potential of *Pseudococcomyxa simplex*: a stepwise extraction for cosmetic applications

Paola Imbimbo[1] · Enrica Giustino[1] · Alfonso Ferrara[1] · Gerardo Alvarez-Rivera[2] · Hassan Annaz[3] · Elena Ibanez[2] · Maria Chiara Di Meo[4] · Armando Zarrelli[1] · Daria Maria Monti[1]

Received: 3 April 2024 / Revised: 24 May 2024 / Accepted: 7 June 2024

Abstract
Microalgae are gaining attention as they are considered green fabrics able to synthesize many bioactive metabolites, with unique biological activities. However, their use at an industrial scale is still a challenge because of the high costs related to upstream and downstream processes. Here, a biorefinery approach was proposed, starting from the biomass of the green microalga *Pseudococcomyxa simplex* for the extraction of two classes of molecules with a potential use in the cosmetic industry. Carotenoids were extracted first by an ultrasound-assisted extraction, and then, from the residual biomass, lipids were obtained by a conventional extraction. The chemical characterization of the ethanol extract indicated lutein, a biosynthetic derivative of α-carotene, as the most abundant carotenoid. The extract was found to be fully biocompatible on a cell-based model, active as antioxidant and with an in vitro anti-aging property. In particular, the lutein-enriched fraction was able to activate Nrf2 pathway, which plays a key role also in aging process. Finally, lipids were isolated from the residual biomass and the isolated fatty acids fraction was composed by palmitic and stearic acids. These molecules, fully biocompatible, can find application as emulsifiers and softener agents in cosmetic formulations. Thus, an untapped microalgal species can represent a sustainable source for cosmeceutical formulations.

Key points
- *Pseudococcomyxa simplex has been explored in a cascade approach.*
- *Lutein is the main extracted carotenoid and has antioxidant and anti-aging activity.*
- *Fatty acids are mainly composed of palmitic and stearic acids.*

Keywords *Pseudococcomyxa simplex* · Carotenoids · Fatty acids · Biorefinery · Cosmetics

Introduction

Cosmetic is one of the most remunerative industrial sectors in the world, constantly growing since 2004. It has been estimated that, in 2028, the revenues of the global cosmetic market will be nearly 129 billion USD. In particular, the beauty market is dominated by skincare, which is expected to reach 221.38 billion UDS by 2030 with a CAGR of 4.79% (https://straitsresearch.com/report/facial-skincare-products-market, accessed on 14 March 2024). Nowadays, consumers prefer to use natural cosmetics that are produced from natural sources that can be considered safe for humans and environment. This trend inversion is due not only to the growing environmental consciousness of the consumers, but also to their awareness of health issues that can occur by using synthetic compounds, such as hyperactivity, allergic

✉ Paola Imbimbo
paola.imbimbo@unina.it

✉ Daria Maria Monti
mdmonti@unina.it

[1] Department of Chemical Sciences, University of Naples Federico II, Via Cinthia 4, 80126 Naples, Italy

[2] Laboratory of Foodomics, Institute of Food Science Research, CIAL, CSIC, Nicolás Cabrera 9, 28049 Madrid, Spain

[3] College of Agriculture and Environmental Science, AgroBioSciences Program, University Mohammed VI Polytechnic, Ben Guerir, Morocco

[4] Department of Sciences and Technologies (DST), University of Sannio, 82100 Benevento, BN, Italy

Published online: 24 June 2024

reactions, or other side effects (Tang et al. 2020). Thus, different cosmetic companies are using biotechnology to ensure quality, efficacy, and safety of natural products (Bouzroud et al. 2023). Among natural sources, microalgae have gained attention as they are considered green fabrics able to synthesize a plethora of bioactive metabolites, endowed with unique biological activities (Liberti et al. 2023). Moreover, they are perceived as vegan, natural, and healthy by consumers. To date, only a few strains have been exploited for cosmetic purposes, such as *Spirulina*, *Dunaliella*, *Chlorella*, and *Haematococcus* (Yarkent et al. 2020). Despite the considerable potential of microalgae, some issues still limit their full industrialization, such as high upstream and downstream costs (Imbimbo et al. 2020). To make the use of microalgae sustainable and feasible, the biorefinery approach has been proposed as the technology is able to implement the circular economy and lowers the overall process costs (Igbokwe et al. 2022).

Carotenoids are pigments which can be used in different fields, such as the food and pharmaceutical industry, and recently, due to the potent antioxidant activity, they have attracted interest to be used as active ingredients in cosmetic formulations. Currently, the market is dominated by astaxanthin, β-carotene, zeaxanthin, lutein, and lycopene (Sathasivam and Ki 2018),

Lipids, and more in general oils, are one of the major components in cosmetic cream formulations (Franco et al. 2022). Based on their nature, they can be used for different purposes, such as softener agents, emulsifiers, detergents, and skin lighteners (De Luca et al. 2021). Fatty acids are used in cosmetics as emollients to improve the skin hydration, and as emulsifiers, since they can act as thickening agents. It has been reported that the ideal length of the carbon chain for fatty acids-based emulsion is 16–18, which correspond to palmitic and stearic acid (Cochran and Anthonavage 2015). Fatty acids are also physiological skin components that ensure the maintenance of skin barrier functions (Knox and O'Boyle 2021). In this paper, we proposed a biorefinery approach starting from the biomass of the green microalga *Pseudococcomyxa simplex* for the extraction of two classes of molecules with a potential use in cosmetic industry. Carotenoids were extracted as the first class of molecules by an ultrasound-assisted extraction coupled to maceration, and then, from the residual biomass, lipids were obtained by a conventional extraction. Finally, a chemical and biological characterization of both classes of molecules has been carried out to investigate a possible use of these molecules in cosmetic field.

Materials and methods

Reagents

All the reagents, unless differently specified, were purchased from Sigma-Aldrich (Milan, Italy).

Microalgae strain and cultivation

Pseudococcomyxa simplex (ACUF 127) was provided by the Algal Collection of the University Federico II (ACUF, www.acuf.net). The cultivation was carried out in bubble column photobioreactors in Bold Basal Medium (BBM) at 24 ± 2 °C with a constant light intensity of 100 PARs [($\mu mol_{photons}/m^2$)/s]. The culture was mixed by bubbling air through a sintered glass tube placed at the bottom of each reactor. Algal growth was monitored by measuring the absorbance at 730 nm.

The dry weight determination was carried out via conversion between the Optical Density (O.D.) and the biomass dry weight at the end of the exponential growth phase. The conversion factor was 1 O.D. corresponded to 0.22 mg dry weight. The biomass concentration achieved at the end of the exponential growth phase was 0.7 $g_{D.W.}/L$.

Pigments extraction and characterization

Pigments were extracted using ethanol as solvent, as previously reported (Imbimbo et al. 2023). Briefly, 200 mg of dry weight (D.W.) of alga were suspended in 4 mL of pure ethanol and disrupted by ultrasonication (40% amplitude, 4 min on ice, Bandelin SONOPULS HD 3200, tip MS73). The volume was adjusted to 20 mL and the mixture was shaken for 24 h at 250 rpm at 4 °C in the dark. Pigments were recovered in the supernatants by centrifugation at 5000 *g* for 10 min, and then, ethanol was removed under N_2 stream. The extraction yield was determined gravimetrically.

Carotenoids and pigment identification was performed by HPLC–DAD-APCI-QTOF-MS/MS. The analysis of the extracts was carried out in an Agilent 1290 UHPLC system (ultrahigh performance liquid chromatography) equipped with a diode-array detector (DAD), coupled to an Agilent 6540 quadrupole-time-of-flight mass spectrometer (q-TOF MS) equipped with an atmospheric pressure chemical ionization (APCI) source. A Thermo Fisher Scientific Accucore C30 column (2.6 µm, 4.6 × 50 mm) was used at 30 °C. Separation was achieved using a 12-min gradient program from 100% mobile phase A (90% methanol, 7% MTBE, 3% water) and 0% mobile phase B (90% MTBE, 10% methanol)

to 0% mobile phase A and 100% mobile phase B, and kept constant for 1.5 min before returning to the initial conditions within 1.5 min. The total run time was 15 min at a flow rate of 0.8 mL/min. The mass spectrometer was operated in positive ionization mode (APCI +), with gas temperature at 300 °C; drying gas at 8 L/min; vaporizer temperature at 350 °C; nebulizer pressure at 40 Psi; capillary voltage at 3500 V; corona + : 4 µA; fragmentor voltage at 110 V; and skimmer voltage at 45 V. The MS and auto MS/MS modes were set to acquire m/z values ranging between 25 and 1500, at a scan rate of 10 spectra per second. Auto MS/MS mode was operated at two collision-induced dissociation energies: 20 and 40 eV and selecting 4 precursor ions per cycle at a threshold of 200 counts.

Lipids extraction and characterization

Lipids were recovered by using the original Bligh and Dyer protocol (Bligh and Dyer 1959). Extractions were carried out on 300 mg of both freeze-dried biomass and residual freeze-dried biomass (i.e., after pigment extraction) using chloroform, methanol, and water in a ratio 2:2:1 (v/v/v) for 1 h at room temperature. At the end of the extraction, the hydrophobic phase was recovered by centrifugation and the extract was dried under N_2 stream. The lipid extract was then fractionated in three different lipid classes (i.e., neutral lipids, fatty acids, and phospholipids) by performing a solid-phase extraction (SPE) as previously described (Imbimbo et al. 2019). The recovered fatty acids were first derivatized by transforming them into the corresponding methyl esters and then identified and quantified by GC – MS analysis (Crescenzo et al. 2015).

Biological characterization

In vitro anti-aging assays

The in vitro anti-aging activity was evaluated by anti-tyrosinase and anti-elastase assays, as described by Mahdi et al. (Mahdi et al. 2024). Kojic acid was used as a commercial inhibitor. Values are reported as inhibitory concentration (IC_{50}), which represents the concentration of molecule able to inhibit 50% of the enzyme activity and expressed as milligram *per* milliliter (mg/mL).

Cell culture and biocompatibility of ethanol extract

Immortalized human keratinocytes (HaCaT) were from Innoprot (Biscay, Spain) and immortalized murine fibroblasts (BALB/c-3T3) were from ATCC (VA, USA). Cells were cultured in Dulbecco's modified Eagle's medium (DMEM), supplemented with 10% fetal bovine serum (HyClone), 2 mM L-glutamine, and antibiotics, under a 5% CO_2 humidified atmosphere at 37 °C. The biocompatibility of either ethanol extract or FAs was tested. HaCaT cells were seeded in 96-well plate at a density of 2.5×10^3 cells per well, whereas BALB/c-3T3 at a density of 3×10^3 cells per well. HaCaT cells were incubated with increasing concentration (from 0.5 to 100 µg/mL) of both ethanol extract and FAs for 24 and 48 h, whereas BALB/c-3T3 only with ethanol extract. At the end of the incubation, cell viability was assessed by the MTT assay, as previously reported (Liberti et al. 2023). Cell viability was expressed as the percentage of viable cells in the presence of the extract compared to the controls, represented by untreated cells and cells supplemented with identical volumes of DMSO.

Sodium arsenite stress induction and biochemical analyses

HaCaT cells were pre-treated with 90 µg/mL of ethanol extract for 2 h. Then, cells were stressed with 300 µM sodium arsenite ($NaAsO_2$) for 1 h as previously described (Sobeh et al. 2019). Immediately after $NaAsO_2$ stress induction, intracellular ROS levels were determined by DCFDA assay, as previously reported (Imbimbo et al. 2023), whereas intracellular glutathione (GSH) levels were measured by performing 5,5′-dithiobis-(2-nitrobenzoic acid) (DTNB) assay, as reported by (Laezza et al. 2024).

Western blot analysis

Ninety minutes after stress induction, HaCaT cells were detached by trypsin and lysate in lysis buffer (0.1 M Tris HCl pH 7.4, 0.3 M NaCl, and 0.5% NP40), supplemented with proteases and phosphatases inhibitors. After 30-min incubation on ice, lysates were centrifuged at 14,000 *g* for 30 min at 4 °C. Supernatants were collected and protein concentration was determined by the Bradford assay. Eighty micrograms of proteins were separated by SDS-PAGE and analyzed by Western blotting using specific antibodies: anti-phospho-p38, anti-phospho-MAPKAPK-2 from Cell Signaling (Danvers, MA, USA); anti-Nrf2 from Bioss Antibodies (Woburn, MA, USA); anti-HO-1 from Bethyl laboratories INC. (Montgomery, TX, USA), anti-B-23, and anti-β-actin. Band detection and densitometric analyses were performed using a ChemiDoc (Biorad, Hercules, CA, USA), according to the manufacturer's instruction.

Statistical analyses

Samples were tested in three independent analyses, each carried out in triplicate. Results are presented as the mean of results obtained after three independent experiments (mean ± SD) and compared by one-way ANOVA according to Bonferroni's method (post hoc) using Graphpad Prism for Windows, version 6.01.

Results

Pigments extraction and characterization

The proposed biorefinery strategy consists in the extraction of two different classes of molecules, pigments and lipids, starting from *P. simplex* biomass. The order of the extraction was chosen by following two different criteria: the polarity of the target molecules, to ensure that the extraction solvent would not affect the quality of the residual biomass, and the market value of the molecules to be extracted.

To obtain pigments, the biomass was harvested, freeze-dried, and treated as described in the "Materials and methods" section. At the end of the extraction, the mixture was centrifuged, the supernatant dried under N_2 stream, and cells debris were dried and stored for further extraction. The yield of the ethanol extract was 26 ± 3%. To investigate the composition of the ethanol extract, a profiling analysis using a chromatographic HPLC–DAD system hyphenated to a QTOF-MS analyzer was used to obtain complementary structural information. UV–vis profiles and HRMS/MS data acquired in positive ionization mode (APCI+) were jointly analyzed to increase structural elucidation capacity.

The UHPLC-DAD chromatographic profile, shown in Fig. 1, revealed the presence of 7 major carotenoids and 6 chlorophylls/chlorophyll derivatives, tentatively identified according to their maximum absorption wavelength (λ_{max}), molecular ion (m/z), and main MS/MS fragments obtained by LC-APCI(+)-MS/MS analysis. Structural information of the annotated pigments is summarized in Table S1. From their calculated molecular formulae, chromatographic peaks 1 to 5 were annotated as compounds belonging to the xanthophylls (oxygen-containing carotenoids), whereas compounds 12 and 13 were classified as carotenes (hydrocarbon carotenoids). The nitrogen-containing pigments (peaks 6 to 11) were classified as chlorophylls and chlorophyll derivatives. Concentration values were estimated for the identified carotenoids following a semi-quantitative approach using β-carotene as reference standard (Table 1).

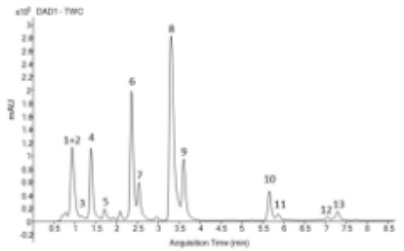

Fig. 1 Representative LC-DAD chromatogram of pigments extracted from *P. simplex*. The TWC (total wavelength chromatogram), in the range 190 to 640 nm, is reported. Peaks identification is reported in Table S1

Table 1 Concentration values ($mg/g_{extract}$) of carotenoids identified in the ethanol extract of *P. simplex*

Peak N°	Compound	Concentration ($mg/g_{extract}$)
1+2	Diatoxanthin/monadoxanthin/ neoxanthin	30 ± 1
3	Mutatoxanthin-type	2.5 ± 0.2
4	Lutein	30 ± 1
5	Crocoxanthin	6 ± 1
12	α-Carotene	1.6 ± 0.3
13	β-Carotene	4.6 ± 0.1

Carotenoids 1–5, 12, and 13 showed three typical maximum absorption wavelengths ranging from 400 to 475 nm in their UV–vis spectra. Compounds 1 and 2 are two major carotenoids in *P. simplex*, that coelute under the same peak and show molecular ions at m/z 567.4196 ($C_{40}H_{54}O_2$) and m/z 601.4251 ($C_{40}H_{56}O_4$), respectively. Compound 3 with m/z 585.4302 ($C_{40}H_{56}O_3$) shares similar UV–vis absorption profile to compound 2. The first compound was annotated as a didehydro-carotenediol (e.g., diatoxanthin/monadoxanthin), whereas the second and the third were annotated as neoxanthin and the third one as mutatoxanthin-type, respectively; two biosynthetically related epoxycarotenoids and β-carotene derivatives. Peak 4 (m/z 569.4353, $C_{40}H_{56}O_2$) was unambiguously annotated as lutein, the most abundant carotenoid identified in the ethanol extract of *P. simplex*, whereas peak 5 (m/z 551.4247, $C_{40}H_{54}O$) was tentatively identified as crocoxanthin. Both compounds 4 and 5 are biosynthetic derivatives of α-carotene. Additionally, two non-oxygenated carotenoid isomers (peaks 12 and 13) were identified as α- and β-carotene (m/z 537.4455, $C_{40}H_{56}$) and exhibited a higher retention time, in agreement with their higher lipophilicity. Chlorophylls and their derivatives

exhibit two major absorption bands in the visible range, corresponding to the cyclic tetrapyrrole (porphyrin) skeleton, at around 420–460 nm and above 650 nm. Due to operational restrictions, only the first band could be measured in this work. In agreement with λ_{max} values in literature (Almela et al. 2000), compounds 6–7 and 8–9 were annotated as chlorophyll *b* and chlorophyll *a* isomers, corresponding to molecular ions at *m/z* 907.5218 ($C_{55}H_{70}MgN_4O_6$) and *m/z* 893.5426 ($C_{55}H_{72}MgN_4O_5$), respectively. Two additional chlorophyll derivatives, lacking the central Mg-atom, were annotated as pheophytin *a* isomers (compounds 10–11). These demetallized forms are less polar than the corresponding chlorophylls, showing higher retention time in reverse phase columns. The most abundant fragment ions in MS/MS spectra of chlorophyll and its derivatives usually correspond to the fragmentation with the loss of the phytyl chain $[M\text{-}278]^+$.

Lipid extraction and characterization

Lipids were extracted as the second class of molecules by an organic solvent extraction. The extraction was carried out on the residual biomass (i.e., biomass recovered after pigment extraction) after a drying step. In a parallel experiment, lipids were extracted also from the raw biomass, as benchmark, to verify if the lipids extraction could be affected by the previous pigment extraction. As shown in Fig. 2a, the yield of the hydrophobic fraction obtained from the residual biomass was 7 ± 1% (gray bar). This value represents a threefold decrease compared to the extraction yield of the raw biomass (black bar, 24 ± 3%), thus suggesting that lipids extraction was significantly affected from the pigment extraction.

To understand the composition of the isolated lipids, a solid-phase extraction (SPE) was carried out to isolate the three lipid classes: neutral lipids, fatty acids, and phospholipids. As shown in Fig. 2b, no significant alteration in neutral lipids was observed, whereas phospholipids significantly decreased (from 28 to 13%). However, it is interesting to notice a significant increase in relative fatty acid content in the extract obtained from the residual biomass (24 ± 1%) in comparison with the one obtained from the raw one (7 ± 2%).

Finally, a gas chromatography analysis was performed on fatty acids fraction obtained from raw and residual biomass. The results, reported in Table 2, suggest that *P. simplex* biomass is enriched in saturated fatty acids (SFA), particularly palmitic and stearic acids. Notably, when fatty acids were recovered from the residual biomass, the total SFA content increased, to such an extent that the extract appears to be composed only of palmitic and stearic acids.

Biological characterization

In vitro anti-aging activity

Skin aging is a complex mechanism which depends on endogenous and exogenous factors, such as physiological aging and the continuous exposure to stress factors (Gu et al. 2020). Thus, there is a direct link between aging and oxidative stress. Different enzymes are involved in skin aging, such as tyrosinase and elastase. The first is involved in the early steps of melanogenesis, whereas the second is involved in elastin degradation, a protein that plays a key role in the maintenance of the elasticity of the overall skin tone (Panwar et al. 2020). The inhibition of these two enzymes can be a way to slow down skin aging, so that a possible inhibitor effect of *P. simplex* carotenoids extract was evaluated in vitro. The carotenoids extract was able to inhibit both enzymes, but with a lower extent with respect to kojic acid, a commercial inhibitor. The amount of extract needed to inhibit 50% of the enzyme activity (IC_{50}) was calculated and reported in Table 3.

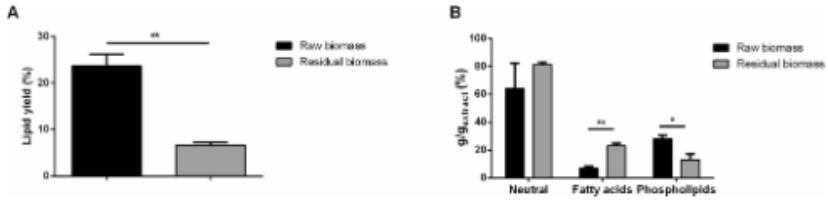

Fig. 2 Lipid extraction and fractionation. **a** Yields of lipids extracted from *P. simplex* and reported as % with respect to dry weight biomass; **b** Yield of neutral lipids, fatty acids and phospholipids obtained upon SPE and reported as % with respect of dry weight extract. Black bars refer to raw biomass; gray bars refer to the residual biomass after pigments extraction. Results are reported as means ± SD of at least three independent experiments. * Indicates $p < 0.05$; ** indicates $p < 0.001$. The lines above the bars indicate the samples compared for statistical analysis

Table 2 Fatty acids composition by gas chromatography analysis on samples obtained from raw and residual biomass after pigment extraction. Saturated fatty acids (SFA), monounsaturated fatty acids (MUFA), and polyunsaturated fatty acids (PUFA) are reported as relative percentages

Fatty acids		Raw biomass (%)	Residual biomass (%)
SFA			
14:0	Myristic	0.56 ± 0.08	0.4 ± 0.1
16:0	Palmitic	30.0 ± 0.8	62 ± 2
18:0	Stearic	15 ± 1	37 ± 2
24:0	Lignoceric	0.13 ± 0.04	0.02 ± 0.01
MUFA			
16:1n7t	*Trans* palmitoleic	0.04 ± 0.01	0.09 ± 0.01
16:1n7	Palmitoleic	0.20 ± 0.02	0.05 ± 0.04
18:1n9t	*Trans* oleic	0.13 ± 0.05	0.04 ± 0.01
18:1n9	Oleic	12 ± 1	0.30 ± 0.08
20:1n9	Eicosenoic	0.09 ± 0.01	0.11 ± 0.03
24:1n9	Nervonic	0.03 ± 0.03	0.010 ± 0.001
PUFA			
18:2n6t	*Trans* linoleic	0.21 ± 0.08	0.06 ± 0.04
18:2n6	Linoleic	20 ± 1	0.24 ± 0.06
18:3n6	γ-Linoleic	21.0 ± 0.8	0.10 ± 0.03
18:3n3	α-Linoleic	0.06 ± 0.01	0.07 ± 0.04
20:2n6	Eicosadienoic	0.73 ± 0.17	0.03 ± 0.03
20:3n6	Dihomo γ-Linoleic	0.03 ± 0.01	0.20 ± 0.02
20:4n6	Arachidonic (AA)	0.06 ± 0.03	0.02 ± 0.01
20:5n3	Eicosapentaenoic (EPA)	0.02 ± 0.01	0.04 ± 0.02
22:4n6	Docosatetraenoic	0.06 ± 0.04	0.010 ± 0.001
22:5n6	Docosapentaenoic-n6	0.05 ± 0.04	0.01 ± 0.01
22:5n3	Docosapentaenoic-n3	N.D	0.01 ± 0.01
22:6n3	Docosahexaenoic (DHA)	N.D	0.010 ± 0.001

Table 3 Anti-tyrosinase and anti-elastase activity of *P. simplex* carotenoids extract. Values are reported as IC_{50} (mg/mL). Data shown are means ± S.D. of three independent experiments

Assay	Kojic acid IC_{50} (mg/mL)	*P. simplex* extract IC_{50} (mg/mL)
Anti-tyrosinase	0.072 ± 0.003	0.48 ± 0.05
Anti-elastase	0.116 ± 0.005	0.55 ± 0.04

Effect of carotenoid extract on cell viability

The biocompatibility of the carotenoid extract was evaluated on immortalized human keratinocytes (HaCaT) and on immortalized murine fibroblasts (BALB/c-3T3) by dose- and time-dependent tests. Cell viability was assessed by the tetrazolium salt colorimetric (MTT) assay, and cell viability was expressed as the percentage of viable cells in the presence of the extract compared to that of control samples. As shown in Fig. 3, the extract was fully biocompatible on both HaCaT (Fig. 3a) and BALB/c-3T3 cells (Fig. 3b), as no reduction in cell viability was observed at any of the experimental conditions tested.

Protective effect of carotenoid extract against sodium arsenite-induced oxidative stress

It is known that carotenoids are excellent antioxidants. Thus, their protective effect was tested on a cell-based system, in which cells were stressed with sodium arsenite. Humans are constantly exposed to this contaminant *via* ingestion, inhalation, and also skin absorption (Ozturk et al. 2022), with severe health problems, such as cancer, cardiovascular disease, diabetes, and skin diseases (Rahaman et al. 2021). All these conditions are triggered by oxidative stress (Sharifi-Rad et al. 2020). Thus, HaCaT cells were treated as described in the "Materials and methods" section, and immediately after $NaAsO_2$-stress induction, intracellular ROS levels were measured by using the fluorescent probe 2',7'-dichlorofluorescin diacetate (H_2-DCFDA). As shown in Fig. 4a, in the absence of oxidative stress, no alteration in ROS production was observed when cells were treated with the carotenoid extract, whereas a significant increase in intracellular ROS levels was observed when cells were stressed with $NaAsO_2$. Interestingly, when cells were pre-incubated with ethanol extract prior to stress exposure, an inhibition in ROS production was observed. The protective effect against oxidative stress was confirmed by analyzing

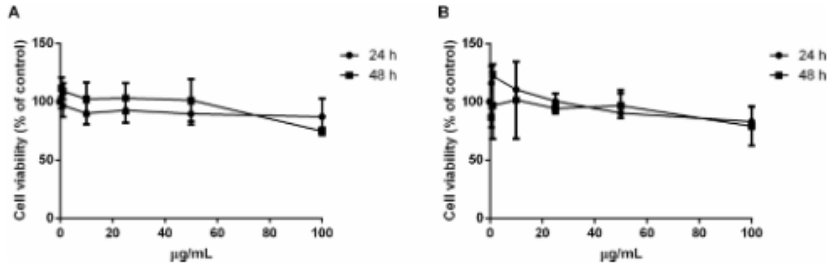

Fig. 3 Cell viability of carotenoid extract on eukaryotic cells. HaCaT cells (**a**) and BALB/c-3T3 (**b**) incubated for 24 h (black circles) or 48 h (black squares) with increasing concentrations (0.5–100 µg/mL) of the extract. Cell viability is expressed as a percentage of viable cells in the presence of carotenoids with respect to control cells grown in the absence of the extract. Data shown are means ± S.D. of three independent experiments

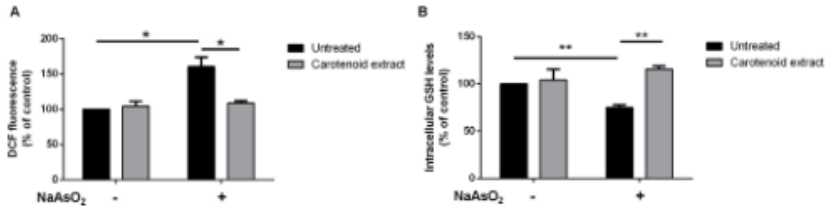

Fig. 4 Effect of carotenoid extract on stressed HaCaT cells. Cells were incubated with 90 µg/mL of *P. simplex* carotenoid extract for 2 h in the absence (−) or in the presence (+) of oxidative stress induced by incubating cells with 300 µM $NaAsO_2$ for 1 h. **a** Intracellular ROS levels measured by DCFDA assay; **b** intracellular GSH levels measured by DTNB assay. Values are expressed as fold increase with respect to untreated cells. Data shown are means ± S.D. of three independent experiments. * Indicates $p < 0.05$; ** indicates $p < 0.001$. Lines above the bars indicate the samples compared for statistical analysis

the intracellular glutathione levels, a molecule which is normally oxidized during oxidative stress. The intracellular GSH levels were assessed using the 5,5'-dithiobis-2-nitrobenzoic acid (DTNB) assay. As shown in Fig. 4b, the exposure of the cells to $NaAsO_2$ resulted in a significant GSH depletion. Nevertheless, the pre-treatment with carotenoids resulted in the inhibition of GSH depletion, thus confirming the protective effect of the extract against $NaAsO_2$-induced oxidative stress.

Activation of Mitogen-Activated Protein Kinases (MAPK) Mediated by Carotenoid Extract

Oxidative stress usually results in the activation of MAP (mitogen-activated protein) kinases pathway. Following oxidative stress insult, p38 is phosphorylated and this causes, in turn, the phosphorylation of its direct target, MAPKAPK-2. Thus, Western blotting analyses were performed to evaluate the protective effect of carotenoids extracted from *P. simplex* biomass. As shown in Fig. 5, the carotenoid extract was able to inhibit the phosphorylation of both p38 and MAPKAPK-2. A complete inhibition in the phosphorylation of p38 and MAPKAPK-2 levels was observed when cells were pre-treated with the extract prior to be stressed.

Protection against oxidative stress *via* the activation of Nrf2 pathway

The nuclear factor E2-related factor 2 (Nrf2) plays a pivotal role in cellular responses to oxidative stress (Li and Kong 2009), as it regulates the expression of antioxidant enzymes and maintains the redox homeostasis (Mansouri et al. 2022). Under physiological conditions, Nrf2 is in the cytosol, associated with the kelch-like ECH-associated

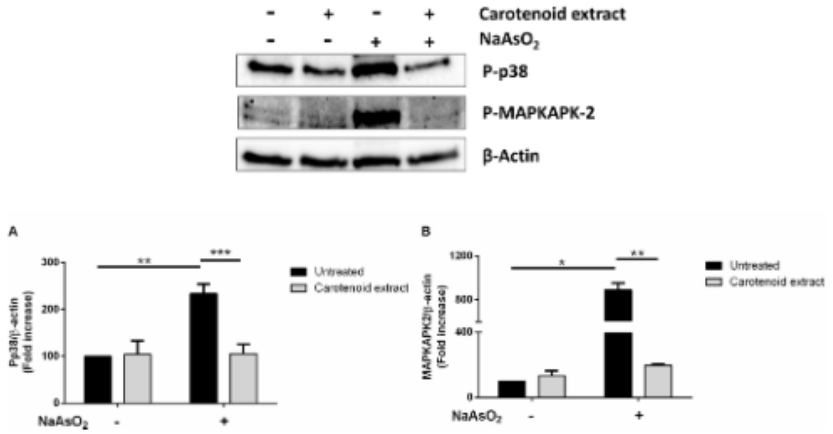

Fig. 5 Effect of carotenoid extract on the activation of mitogen-activated protein kinase (MAPK) cascade upon $NaAsO_2$ stress induction. HaCaT cells were treated as described in the "Materials and methods" section. Phosphorylation levels of p38 and MAPKAPK-2 were analyzed by Western blotting. β-Actin was used as an internal standard. The relative densitometric analysis of P-p38 (**a**) and P-MAPKAPK-2 (**b**) levels is reported. Black bars refer to control cells in the absence (–) or in the presence (+) of sodium arsenite; light gray bars refer to cells incubated with 90 µg/mL of carotenoids. Data shown are the means ± S.D. of three independent experiments. * Indicates $p < 0.05$, ** indicates $p < 0.01$, *** indicates $p < 0.001$. Lines above the bars indicate the samples compared for statistical analysis

protein 1 (KEAP1). In the presence of external stimuli, such as oxidative stress or low exposure to antioxidants, Nrf2 dissociates from KEAP1 and rapidly translocates into the nucleus where it binds the antioxidant responsive elements (ARE) sequences, thus initiating the transcription of over 200 genes involved in the antioxidant response, among which heme oxygenase 1 (HO-1) (Mallard et al. 2020). For this reason, the effect of carotenoid extract in the activation of Nrf2 pathway was analyzed. HaCaT cells were treated with 90 µg/mL of carotenoid extract for 10 or 20 min, and then, lysates were analyzed by Western blot analysis, using Nrf2 antibody. As shown in Fig. 6a, a significant increase in nuclear Nrf2 levels was observed upon 10-min incubation. To corroborate this result, HO-1 levels were also analyzed by Western blot, upon 20- and 30-min incubation. As shown in Fig. 6b, a significant increase in HO-1 levels was observed after 20 min incubation.

Biocompatibility of FAs

Finally, the biocompatibility of palmitic and stearic acids was tested on HaCaT cells. In particular, the FAs obtained at the end of the biorefinery were analyzed following the same procedure used above. As shown in Fig. 7, no effect on cell viability was observed at any of the experimental conditions under test, thus indicating the safeness of the isolated FAs.

Discussion

In the last years, the use of natural molecules to be used in the cosmeceutical field is emerging and the biotech industries are focusing their attention on safe, sustainable, and economical natural sources. The blue biotechnology, based on the use of aquatic resources as raw materials, is meeting consumer demands for natural active molecules to be used in cosmetics and cosmeceuticals. In this context, microalgae represent a versatile reservoir of active molecules with many potential applications, ranging from antioxidants (Imbimbo et al. 2019), anticancer (Ferraro et al. 2020) to anti-aging (Khemiri et al. 2023), as its biomass contains an array of valuable metabolites, such as proteins, lipids, polysaccharides, pigments and vitamins, all known for their antioxidant, anti-aging, and moisturizing activities.

However, several drawbacks hinder microalgae large-scale use, which eventually lead to an increase in overall costs (Imbimbo et al. 2020; Abdur Razzak et al. 2023). A possible solution to lower the costs is the biorefinery approach: a stepwise extraction of more than one product to

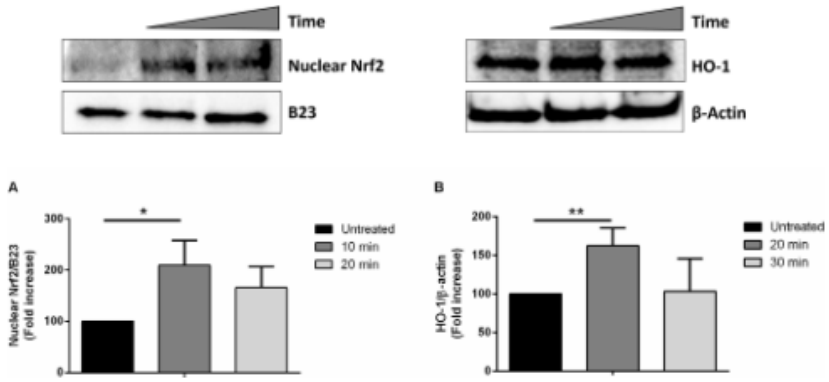

Fig. 6 Effect of carotenoid extract on Nrf2 activation. HaCaT cells were incubated with 90 µg/mL of ethanol extract for different length of times. **a** Western blot analysis of nuclear Nrf2 of untreated cells (black bars), after 10 min (dark gray bar) and 20 min (light gray bar) incubation. **b** Western blot analysis of cytosolic HO-1 of untreated cells (black bars), after 20 min (dark gray bar) and 30 min (light gray bar) incubation. Anti-B23 antibody was used as internal standard for nuclear lysate, whereas anti-β-actin antibody was used for cytosol. Images were quantified by densitometric analysis. Data shown are means ± S.D. of three independent experiments. * Indicates $p < 0.05$, ** indicates $p < 0.01$ with respect to control cells. Lines above the bars indicate the samples compared for statistical analysis

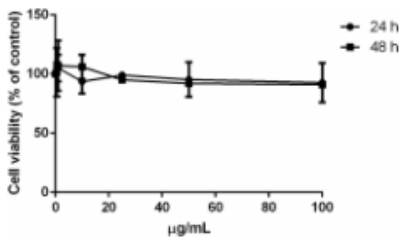

Fig. 7 Biocompatibility of isolated FAs on human keratinocytes. HaCaT cells were incubated for 24 h (black circles) or 48 h (black squares) with increasing concentrations (0.5–100 µg/mL) of FAs isolated from the residual biomass of *P. simplex*. Cell viability is expressed as a percentage of viable cells in the presence of the extracts under test with respect to control cells grown in the absence of the FAs. Data shown are means ± S.D. of three independent experiments

reduce the environmental footprint (Chanana et al. 2023). This should be combined to eco-friendly extraction techniques to obtain biologically active and safe extracts, in terms of negligible cytotoxicity.

Here, an unexplored green microalga strain has been used to isolate different classes of molecules with biological activity. Starting from *Pseudococcomyxa simplex* biomass, carotenoids were extracted first using a green approach. It is well known that carotenoids can exert a potent antioxidant activity, thus protecting skin cells from stress agents and improving skin appearance (Mussagy et al. 2023). Lutein, the most abundant one, is a high added value carotenoid with reported anticancer, antibacterial, anti-neurodegenerative, and anti-inflammatory activities (Desai and Mane 2024), sold at 455,000 €/g. The obtained extract shows a strong antioxidant activity and can activate the Nrf2 pathway, which has been primarily identified as a key player in the antioxidant response. The activation of Nrf2 pathway is also involved in the modulation of skin pigmentation, in wound healing, and in the overall protection of the skin from the environmental stresses, so that the use of Nrf2 modulators is considered a useful tool in dermo-cosmetic applications. Recent studies linked the pivotal role of Nrf2 to other key pathways, such as anti-inflammatory and skin aging (Frantz et al. 2023). Wrinkles, loss of elasticity, hyperpigmentation, and dryness are classical symptoms of skin aging, mainly due to the activity of key enzymes, such as those involved in elastin degradation or in the early steps of melanogenesis (Shin et al. 2023). In particular, melanin overproduction can cause different dermatological problems, such as hyperpigmentation, which can finally lead to melanoma (Bayrakçeken Güven et al. 2023). Our data strongly

support the connection between antioxidants, Nrf2 activation, and skin aging, as the extract shows an inhibitory effect towards tyrosinase and elastase enzymes. Our results are in line with those reported in literature on carotenoids extracted from different strains, such as astaxanthin (Mourelle et al. 2017; Dutta et al. 2023), lutein (Jiang et al. 2024), and β-carotene (Yeager and Lim 2019). Accordingly, microalgae extracts are currently being formulated into skin-care products for providing anti-aging, moisturizing, antioxidant, and anti-irritant benefits (Desai and Mane 2024). The lipids isolated from the residual biomass belong to saturated fatty acids, a neglected class of lipids which are now more considered, as they can find application as antibacterial molecules, in cosmetics and in drug delivery (Liberti et al. 2022). Lipid yield obtained from the raw biomass (24%) is in agreement with the literature (Santhakumaran et al. 2018), whereas lipid yield from the residual biomass is almost three times lower, probably because of the first extraction with ethanol. However, from the residual biomass, a pure class of fatty acids is obtained by a single purification step. We can hypothesize that lipid yield is affected by the first extraction solvent: the more hydrophobic solvent is used for the first extraction, the lower is the lipid yield obtained from the residual biomass. According to this hypothesis, when an aqueous buffer is used as the first extraction solvent, an increase in the lipid yield is observed during the further extraction, as all the lipophilic molecules cannot be extracted by the polar solvent. Moreover, if lipid recovery is preceded by an ethanol extraction, the lipid content decreases, as some class of lipids (those with a lower hydrophobicity) can be co-extracted by ethanol (Imbimbo et al. 2019; Liberti et al. 2022), and an increase in SFA content is observed (Liberti et al. 2022). In cosmetics, fatty acids can be used as oily raw materials, as emulsifiers, and as softeners because they can deposit between desquamating cells (De Luca et al. 2021). The isolated fatty acids were fully biocompatible, thus suggesting a possible role in cosmetics.

The main objective of cosmetic formulations is to use extracts endowed with antioxidant, anti-aging, and moisturizing potential, so that microalgae fulfill these requirements. They also represent a sustainable vegan alternative to replace potentially harmful chemicals, traditionally used in skin care products. Algae molecules can protect from aging, UV, and oxidative stress, but only few strains are commercialized. Currently, molecules or extracts from *Chlorella vulgaris*, *Haematococcus pluvialis*, *Dunaliella salina*, *Nannochloropsis oculata*, and *Phaeodactylum tricornutum* are normally employed, so that the exploration of untapped species is now mandatory. This study represents a milestone but also a starting point for process improvement. Indeed, biomass concentration, advances in extraction technologies, formulation strategies, and a detailed cost analysis are expected to accelerate the adoption of *P. simplex* in the cosmetics industry.

Supplementary Information The online version contains supplementary material available at https://doi.org/10.1007/s00253-024-13229-9.

Acknowledgements The authors thank Dr. Laura Di Rienzo for her work during her Master thesis. G.A.R. would like to acknowledge MICINN for a "Juan de la Cierva-Incorporación" postdoctoral grant IJC2019–041482-I.

Author contribution P.I.: conceptualization, investigation, data analysis, and writing original draft; E.G.: investigation, data analysis, and writing original draft; A.F.: investigation and writing original draft; G.A.R.: investigation, writing original draft; H.A. investigation; E.I. methodology, review-editing; M.C.D.M.: investigation, writing original draft; A.Z.: methodology, review-editing; D.M.M: conceptualization, supervision, and writing original draft, review-editing. All authors read and approved the manuscript.

Funding Open access funding provided by Università degli Studi di Napoli Federico II within the CRUI-CARE Agreement.

Data availability All data generated during this study are included in this published article and its supplementary information file.

Declarations

Ethics approval This article does not contain any studies with human participants or animals performed by any of the authors.

Conflict of interest The authors declare no competing interests.

References

Abdur Razzak S, Bahar K, Islam KMO, Haniffa AK, Faruque MO, Hossain SMZ, Hossain MM (2023) Microalgae cultivation in photobioreactors: Sustainable solutions for a greener future. Green Chem Eng. https://doi.org/10.1016/j.gce.2023.10.004

Almela L, Fernández-López JA, Roca MJ (2000) High-performance liquid chromatographic screening of chlorophyll derivatives produced during fruit storage. J Chromatogr A 870:483–489. https://doi.org/10.1016/S0021-9673(99)00999-1

BayrakçekenGüven Z, Saracoglu I, Nagatsu A, Yilmaz MA, Basaran AA (2023) Anti-tyrosinase and antimelanogenic effect of cinnamic acid derivatives from *Prunus mahaleb L.*: Phenolic composition, isolation, identification and inhibitory activity. J Ethnopharmacol 310:116378. https://doi.org/10.1016/j.jep.2023.116378

Bligh EG, Dyer WJ (1959) A rapid method of total lipid extraction and purification. Can J Biochem Physiol 37:911–917. https://doi.org/10.1139/o59-099

Bouzroud S, El Maaiden E, Sobeh M, Merghoub N, Boukcim H, Kouisni L, El Kharrassi Y (2023) Biotechnological approaches to producing natural antioxidants: anti-ageing and skin longevity prospects. Int J Mol Sci 24. https://doi.org/10.3390/ijms24021397

Chanana I, Kaur P, Kumar L, Kumar P, Kulshreshtha S (2023) Advancements in microalgal biorefinery technologies and their economic analysis and positioning in energy resource market. Fermentation 9. https://doi.org/10.3390/fermentation9030202

Cochran S, Anthonavage M (2015) Fatty acids, fatty alcohols, synthetic esters and glycerin applications in the cosmetic industry BT - lipids and skin health. In: Pappas A (ed) Springer International Publishing, Cham, pp 311–319. https://doi.org/10.1007/978-3-319-09943-9_21

Crescenzo R, Bianco F, Mazzoli A, Giacco A, Cancelliere R, di Fabio G, Zarrelli A, Liverini G, Iossa S (2015) Fat quality influences the obesogenic effect of high fat diets. Nutrients 7:9475–9491. https://doi.org/10.3390/nu7115480

De Luca M, Pappalardo I, Limongi AR, Viviano E, Radice RP, Todisco S, Martelli G, Infantino V, Vassallo A (2021) Lipids from microalgae for cosmetic applications. Cosmetics 8. https://doi.org/10.3390/cosmetics8020052

Desai SS, Mane VK (2024) Biotechnological advances in cosmetic industry. In: Sustainable production innovations. Wiley, pp 103–136. https://doi.org/10.1002/9781119792888.ch3

Dutta S, Kumar SPJ, Banerjee R (2023) A comprehensive review on astaxanthin sources, structure, biochemistry and applications in the cosmetic industry. Algal Res 74:103168. https://doi.org/10.1016/j.algal.2023.103168

Ferraro G, Imbimbo P, Marseglia A, Illiano A, Fontanarosa C, Amoresano A, Olivieri G, Pollio A, Monti DM, Merlino A (2020) A thermophilic C-phycocyanin with unprecedented biophysical and biochemical properties. Int J Biol Macromol 150. https://doi.org/10.1016/j.ijbiomac.2020.02.045

Franco A, Salvia R, Scieuzo C, Schmitt E, Russo A, Falabella P (2022) Lipids from insects in cosmetics and for personal care products. Insects 13. https://doi.org/10.3390/insects13010041

Frantz MC, Rozot R, Marrot L (2023) NRF2 in dermo-cosmetic: from scientific knowledge to skin care products. BioFactors 49:32–61. https://doi.org/10.1002/biof.1907

Gu Y, Han J, Jiang C, Zhang Y (2020) Biomarkers, oxidative stress and autophagy in skin aging. Ageing Res Rev 59:101036. https://doi.org/10.1016/j.arr.2020.101036

Igbokwe VC, Ezugworie FN, Onwosi CO, Aliyu GO, Obi CJ (2022) Biochemical biorefinery: a low-cost and non-waste concept for promoting sustainable circular bioeconomy. J Environ Manage 305:114333. https://doi.org/10.1016/j.jenvman.2021.114333

Imbimbo P, D'Elia L, Liberti D, Olivieri G, Monti DM (2020) Towards green extraction methods from microalgae learning from the classics. Appl Microbiol Biotechnol 104:9067–9077. https://doi.org/10.1007/s00253-020-10839-x

Imbimbo P, D'Elia L, Corrado I, Alvarez-Rivera G, Marzocchella A, Ibáñez E, Pezzella C, Branco dos Santos F, Monti DM (2023) An alternative exploitation of *Synechocystis* sp. PCC6803: a cascade approach for the recovery of high added-value products. Molecules 28:3144. https://doi.org/10.3390/molecules28073144

Imbimbo P, Romanucci V, Pollio A, Fontanarosa C, Amoresano A, Zarrelli A, Olivieri G, Monti DM (2019) A cascade extraction of active phycocyanin and fatty acids from *Galdieria phlegrea*. Appl Microbiol Biotechnol 9455–9464. https://doi.org/10.1007/s00253-019-10154-0

Jiang R, Ding Z, Liu Z, Zhao X, Tu Y, Guo B, He Q, Zhou Z, Zheng Z, Sun Z (2024) Protective effects of microalgal carotenoids against glycosylation-induced collagen degradation in skin. J Funct Foods 113:106014. https://doi.org/10.1016/j.jff.2024.106014

Khemiri S, Khelifi N, Messaoud C, Smaali I (2023) Bioprospecting of microalgae for a potential use as enzyme inhibitors, anti-ageing and prebiotic agents. Biocatal Agric Biotechnol 51:102759. https://doi.org/10.1016/j.bcab.2023.102759

Knox S, O'Boyle NM (2021) Skin lipids in health and disease: a review. Chem Phys Lipids 236:105055. https://doi.org/10.1016/j.chemphyslip.2021.105055

Laezza C, Imbimbo P, D'Amelia V, Marzocchi A, Monti DM, Di Loria A, Monti SM, Novellino E, Tenore GC, Rigano MM (2024) Use of yeast extract to elicit a pulp-derived callus cultures from Annurca apple and potentiate its biological activity. J Funct Foods 112:105988. https://doi.org/10.1016/j.jff.2023.105988

Li W, Kong AN (2009) Molecular mechanisms of Nrf2-mediated antioxidant response. Mol Carcinog 48:91–104. https://doi.org/10.1002/mc.20465

Liberti D, Imbimbo P, Giustino E, D'Elia L, Ferraro G, Casillo A, Illiano A, Pinto G, Di Meo MC, Alvarez-Rivera G, Corsaro MM, Amoresano A, Zarrelli A, Ibáñez E, Merlino A, Monti DM (2022) Inside out *Porphyridium cruentum*: beyond the conventional biorefinery concept. ACS Sustain Chem Eng. https://doi.org/10.1021/acssuschemeng.2c05869

Liberti D, Imbimbo P, Giustino E, D'Elia L, Silva M, Barreira L, Monti DM (2023) Shedding light on the hidden benefit of *Porphyridium cruentum* culture. Antioxidants 12:1–12. https://doi.org/10.3390/antiox12020337

Mahdi I, Imbimbo P, Ortaakarsu AB, Adhiambo Ochieng M, Ben Bakrim W, Drissi BE, Ibrahim MA, Abdelfattah MAO, Mahmoud MF, Monti DM, Sobeh M (2024) Chemical profiling and dermatological and anti-aging properties of *Syzygium jambos L.* (Alston): evidence from molecular docking, molecular dynamics, and in vitro experiments. Front Mol Biosci 10:1–18. https://doi.org/10.3389/fmolb.2023.1331059

Mallard AR, Spathis JG, Coombes JS (2020) Nuclear factor (erythroid-derived 2)-like 2 (Nrf2) and exercise. Free Radic Biol Med 160:471–479. https://doi.org/10.1016/j.freeradbiomed.2020.08.024

Mansouri A, Reiner Ž, Ruscica M, Tedeschi-Reiner E, Radhakhsh S, Ekta MB, Sahebkar A (2022) Antioxidant effects of statins by modulating Nrf2 and Nrf2/HO-1 signaling in different diseases. J Clin Med 11:1–21. https://doi.org/10.3390/jcm11051313

Mourelle ML, Gómez CP, Legido JL (2017) The potential use of marine microalgae and Cyanobacteria in cosmetics and thalassotherapy. Cosmetics 4. https://doi.org/10.3390/cosmetics4040046

Mussagy CU, Oshiro A, Farias FO, Haddad FF, dos Santos JL, Scarim CB, Herculano RD, Pessoa A, Santos-Ebinuma VC (2023) Emerging role of bio-based solvents mixtures to increase the solubility and recovery of carotenoids from processed carrot wastes for potential skin care application. Ind Crops Prod 205:117436. https://doi.org/10.1016/j.indcrop.2023.117436

Ozturk M, Metin M, Altay V, Bhat RA, Ejaz M, Gul A, Unal BT, Hasanuzzaman M, Nibir L, Nahar K, Bukhari A, Dervash MA, Kawano T (2022) Arsenic and human health: genotoxicity, epigenomic effects, and cancer signaling. Biol Trace Elem Res 200:988–1001. https://doi.org/10.1007/s12011-021-02719-w

Panwar P, Hedtke T, Heinz A, Andrault P-M, Hoehenwarter W, Granville DJ, Schmelzer CEH, Brömme D (2020) Expression of elastolytic cathepsins in human skin and their involvement in age-dependent elastin degradation. Biochim Biophys Acta - Gen Subj 1864:129544. https://doi.org/10.1016/j.bbagen.2020.129544

Rahaman MS, Rahman MM, Mise N, Sikder MT, Ichihara G, Uddin MK, Kurasaki M, Ichihara S (2021) Environmental arsenic exposure and its contribution to human diseases, toxicity mechanism

and management. Environ Pollut 289:117940. https://doi.org/10.1016/j.envpol.2021.117940

Santhakumaran P, Kookal SK, Ray JG (2018) Biomass yield and biochemical profile of fourteen species of fast-growing green algae from eutrophic bloomed freshwaters of Kerala, South India. Biomass Bioenerg 119:155–165. https://doi.org/10.1016/j.biombioe.2018.09.021

Sathasivam R, Ki JS (2018) A review of the biological activities of microalgal carotenoids and their potential use in healthcare and cosmetic industries. Mar Drugs 16:26. https://doi.org/10.3390/md16010026

Sharifi-Rad M, Anil Kumar N V, Zucca P, Varoni EM, Dini L, Panzarini E, Rajkovic J, Tsouh Fokou PV, Azzini E, Peluso I, Prakash Mishra A, Nigam M, El Rayess Y, Beyrouthy M El, Polito L, Iriti M, Martins N, Martorell M, Docea AO, Setzer WN, Calina D, Cho WC, Sharifi-Rad J (2020) Lifestyle, oxidative stress, and antioxidants: back and forth in the pathophysiology of chronic diseases. Front Physiol 11. https://doi.org/10.3389/fphys.2020.00694

Shin SH, Lee YH, Rho NK, Park KY (2023) Skin aging from mechanisms to interventions: focusing on dermal aging. Front Physiol 14:1–10. https://doi.org/10.3389/fphys.2023.1195272

Sobeh M, Petruk G, Osman S, El Raey MA, Imbimbo P, Monti DM, Wink M (2019) Isolation of myricitrin and 3,5-di-O-methyl gossypetin from *Syzygium samarangense* and evaluation of their involvement in protecting keratinocytes against oxidative stress via activation of the Nrf-2 pathway. Molecules 24. https://doi.org/10.3390/molecules24091839

Tang DYY, Khoo KS, Chew KW, Tao Y, Ho SH, Show PL (2020) Potential utilization of bioproducts from microalgae for the quality enhancement of natural products. Bioresour Technol 304:122997. https://doi.org/10.1016/j.biortech.2020.122997

Yarkent Ç, Gürlek C, Oncel SS (2020) Potential of microalgal compounds in trending natural cosmetics: a review. Sustain Chem Pharm 17. https://doi.org/10.1016/j.scp.2020.100304

Yeager DG, Lim HW (2019) What's new in photoprotection: a review of new concepts and controversies. Dermatol Clin 37:149–157. https://doi.org/10.1016/j.det.2018.11.003

Supporting information

Table S1. Tentatively identified carotenoids and chlorophylls in *Pseudococcomyxa simplex* by HPLC-DAD-APCI-QTOF analysis, including peak annotation, high-resolution mass spectrometry features and UV–Vis maxima.

Peak N°	RT (min)	Identification	Molecular formula	Monoisotopic mass	Theoretical $[M+H]^+$ *m/z*	Error (ppm)	MS/MS product ions	UV–Vis maxima (nm)	% of total pigments
1	0.815	Diatoxanthin/Monadoxanthin	$C_{40}H_{54}O_2$	566.4123	567.4196	2.2	549, 427, 121	424s, 447, 477	13 ± 1
2	0.922	Neoxanthin	$C_{40}H_{56}O_4$	600.4179	601.4251	2.1	583, 333, 167	417, 440, 467	
3	1.095	Mutatoxanthin-type	$C_{40}H_{56}O_3$	584.4229	585.4302	1.2	567, 476, 133	417, 440, 467	1 ± 0.1
4	1.315	Lutein*	$C_{40}H_{56}O_2$	568.4280	569.4353	3.0	551, 431, 337	422s, 445, 473	13 ± 1
5	1.642	Crocoxanthin	$C_{40}H_{54}O$	550.4175	551.4247	4.6	533, 495, 175	417s, 440, 467	2.6 ± 0.6
6	2.289	Chlorophyll *b*	$C_{55}H_{70}MgN_4O_6$	906.5146	907.5219	1.8	630, 601, 569	468	16.8 ± 0.1
7	2.462	Chlorophyll *b*	$C_{55}H_{70}MgN_4O_6$	906.5146	907.5219	2.4	630, 601, 569	468	5.1 ± 1.3
8	3.235	Chlorophyll *a*	$C_{55}H_{72}MgN_4O_5$	892.5353	893.5426	4.5	615, 583, 555	339, 390s, 420s, 432	37.3 ± 4.5
9	3.542	Chlorophyll *a*	$C_{55}H_{72}MgN_4O_5$	892.5353	893.5426	4.5	615, 583, 555	339, 390s, 420s, 432	6.6 ± 4.5
10	5.595	Pheophytin *a*	$C_{55}H_{74}N_4O_5$	870.5659	871.5732	2.8	593, 533	408	2.4 ± 2.6
11	5.809	Pheophytin *a*	$C_{55}H_{74}N_4O_5$	870.5659	871.5732	2.8	593, 533	408	0.6 ± 0.8
12	7.008	Alpha-carotene*	$C_{40}H_{56}$	536.4382	537.4455	3.4	457, 177, 123	425s, 446, 473	0.7 ± 0.1
13	7.248	Beta-carotene*	$C_{40}H_{56}$	536.4382	537.4455	3.4	457, 321, 203	430s, 452, 478	1.9 ± 0.1

*Confirmed by commercial standard.

International Journal of
Molecular Sciences

MDPI

Article

Microalgae Flocculation: Assessment of Extraction Yields and Biological Activity

Paola Imbimbo [1,†], Alfonso Ferrara [1,†], Enrica Giustino [1], Davide Liberti [2] and Daria Maria Monti [1,*]

[1] Department of Chemical Sciences, University of Naples Federico II, via Cinthia 4, 80126 Naples, Italy; paola.imbimbo@unina.it (P.I.); alfonso.ferrara@unina.it (A.F.); enrica.giustino@unina.it (E.G.)
[2] Centre of Marine Sciences, University of Algarve, Campus de Gambelas, 8005-139 Faro, Portugal; dliberti@ualg.pt
* Correspondence: mdmonti@unina.it; Tel.: +39-081-679150
† These authors equally contributed to this work.

Abstract: Downstream costs represent one of the main obstacles to enabling microalgae to become widespread. The development of an economical, easily scaled-up strategy could reduce the overall process costs. Here, different flocculants were tested on different microalgae strains and a cyanobacterium. The results indicate that flocculation could be an alternative to centrifugation, as $CaCl_2$ induced a complete flocculation of green and red marine strains (96 ± 4% and 87.0 ± 0.5%, respectively), whereas Chitosan was the only agent able to induce flocculation on the cyanobacterium (46 ± 1%). As for the thermoacidophilic red microalga, 100% flocculation was achieved only by increasing the pH. Carotenoids were extracted from the flocculated biomass, and the strategy improved with the use of the wet biomass. The results indicate that flocculation does not affect carotenoid yield, which is at least the same than that obtained upon centrifugation and extraction from the wet biomass. Then, for the first time, the biological activity of the extracts obtained from the flocculated biomasses was evaluated. The results indicate that only the green microalga extract shows increased antioxidant activity. In conclusion, this work highlights that a general downstream procedure cannot be developed for microalgae strains but should be rationally tailored.

Keywords: microalgae; flocculation; harvesting; green extraction; antioxidant activity; industrial processes

Citation: Imbimbo, P.; Ferrara, A.; Giustino, E.; Liberti, D.; Monti, D.M. Microalgae Flocculation: Assessment of Extraction Yields and Biological Activity. *Int. J. Mol. Sci.* **2024**, *25*, 10238. https://doi.org/10.3390/ijms251910238

Academic Editors: María Serrano and Ana Paula Coelho Duarte

Received: 25 July 2024
Revised: 16 September 2024
Accepted: 19 September 2024
Published: 24 September 2024

1. Introduction

In the last few years, microalgae biomass has been deeply explored as a sustainable alternative to conventional feedstocks, mainly for the presence of a wide array of bioactive molecules. Indeed, carotenoids, polyunsaturated fatty acids and proteins are all endowed with beneficial properties for human health [1,2]. However, despite microalgae's enormous potential, large-scale production is still limited by the high cultivation, harvesting and processing costs [3,4]. It has been estimated that the harvesting step could represent up to 30% of the overall downstream costs [5,6], meaning that the optimization of an efficient and economic harvesting procedure is still a challenge. Indeed, the selection of the right technology to harvest the biomass could be a turning point for rendering microalgae exploitation cost-effective at a large scale.

The main drawbacks related to microalgae harvesting are due to cell size, to their overall negative charge and to their low density; for all these reasons, microalgae cells require an economically expensive and energetically intensive dewatering step. To date, the most used harvesting procedures are sedimentation, centrifugation, filtration, flocculation and flotation [7–9]. Each procedure presents different advantages and drawbacks, and the choice of technique is usually based on the market value of the molecule to be isolated. Among all the harvesting techniques, filtration and centrifugation are the most effective in terms of biomass recovery [10,11], but they require a high energy input. In the case of filtration, the frequent replacement of filters makes the technique prohibitive

at an industrial scale [12,13]. Sedimentation, on the other hand, is an easy and low-cost procedure, but its efficiency strictly depends on culture density, thus making this procedure time-consuming [14]. Flotation and flocculation are the most promising techniques for microalgae biomass harvesting as they are cheap, easy, fast and scalable. Despite its potential, flotation has limited efficiency due to the interaction between cells and air bubbles in the culture medium, as the collapsing of the bubbles could result in flocs breaking [15]. To overcome this limitation, flotation could be performed in the presence of surfactants, but this would increase the overall costs [13]. On the other hand, flocculation is considered the most cost-effective method, as it requires low energy consumption and is suitable with algal scaling-up systems and the costs are mainly related to the flocculating agent chosen [16]. Flocculants based on metal salts, such as $AlCl_2$, $AlCl_3$, $FeCl_3$, $Al_2(SO_4)_3$ and $Fe_2(SO_4)_3$, are generally used for their low costs and are commonly used for biofuel production or wastewater treatments, without considering the effects of flocculants on biomass quality or the environment [6,17,18]. However, due to their non-biodegradable nature, these flocculants may irreversibly affect water reuse. Thus, organic flocculants, such as chitosan and starch, have been proposed as green alternatives. Flocculation can also be achieved by increasing the pH of the culture medium (autoflocculation), avoiding the use of flocculants, with low energy consumption [18]. Recently, new approaches based on magnetic particles have emerged, but their economic feasibility and biocompatibility still need to be evaluated [19].

Besides harvesting, the extraction of biologically active molecules from the biomass represents another challenge to be overcome to fully exploit microalgae's potential [20]. Conventional extractions usually require large amounts of organic solvents, which are considered not eco-friendly, require long times, give low yields and are generally used on dried biomass, with a consequent increase in the final costs [21–23]. Recently, some green extraction techniques were developed, such as pressurized/supercritical liquid extractions and ultrasound- or microwave-assisted extractions. However, these procedures still present some drawbacks, such as scaling-up difficulty, energy consumption, the quality and selectivity of the extractions, cost validation and long extraction times [24,25].

Interestingly, many papers have been published providing alternatives for harvesting the biomass, but the literature is quiescent on the effects that the harvesting methods may have on the quality of the biomass and thus on the extracted molecules. Here, different alternatives, based on eco-friendly and cost-effective flocculation procedures, were provided by taking into account different microalgae strains and flocculants. Moreover, evidence of the effect of flocculants on the subsequent carotenoid extractions was provided. The extraction step was improved, avoiding the use of a dried biomass and using a GRAS solvent, and the whole procedure was validated by assaying the in vitro antioxidant activity of carotenoids.

2. Results

2.1. Flocculation

To obtain a general understanding of the procedure, different microalgae strains were analyzed: two Rhodophyta (*Porphyridium cruentum* and *Galdieria phlegrea*), a Chlorophyta (*Pseudococcomyxa simplex*) and a Cyanobacterium (*Synechococcus bigranulatus*). Different flocculants, based on their mechanism of action, were tested on each strain: a carbohydrate, chitosan, known to induce flocculation through a bridging mechanism; two salts, calcium chloride and sodium glutamate, which should induce charge neutralization; and the increase of the pH of the cell culture, which causes flocculation through a sweeping mechanism. Flocculants were added to the culture, as described in the Materials and Methods section. For each experimental procedure, the culture was collected when the cell concentration reached 7 ± 0.1 O.D./mL, and then each flocculant was added to the culture medium at three different concentrations (or pH values). Solutions were stirred and analyzed immediately (0 min). To verify the effects of incubation time on flocculation efficiency, longer incubations (10 and 20 min) were performed before reading the absorbance of the culture. Samples were analyzed spectrophotometrically, by reading the absorbance at 730 nm. Each sample was compared to an untreated cell culture.

2.1.1. Chitosan

Chitosan (CS) was tested at 0.1, 0.15 and 0.2 g/L. Results are reported in Figure 1. In the case of the *P. cruentum* culture, a direct correlation between the concentration of polymer added and flocculation efficiency was observed: from 66% of flocs immediately formed (0.1 g/L of CS), up to 90% with 0.15 g/L, and 100% flocculation in the presence of the highest concentration tested (0.2 g/L). *P. cruentum* was completely flocculated in the presence of any CS concentration tested after 10 or 20 min. On the other hand, the other red microalga analyzed, *G. phlegrea*, did not flocculate at any time with any tested CS concentration. *G. phlegrea* was incubated up to 90 min in the presence of increasing CS concentrations (0.10–0.20 g/L), but no flocculation occurred. CS induced an immediate 84% flocculation in the green microalga *P. simplex*, independently from the amount of polymer added to the culture. *P. simplex* completely flocculated after 10 or 20 min incubation, independently from the CS concentration. Similar results were obtained with the *S. bigranulatus* culture, even if at a lower extent, as only 40% flocculation was observed independently from the concentration of CS used. It is interesting to note that no significant increase in the efficiency of the process was observed upon 10 or 20 min incubation.

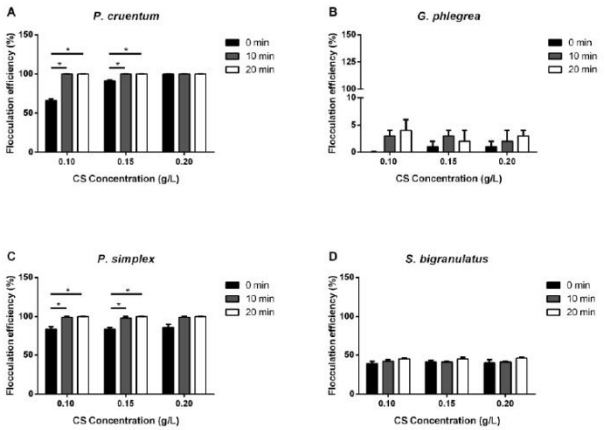

Figure 1. Flocculation efficiency (%) of chitosan (CS). Effect of different CS concentrations on the flocculation efficiency of microalgae strains analyzed immediately (0 min, black bars), 10 min (grey bars) and 20 min (white bars) after stirring. (**A**), *P. cruentum*; (**B**), *G. phlegrea*; (**C**), *P. simplex*; (**D**), *S. bigranulatus* upon different flocculation times. Data are obtained by means of three independent experiments (mean ± S.D.). * $p < 0.05$. The lines above the bars indicate the two samples compared for statistical analysis.

2.1.2. Calcium Chloride and Sodium Glutamate

The same set of experiments was carried out using two salts, sodium glutamate (SG) and calcium chloride (CC). SG was tested as a possible cost-effective alternative to polyglutamic acid, normally used in the cosmeceutical industry [26]. When SG was tested, no effect was observed at any concentration used on any strain, independently of the incubation time used. The case of CC was different. As shown in Figure 2, the red microalga *P. cruentum* showed a time- and concentration-dependent flocculation efficiency, reaching about 90% flocculation at the highest CC concentration tested. CC was unable to induce flocculation on the other red microalga (*G. phlegrea*), at any analyzed experimental condition. *P. simplex* flocs were observed after 10 min incubation, with a 90% flocculation

efficiency, but independently from the concentration of salt used. No flocculation was observed for *S. bigranulatus* at any analyzed condition.

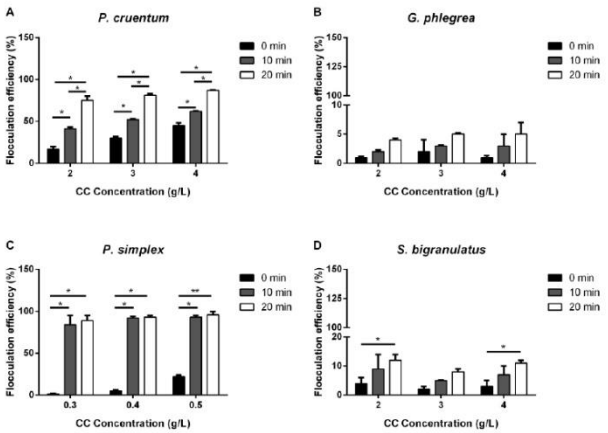

Figure 2. Flocculation efficiency (%) of calcium chloride (CC). Effect of different CC concentrations on the flocculation efficiency of microalgae strains analyzed immediately (0 min, black bars), after 10 min (grey bars) and after 20 min (white bars) from stirring. (**A**), *P. cruentum*; (**B**), *G. phlegrea*; (**C**), *P. simplex*; (**D**), *S. bigranulatus* upon different flocculation times. Data are obtained by means of three independent experiments (mean ± S.D.). * $p < 0.05$, ** $p < 0.005$. The lines above the bars indicate the two samples compared for statistical analysis.

2.1.3. pH-Mediated Flocculation

Finally, pH increase was tested to analyze autoflocculation. Sodium hydroxide was used to increase the pH of the culture medium, and two pH values were tested for each strain, as indicated in Figure 3. Interestingly, with the exception of the *S. bigranulatus* culture, increasing pH values induced biomass flocculation on all the tested strains. In particular, the increase of the pH value from 7 to 10 immediately induced more than 90% flocculation in the *P. cruentum* culture. This value reached 100% after 10 min incubation. When the pH value was increased from 7 to 12, an immediate and complete flocculation was observed. In the case of the *G. phlegrea* culture, the flocculation efficiency was complete after 10 min incubation. Surprisingly, when the pH of the culture was increased to 13, a complete and immediate flocculation occurred, but a bleaching phenomenon in the biomass happened. Different results were observed for *P. simplex*, in which the switch in the pH value from 8 to 12 induced about 80% flocculation after 20 min incubation, whereas the increase in the pH to 13 sped up the process, and the biomass was totally and immediately flocculated. *S. bigranulatus*, instead, showed a small flocculation efficiency over time at pH 12 (from 1 to 38%) and up to 51% after 20 min at pH 13.

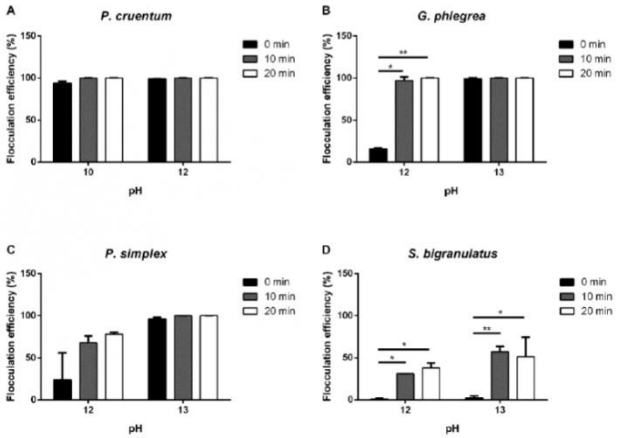

Figure 3. Flocculation efficiency (%) after pH increase. Effect of pH on the flocculation efficiency of microalgae strains analyzed immediately (0 min, black bars), after 10 min (grey bars) and after 20 min (white bars) from stirring. (**A**), *P. cruentum*; (**B**), *G. phlegrea*; (**C**), *P. simplex*; (**D**), *S. bigranulatus* upon different flocculation times. Data are obtained by means of three independent experiments (mean ± S.D.). * $p < 0.05$, ** $p < 0.005$. The lines above the bars indicate the two samples compared for statistical analysis.

Thus, according to the literature, a high variability of flocculation is observed among microalgae strains, so that each strain represents a different case study [27]. Based on the overall results, for each strain the best flocculation condition was chosen and reported in Table 1. In the case of *P. cruentum*, despite the fact that CS provided the best results, the choice fell on CC, as the latter is a valid and economical alternative (about 1000 vs. 44 €/kg, from Sigma-Aldrich, St Louis, MO, USA).

Table 1. Summary of the selected flocculation conditions for each strain.

Strain	Flocculation Condition	Flocculation Efficiency 20 Min
P. cruentum	4.0 g/L CC	87.0 ± 0.5
G. phlegrea	pH 12 pH 13	100.0 ± 0.1 100.0 ± 0.1
P. simplex	0.5 g/L CC	96 ± 4
S. bigranulatus	0.2 g/L CS	46 ± 1

2.2. Pigment Extraction

In order to verify whether flocculation has any effect on the subsequent pigment extraction in terms of yield and activity, each strain was flocculated based on the selected conditions, and pigments were extracted from the resulting wet biomass. Pigments were extracted by using ethanol as a solvent, as it is GRAS, non-toxic for humans and widely used in many applications. The idea of using wet biomass is another small step forward for the use and application of microalgae, as the drying step is avoided, thus saving energy and reducing the overall costs. Each extraction was compared to two benchmarks, i.e., a biomass harvested by centrifugation and extracted bypassing the drying step (named wet biomass) or after lyophilization (named dry biomass). As described in Materials and

Methods, for each extraction, the same amount of biomass was used for pigment extraction by resuspending the biomass in 4 mL of pure ethanol and disrupting by ultrasonication. The volume was then diluted 2.5-fold, in order to increase the efficiency of the extraction procedure, by moving forward the equilibrium between the components still bound to the matrix and those already solubilized in the solvent. In the case of *P. cruentum* (Figure 4A), the yield of the extract obtained from the biomass flocculated with 4 g/L of CC (light grey bar, 15%) showed an increase in flocculation efficiency compared to both untreated samples (black bar, 7.5%, dark grey bar, 8.5%). No significant differences ($p > 0.05$) were observed between the extracts obtained from dry and wet biomass (black bar and dark grey bar, respectively). *G. phlegrea* pigment extraction was performed either on the biomass obtained upon flocculation at pH 12 or on the bleached biomass (obtained at pH 13). As shown in Figure 4B, the yield of the extract obtained from dry biomass (black bar, 16%) was significantly higher than that obtained from the wet biomass (dark grey bar, 13%, $p < 0.05$), whereas no significant difference was observed with respect to the flocculated biomass at pH 12 (light grey bar, 16%, $p > 0.05$). The yield of extraction from the flocculated biomass at pH 12 was significantly higher than that obtained from the wet one (16 and 13%, respectively, $p < 0.05$). In the case of the extract obtained from the flocculated biomass at pH 13 (white bar, 12%), a significant decrease in the extraction yield was observed with respect to dry biomass and to the biomass flocculated at pH 12 ($p < 0.05$). No differences were observed between the extract obtained from the wet biomass and that obtained after flocculation at pH 13 ($p > 0.05$). The extracts obtained from *P. simplex* biomass (Figure 4C) did not show a statistically significant difference among them, suggesting that flocculation does not affect extraction yield. In Figure 4D, the extracts obtained from *S. bigranulatus* biomass are reported. The same yield of extraction (22%) was obtained in the centrifuged wet biomass (dark grey bar) and the flocculated one (light grey bar), and the values were significantly higher ($p < 0.01$) than the yield obtained from the centrifuged dry biomass (black bar, 12%).

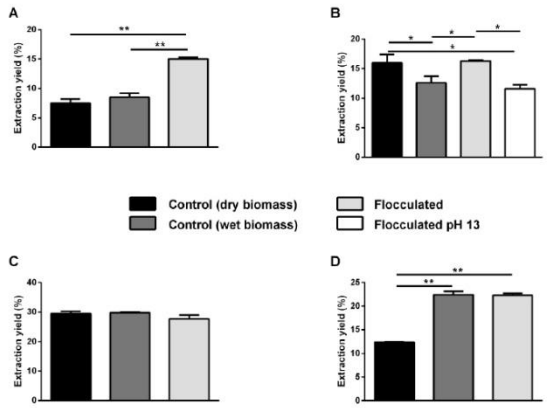

Figure 4. Pigments extraction. Extraction yields (%) are reported as mg of extract with respect to mg of D.W. biomass. Black bars indicate centrifuged dry biomass, dark grey bars indicate centrifuged wet biomass, light grey bars indicate flocculated wet biomass. The white bar refers to flocculated biomass at pH 13. (**A**), *P. cruentum*; (**B**), *G. phlegrea*; (**C**), *P. simplex*; (**D**), *S. bigranulatus*. Results are expressed as the mean ± S.D. of three independent experiments. * indicates $p < 0.05$, ** indicates $p < 0.01$. The lines above the bars indicate the two samples compared for statistical analysis.

2.3. In Vitro Antioxidant Activity

From previous data, it is known that the ethanol extract from *P. cruentum* mainly contains zeaxanthin [28], whereas *S. bigranulatus* extract is enriched in zeaxanthin and xanthophylls [29], *G. phlegrea* contains zeaxanthin and β-carotene [30], and *P. simplex* is enriched in lutein [31]. The ethanol extracts, obtained from either centrifuged or flocculated wet biomasses, were analyzed for their antioxidant capacity by in vitro ABTS assay. The results of the ABTS assay, shown in Figure 5, report, for each analyzed condition, the IC_{50} values obtained (i.e., the concentration of extract necessary to inhibit 50% of the free radicals of the $ABTS^{\bullet+}$). In particular, the experiments carried out on the extract obtained from the flocculated biomass of *P. cruentum* revealed a significant increase in the IC_{50} value (187.0 ± 1.1 μg/mL) compared to the extract obtained from centrifuged wet biomass (125.0 ± 1.4 μg/mL, $p < 0.001$). Furthermore, in the case of *G. phlegrea* extract, a significant increase ($p < 0.001$) in the IC_{50} value was observed in the flocculated biomass with respect to the benchmark extraction (i.e., centrifuged wet biomass) (93 ± 1 μg/mL and 63 ± 1 μg/mL, respectively), whereas the extract obtained from the biomass flocculated at pH 13 had an IC_{50} value of and of 109 ± 22 μg/mL ($p < 0.05$ compared to the other tested samples). These results suggest that flocculation can negatively affect the antioxidant activity of the extracts. However, the IC_{50} values obtained from *P. simplex* extracts after flocculation showed a significant reduction in comparison to that obtained from the centrifuged biomass (63 ± 1 μg/mL and 93 ± 1 μg/mL, respectively, $p < 0.001$), thus representing an improvement in the antioxidant activity of the extract. Unfortunately, CS showed a small negative effect on *S. bigranulatus* extract, as the IC_{50} values increased from 48 ± 1 to 63 ± 1 μg/mL ($p < 0.01$). It can be hypothesized that the flocculant may interact with the extracted carotenoid, as CC negatively affects the antioxidant activity of *P. cruentum* (enriched in zeaxanthin) but positively affects the antioxidant activity of *P. simplex* (enriched in lutein).

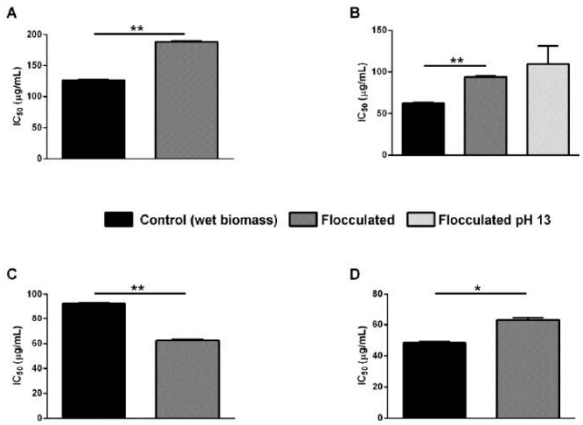

Figure 5. Antioxidant activity of ethanol extracts. Values are expressed as IC_{50} (μg/mL), i.e., the concentration required to scavenge 50% of free radical ABTS. Black bars indicate centrifuged wet biomass, dark grey bars indicate flocculated wet biomass, and the light grey bar indicates flocculated wet biomass at pH 13. (**A**), *P. cruentum*; (**B**), *G. phlegrea*; (**C**), *P. simplex*; (**D**), *S. bigranulatus*. Data are shown as means ± S.D. Three independent measurements were carried out. * indicate $p < 0.01$; ** indicate $p < 0.001$ with respect to centrifuged wet biomass. The lines above the bars indicate the two samples compared for statistical analysis.

3. Discussion

In the last few years, flocculation has been studied as a cost-effective alternative to centrifugation, with the aim to lower energy consumption and the costs related to the downstream at an industrial level. However, due to the complexity of living systems, such as microalgae and cyanobacteria, it is hard to develop a standardized flocculation procedure that can be effective on different strains [32]. Here, a study on the effect of four flocculants of different natures was carried out on three microalgae strains and one cyanobacterium. Generally speaking, a systematic comparison of different strains could be challenging, as cultivation conditions can differ in some aspects, such as cell concentration or cultivation techniques [27]. For this reason, algae cultures with the same biomass concentrations (7 O.D./mL) were used for all the experiments. Different flocculants were used, and flocculation time was set-up considering the nature of the flocculant as well as the strain analyzed. Typically, an incubation between 0 and 20 min was used, as a prolonged time could overlap with the spontaneous sedimentation that naturally occurs when a culture is in a static mode. Chitosan (CS) was selected as it is a natural and environmentally friendly agent. From a chemical point of view, CS is a polymer obtained from the deacetylation of chitin, and due to its cationic nature, it can interact with negatively charged microorganisms. When the effect of CS was studied on the *P. cruentum* culture, a dose-dependence was observed, as 66% of flocs immediately formed at the lowest concentration tested (0.1 g/L), reaching 100% flocculation in the presence of the highest concentration tested (0.2 g/L). These results indicate a higher flocculation efficiency compared to those reported by Endrawati and colleagues, who found 67% flocculation after 10 min of incubation with 0.1 g/L CS and 100% flocculation only after 40 min [33]. In the case of *G. phlegrea*, no flocculation occurred at any of the experimental conditions tested, whereas CS was able to induce 84% flocculation at time 0 in the green microalga *P. simplex*, independently from the concentration used. Similar results were obtained with *S. bigranulatus*, but at a lower extent (40% flocculation efficiency independently from the concentration). Except for *P. cruentum* flocculated in the presence of CS [33], no data are present in the literature on the other analyzed strains. However, it is generally recognized that in CS-induced flocculation, the incubation time, as well as CS concentration, can affect efficiency. As an example, Ahmad and colleagues reported the flocculation of *Chlorella* sp. in the presence of CS, but the authors found a negative correlation between algal coagulation, the amount of CS used, incubation time and speed rate [34].

Among chemical flocculants, metal ions have been extensively studied for microalgae harvesting, as they are considered highly effective in terms of flocculation efficiency; however, several issues may occur as a possible transfer of the metal ion to microalgae biomass could turn out to be highly toxic [35]. Aluminum sulfate is one of the most used chemical flocculants, generally used for waste water treatment, but it was not used in this study, as it is toxic and its presence would affect biomass valorization [36]. Alternatively, calcium chloride (CC) is a non-toxic alkali metal generally used as a food preservative, and therefore it could represent a green alternative to metal-based salts, to preserve both the biomass integrity and the environment [37]. Indeed, CC was found to be effective on *P. cruentum* in a time- and concentration-dependent manner, whereas *P. simplex* biomass flocculated after 10 min incubation without a dose-effect dependency. Unfortunately, no effects were observed on *G. phlegrea* and *S. bigranulatus*. Overall, the results obtained on the green microalga are consistent with those reported by Singh et al. [37] on *Chlorella pyrenoidosa*. Authors reached almost 98% of flocculation in the presence of~0.3 g/L of CC but with a longer incubation time then that reported in the present paper. Further analyses are needed to verify its effects on cell morphology. Another unexplored chemical flocculant, sodium glutamate (SG), was tested. SG is the monomer of the normally used polyglutamic acid (PGA) [38]. PGA works as a bridging agent by its negatively charged glutamic residue, so it was decided to use the building block to flocculate the biomass, but no positive results were obtained.

Autoflocculation occurs when microorganisms self-aggregate when the environmental conditions change. This phenomenon is achieved by neutralizing the negatively charged cell surface, thus creating an alkaline environment (pH > 8.0) that allows cells to aggregate. The variation in pH can be facilitated by adding to the microalgae culture a small amount of chemicals, such as NaOH, KOH or $Mg(OH)_2$, thus making this process economically suitable [39]. However, a substantial increase in pH could affect the algae culture and thus the quality of the biomass [12,40]. Here, NaOH was used to increase the pH of the algae culture, and with the exception of *S. bigranulatus*, it was found to be effective on all the other strains. In particular, for *P. cruentum* and *G. phlegrea* a highly efficient flocculation was immediately observed, whereas *P. simplex* completely flocculated upon 10 min incubation. These results are consistent with the literature data, as an increase in pH values has been shown to induce autoflocculation, with NaOH the base working at lower concentrations with respect to KOH, $Mg(OH)_2$ and $Al(OH)_2$ [18,41]. Despite the promising results, the pH variation in the case of *G. phlegrea* from 1.5 to 13 resulted in a dramatic change in the color of the biomass, suggesting that flocculation could affect not only the quality of the biomass but also the quality of the molecules within it. This evidence is supported by data in the literature, which report that pH variations can alter microalgae cell physiology [42]. Having selected the best flocculation parameter for each strain, a pigment extraction was carried out. Conventionally, extractions are performed on dry biomasses; however, it is known that the drying step is energetically expensive [30]. To further decrease the overall process costs, in this work pigment extractions were carried out on a wet biomass. The results clearly indicate that flocculation does not negatively affect the extraction yields when compared to those obtained starting from a centrifuged biomass and that the drying step can be avoided, with a generally positive impact on the overall downstream costs. Finally, the bioactivity of the extracted molecules was determined in vitro to understand more closely whether the flocculation procedure could affect the bioactivity of the extracted molecules. The ABTS assay revealed that flocculation does not affect the quality of the extracted molecules, with the exception of *P. simplex*, in which the antioxidant activity of the extract obtained from the flocculated biomass improved with respect to that obtained from the centrifuged one (IC_{50} values: 63 µg/mL vs. 93 µg/mL). Further analyses are mandatory to understand whether an excess of flocculant may be responsible for the lower antioxidant activity of the extract. These results are important as this is the first report in which flocculants have been related to the quality of the extracted molecules. Many papers have been published so far reporting a simple relationship between the efficiency of flocculation and biomass morphology [18,35,36]. However, no analysis on the bioactivity of the molecules extracted from flocculated biomass has been reported so far, probably because research has been mainly focused on wastewater treatment or biodiesel production [37–39]. To date, only Taghavijeloudar and colleagues successfully extracted proteins, carbohydrates and lipids from a *Chlorella sorokiniana* strain, but no data are reported on the biological activity of the obtained molecules [43]. Understanding the domino effect of flocculants on biomass and molecules to be extracted represents a priority for a safe and mindful use of microalgae, which are now considered in a wider perspective, not only for their lipid content, but as a source of green, vegan and sustainable molecules.

4. Materials and Methods

4.1. Reagents and Chemicals

Solvents and reagents, unless differently specified, were from Sigma-Aldrich.

4.2. Microalgae Strains and Culture Conditions

Porphyridium cruentum (CCALA 415) was acquired from Culture Collection of Autotrophic Organism (CCALA, Centre for Phycology, Institute of Botany of the AS CR, Dukelská 135, TŘEBOŇ CZ-379 82, Czech Republic), and grown in Porphyridium Medium. *Galdieria phlegrea* (ACUF 009), *Pseudococcomyxa simplex* (ACUF 127) and *Synechococcus bigranulatus* (ACUF 680) were kindly provided by Algal Collection of the University Fed-

erico II (ACUF, University of Naples Federico II, Department of Biology, Naples, Italy, www.acuf.net, accessed on 5 July 2024) and grown in Allen medium, BBM and BG11, respectively. Microalgae strains were grown in bubble column photobioreactors at temperatures, and light intensity [Photosynthetic Active Radiations (PAR) ($\mu mol_{photons}/m^2/s$), as previously described [28,29,31,44]. Briefly, cells were cultured as follows: *P. cruentum* at 25 °C and 13 PAR; *G. phlegrea* at 37 °C and 200 PAR; *P. simplex* at 24 °C and 100 PAR and *S. bigranulatus* at 39 °C and 300 PAR. Each culture was mixed by bubbling air through a sintered glass tube placed at the bottom of each reactor. Algal growth was daily monitored by measuring the absorbance at 730 nm.

4.3. Flocculation

At the end of cultivation, different concentrations of high-molecular-weight chitosan (CS), calcium chloride (CC), sodium glutamate (SG) and sodium hydroxide (to increase the pH) were added to each strain. In particular, CS was tested at 0.1, 0.15 and 0.2 g/L; CC at 2, 3, and 4 g/L on *P. cruentum*, *G. phlegrea* and *S. bigranulatus* and at 0.3, 0.4, 0.5 g/L on *P. simplex*. Autoflocculation was induced by adjusting the pH at 10 and 12 for *P. cruentum* and at 12 and 13 for the other strains. Flocculation was carried out at the pH measured at the end of cell growth (7 for *P. cruentum*, 1.5 for *G. phlegrea*, 8 for *S. bigranulatus* and *P. simplex*). After the flocculating agent had been added, each culture was stirred for 30 s at 1000 rpm, and then the O.D. of the solution was measured at 730 nm. Time-course experiments were performed by measuring the O.D. immediately (0 min) and at 10 and 20 min after stirring. Flocculation efficiency was calculated as percentage (%) using the formula:

$$\text{Flocculation effiency}(\%) = \left(1 - \frac{\text{O.D.sample}}{\text{O.D.culture}} \times 100\right)$$

where O.D. sample is the O.D. measured after the treatment and O.D. culture is the value measured before any treatment [45].

4.4. Pigments Extraction and Yields Determination

Pigment extractions were performed using a GRAS solvent, ethanol, as reported by Aremu, with some modifications [46]. Briefly, for each extraction, independently from the harvesting procedure followed, the equivalent of 200 mg of dry weight (D.W.) was used for extractions. The biomass was suspended in 4 mL of pure ethanol and disrupted by ultrasonication (40% amplitude, 4 min on ice, Bandelin SONOPULS HD 3200, tip MS73). The final volume was adjusted to 20 mL, and the mixture was shaken for 24 h at 250 rpm in a dark room at 4 °C. The mixture was then centrifuged at 5000× *g* for 10 min, and the supernatant was stored at −20 °C and dried under an N_2 stream at 30 °C. The extraction yields were determined gravimetrically and expressed using the formula:

$$Extraction\ yield\ (\%) = \frac{mg_{extract}}{mg_{biomass\ dry\ weight}} \times 100$$

4.5. ABTS Assay

The in vitro antioxidant activity of each extract was evaluated by the 2,2′-azinobis-(3-ethylbenzothiazoiline-6-sulfonic acid) ABTS assay, according to Imbimbo et al. [30]. Results are expressed as IC_{50} (µg/mL), i.e., the concentration required to scavenge 50% of free radical ABTS.

4.6. Statistical Analyses

Samples were tested in three independent analyses, each carried out in triplicate. The results are presented as the mean of results obtained after three independent experiments (mean ± S.D.) and compared by one-way ANOVA according to Bonferroni's method (post hoc) using Graphpad Prism for Windows, version 6.01.

5. Conclusions

In the present work, three microalgae strains and a cyanobacterium were harvested using different flocculants, chosen for their different mechanisms of action. The results clearly indicate that a general procedure cannot be developed, as no correlation between the flocculating agent and the microbial strain can be established, but flocculation must be tailored considering the strain, the nature of the flocculant and the incubation time. It is worth noting that, in this paper, a new carotenoid extraction strategy was set up, based on the use of ethanol on a wet-flocculated biomass. Using a GRAS solvent and avoiding the drying step environmental impact and energy consumption can be reduced, without negatively affecting extraction yields. For the first time, the antioxidant activity of the molecules extracted from a flocculated biomass was analyzed. Unexpectedly, a general decrease in the antioxidant activity was observed on the extracts obtained from the flocculated biomass, except for *P. simplex*, whose activity was increased. Despite the energetic sustainability of the whole process, the presented results raise some criticisms that should be overcome to translate flocculation to an industrial level.

Author Contributions: P.I.: Supervision, Investigation, Writing—original draft, Writing—review & editing, Data curation; A.F.: Methodology, Investigation, Data curation, Writing—review & editing; E.G.: Investigation, Writing—review & editing; D.L.: Investigation; D.M.M., Supervision, Conceptualization, Writing—original draft, Writing—review & editing, Project administration. All authors have read and agreed to the published version of the manuscript.

Funding: This research received no external funding.

Institutional Review Board Statement: Not applicable.

Informed Consent Statement: Not applicable.

Data Availability Statement: Data is contained within the article.

Conflicts of Interest: The authors declare no conflicts of interest.

References

1. Siddiqui, A.; Wei, Z.; Boehm, M.; Ahmad, N. Engineering Microalgae through Chloroplast Transformation to Produce High-Value Industrial Products. *Biotechnol. Appl. Biochem.* **2020**, *67*, 30–40. [CrossRef]
2. Levasseur, W.; Perré, P.; Pozzobon, V. A Review of High Value-Added Molecules Production by Microalgae in Light of the Classification. *Biotechnol. Adv.* **2020**, *41*, 107545. [CrossRef]
3. Acién Fernández, F.G.; Fernández Sevilla, J.M.; Molina Grima, E. Chapter 21—Costs Analysis of Microalgae Production. In *Biomass, Biofuels, Biochemicals*; Pandey, A., Chang, J.-S., Soccol, C.R., Lee, D.-J., Chisti, Y.B.T.-B., Eds.; Elsevier: Amsterdam, The Netherlands, 2019; pp. 551–566. ISBN 978-0-444-64192-2.
4. Udayan, A.; Pandey, A.K.; Sharma, P.; Sreekumar, N.; Kumar, S. Emerging Industrial Applications of Microalgae: Challenges and Future Perspectives. *Syst. Microbiol. Biomanuf.* **2021**, *1*, 411–431. [CrossRef]
5. Roy, M.; Mohanty, K. A Comprehensive Review on Microalgal Harvesting Strategies: Current Status and Future Prospects. *Algal Res.* **2019**, *44*, 101683. [CrossRef]
6. Okoro, V.; Azimov, U.; Munoz, J.; Hernandez, H.H.; Phan, A.N. Microalgae Cultivation and Harvesting: Growth Performance and Use of Flocculants—A Review. *Renew. Sustain. Energy Rev.* **2019**, *115*, 109364. [CrossRef]
7. Fuad, N.; Omar, R.; Kamarudin, S.; Harun, R.; Idris, A.; Wan, W.A. Mass Harvesting of Marine Microalgae Using Different Techniques. *Food Bioprod. Process.* **2018**, *112*, 169–184. [CrossRef]
8. Hidayah, N.; Yasin, M.; Shafei, N.I.; Rushan, N.H.; Raihana, N.; Sepian, A.; Said, F.M. ScienceDirect the Effect of Microalgae Harvesting on Lipid for Biodiesel Production. *Mater. Today Proc.* **2019**, *19*, 1582–1590. [CrossRef]
9. Rawat, I.; Kumar, R.R.; Mutanda, T.; Bux, F. Dual Role of Microalgae: Phycoremediation of Domestic Wastewater and Biomass Production for Sustainable Biofuels Production. *Appl. Energy* **2011**, *88*, 3411–3424. [CrossRef]
10. Barros, A.I.; Gonçalves, A.L.; Simões, M.; Pires, J.C.M. Harvesting Techniques Applied to Microalgae: A Review. *Renew. Sustain. Energy Rev.* **2015**, *41*, 1489–1500. [CrossRef]
11. Najjar, Y.S.H.; Abu-Shamleh, A. Harvesting of Microalgae by Centrifugation for Biodiesel Production: A Review. *Algal Res.* **2020**, *51*, 102046. [CrossRef]
12. Min, K.H.; Kim, D.H.; Ki, M.R.; Pack, S.P. Recent Progress in Flocculation, Dewatering, and Drying Technologies for Microalgae Utilization: Scalable and Low-Cost Harvesting Process Development. *Bioresour. Technol.* **2022**, *344*, 126404. [CrossRef] [PubMed]
13. Kumar, N.; Banerjee, C.; Negi, S.; Shukla, P. Microalgae Harvesting Techniques: Updates and Recent Technological Interventions. *Crit. Rev. Biotechnol.* **2023**, *43*, 342–368. [CrossRef]

14. Ortiz, A.; García-Galán, M.J.; García, J.; Díez-Montero, R. Optimization and Operation of a Demonstrative Full Scale Microalgae Harvesting Unit Based on Coagulation, Flocculation and Sedimentation. *Sep. Purif. Technol.* **2021**, *259*, 118171. [CrossRef]
15. Demir-Yilmaz, I.; Ftouhi, M.S.; Balayssac, S.; Guiraud, P.; Coudret, C.; Formosa-Dague, C. Bubble Functionalization in Flotation Process Improve Microalgae Harvesting. *Chem. Eng. J.* **2023**, *452*, 139349. [CrossRef]
16. Xu, H.; Wang, H.; Liang, Z.; Chen, H.; Yang, D.; Tang, Z.; Dai, X. A Novel Biomineralization-Inspired Flocculation Approach for Harvesting High Quality Microalgal Biomass: Dual Action of Cationic Polyelectrolytes and Nanosilica. *Bioresour. Technol.* **2023**, *388*, 129739. [CrossRef]
17. Zhang, J.; Hu, B. A Novel Method to Harvest Microalgae via Co-Culture of Filamentous Fungi to Form Cell Pellets. *Bioresour. Technol.* **2012**, *114*, 529–535. [CrossRef]
18. de Morais, E.G.; Sampaio, I.C.F.; Gonzalez-Flo, E.; Ferrer, I.; Uggetti, E.; García, J. Microalgae Harvesting for Wastewater Treatment and Resources Recovery: A Review. *New Biotechnol.* **2023**, *78*, 84–94. [CrossRef]
19. Zhang, B.; Mao, B. Efficient Magnetic Flocculation for Microalgae Harvesting Using a Novel Composite Flocculant of Fe_3O_4-Based Starch-Grafted-Cationic Polyacrylamide. *J. Water Process Eng.* **2023**, *55*, 104121. [CrossRef]
20. Gifuni, I.; Pollio, A.; Safi, C.; Marzocchella, A.; Olivieri, G. Current Bottlenecks and Challenges of the Microalgal Biorefinery. *Trends Biotechnol.* **2019**, *37*, 242–252. [CrossRef] [PubMed]
21. Mansour, E.A.; Abo El-Enin, S.A.; Hamouda, A.S.; Mahmoud, H.M. Efficacy of Extraction Techniques and Solvent Polarity on Lipid Recovery from Domestic Wastewater Microalgae. *Environ. Nanotechnol. Monit. Manag.* **2019**, *12*, 100271. [CrossRef]
22. Sati, H.; Mitra, M.; Mishra, S.; Baredar, P. Microalgal Lipid Extraction Strategies for Biodiesel Production: A Review. *Algal Res.* **2019**, *38*, 101413. [CrossRef]
23. Sousa, V.; Pereira, R.N.; Vicente, A.A.; Dias, O.; Geada, P. Microalgae Biomass as an Alternative Source of Biocompounds: New Insights and Future Perspectives of Extraction Methodologies. *Food Res. Int.* **2023**, *173*, 113282. [CrossRef] [PubMed]
24. Pocha, C.K.R.; Chia, W.Y.; Chew, K.W.; Munawaroh, H.S.H.; Show, P.L. Current Advances in Recovery and Biorefinery of Fucoxanthin from *Phaeodactylum tricornutum*. *Algal Res.* **2022**, *65*, 102735. [CrossRef]
25. Chong, J.W.R.; Tang, D.Y.Y.; Leong, H.Y.; Khoo, K.S.; Show, P.L.; Chew, K.W. Bridging Artificial Intelligence and Fucoxanthin for the Recovery and Quantification from Microalgae. *Bioengineered* **2023**, *14*, 2244232. [CrossRef] [PubMed]
26. Elbanna, K.; Alsulami, F.S.; Neyaz, L.A.; Abulreesh, H.H. Poly (γ) Glutamic Acid: A Unique Microbial Biopolymer with Diverse Commercial Applicability. *Front. Microbiol.* **2024**, *15*, 1348411. [CrossRef]
27. Lama, S.; Muylaert, K.; Karki, T.B.; Foubert, I.; Henderson, R.K.; Vandamme, D. Flocculation Properties of Several Microalgae and a Cyanobacterium Species during Ferric Chloride, Chitosan and Alkaline Flocculation. *Bioresour. Technol.* **2016**, *220*, 464–470. [CrossRef]
28. Liberti, D.; Imbimbo, P.; Giustino, E.; D'elia, L.; Ferraro, G.; Casillo, A.; Illiano, A.; Pinto, G.; Di Meo, M.C.; Alvarez-Rivera, G.; et al. Inside out *Porphyridium cruentum*: Beyond the Conventional Biorefinery Concept. *ACS Sustain. Chem. Eng.* **2022**, *11*, 381–389. [CrossRef]
29. D'Elia, L.; Imbimbo, P.; Liberti, D.; Bolinesi, F.; Mangoni, O.; Pollio, A.; Olivieri, G.; Monti, D.M. Thermo Resistant Antioxidants from Photoautotrophic Microorganisms: Screening and Characterization. *World J. Microbiol. Biotechnol.* **2021**, *37*, 215. [CrossRef]
30. Imbimbo, P.; Bueno, M.; D'Elia, L.; Pollio, A.; Ibañez, E.; Olivieri, G.; Monti, D.M. Green Compressed Fluid Technologies To Extract Antioxidants and Lipids from *Galdieria phlegrea* in a Biorefinery Approach. *ACS Sustain. Chem. Eng.* **2020**, *8*, 2939–2947. [CrossRef]
31. Imbimbo, P.; Giustino, E.; Ferrara, A.; Alvarez, G.; Hassan, R.; Elena, A.; Chiara, M.; Meo, D.; Zarrelli, A.; Maria, D. Unveiling the Potential of *Pseudococcomyxa simplex*: A Stepwise Extraction for Cosmetic Applications. *Appl. Microbiol. Biotechnol.* **2024**, *108*, 390. [CrossRef]
32. Rosmahadi, N.A.; Leong, W.H.; Rawindran, H.; Ho, Y.C.; Mohamad, M.; Ghani, N.A.; Bashir, M.J.K.; Usman, A.; Lam, M.K.; Lim, J.W. Assuaging Microalgal Harvesting Woes via Attached Growth: A Critical Review to Produce Sustainable Microalgal Feedstock. *Sustainability* **2021**, *13*, 11159. [CrossRef]
33. Endrawati, H.; Widianingsih, W.; Nuraini, R.A.T.; Hartati, R.; Redjeki, S.; Riniatsih, I.; Mahendrajaya, R.T. The Effect of Chitosan Concentration on Flocculation Efficiency Microalgae *Porphyridium cruentum* (Rhodhophyta). *IOP Conf. Ser. Earth Environ. Sci.* **2021**, *919*, 012052. [CrossRef]
34. Ahmad, A.L.; Mat Yasin, N.H.; Derek, C.J.C.; Lim, J.K. Optimization of Microalgae Coagulation Process Using Chitosan. *Chem. Eng. J.* **2011**, *173*, 879–882. [CrossRef]
35. Rossi, S.; Visigalli, S.; Castillo Cascino, F.; Mantovani, M.; Mezzanotte, V.; Parati, K.; Canziani, R.; Turolla, A.; Ficara, E. Metal-Based Flocculation to Harvest Microalgae: A Look beyond Separation Efficiency. *Sci. Total Environ.* **2021**, *799*, 149395. [CrossRef] [PubMed]
36. Zhu, L.; Hu, T.; Li, S.; Nugroho, Y.K.; Li, B.; Cao, J.; Show, P.-L.; Hiltunen, E. Effects of Operating Parameters on Algae *Chlorella vulgaris* Biomass Harvesting and Lipid Extraction Using Metal Sulfates as Flocculants. *Biomass Bioenergy* **2020**, *132*, 105433. [CrossRef]
37. Singh, H.M.; Tyagi, V.V.; Ahmad, S.; Kothari, R. Optimization of Flocculation Efficiency of *Chlorella pyrenoidosa* with $CaCl_2$ Using the Box-Behnken Design of Response Surface Methodology: A Cost Effective Statistical Investigation. *Biomass Convers. Biorefin.* **2024**, *14*, 3261–3273. [CrossRef]

38. Pugazhendhi, A.; Shobana, S.; Bakonyi, P.; Nemestóthy, N.; Xia, A.; Banu, J.R.; Kumar, G. A Review on Chemical Mechanism of Microalgae Flocculation via Polymers. *Biotechnol. Rep.* **2019**, *21*, e00302. [CrossRef]
39. Babakhani, P.; Mahdavi, M.A.; Gheshlaghi, R.; Karimian, A. The Shift in Carbon Source Induces pH Increase and Autoflocculation in Microalgal Suspensions Facilitating Multi-Approach Biomass Harvesting. *Biomass Convers. Biorefin.* **2022**. [CrossRef]
40. Chen, C.Y.; Liu, C.H.; Lo, Y.C.; Chang, J.S. Perspectives on Cultivation Strategies and Photobioreactor Designs for Photo-Fermentative Hydrogen Production. *Bioresour. Technol.* **2011**, *102*, 8484–8492. [CrossRef]
41. Vandamme, D.; Foubert, I.; Fraeye, I.; Meesschaert, B.; Muylaert, K. Flocculation of *Chlorella vulgaris* Induced by High pH: Role of Magnesium and Calcium and Practical Implications. *Bioresour. Technol.* **2012**, *105*, 114–119. [CrossRef]
42. Kuzhiumparambil, U.; Labeeuw, L.; Commault, A.; Vu, H.P.; Nguyen, L.N.; Ralph, P.J.; Nghiem, L.D. Effects of Harvesting on Morphological and Biochemical Characteristics of Microalgal Biomass Harvested by Polyacrylamide Addition, pH-Induced Flocculation, and Centrifugation. *Bioresour. Technol.* **2022**, *359*, 127433. [CrossRef] [PubMed]
43. Taghavijeloudar, M.; Yaqoubnejad, P.; Ahangar, A.K.; Rezania, S. A Rapid, Efficient and Eco-Friendly Approach for Simultaneous Biomass Harvesting and Bioproducts Extraction from Microalgae: Dual Flocculation between Cationic Surfactants and Bio-Polymer. *Sci. Total Environ.* **2023**, *854*, 158717. [CrossRef] [PubMed]
44. Imbimbo, P.; Romanucci, V.; Pollio, A.; Fontanarosa, C.; Amoresano, A.; Zarrelli, A.; Olivieri, G.; Monti, D.M. A Cascade Extraction of Active Phycocyanin and Fatty Acids from *Galdieria phlegrea*. *Appl. Microbiol. Biotechnol.* **2019**, *103*, 9455–9464. [CrossRef] [PubMed]
45. Chua, E.T.; Shekh, A.Y.; Eltanahy, E.; Thomas-Hall, S.R.; Schenk, P.M. Effective Harvesting of *Nannochloropsis* Microalgae Using Mushroom Chitosan: A Pilot-Scale Study. *Front. Bioeng. Biotechnol.* **2020**, *8*, 771. [CrossRef]
46. Aremu, A.O.; Masondo, N.A.; Molnár, Z.; Stirk, W.A.; Ördög, V.; Van Staden, J. Changes in Phytochemical Content and Pharmacological Activities of Three Chlorella Strains Grown in Different Nitrogen Conditions. *J. Appl. Phycol.* **2016**, *28*, 149–159. [CrossRef]